RISK ANALYSIS AND MODELING OF THE MARITIME TRAFFIC IN THE STRAIT OF ISTANBUL

by

Şirin Özlem

B.S., Industrial Engineering, Uludağ University, 2008
M.S., Industrial Engineering, Boğaziçi University, 2011

Submitted to the Institute for Graduate Studies in
Science and Engineering in partial fulfillment of
the requirements for the degree of
Doctor of Philosophy

Graduate Program in Industrial Engineering

Boğaziçi University

2018

ACKNOWLEDGEMENTS

I express my gratitude to my thesis supervisor Prof. İlhan Or. We spent nine years together and during these years, his wisdom, scientific experience, kindness, and helpfulness contributed tremendously not only to this study but also to my life perspective, academic vision and stability.

I would like to thank Assoc. Prof. Emre Otay for countless contribution and interest to this study. With a continuous motivation, he always assisted me at my toughest times. I would also like to thank Prof. Taner Bilgiç for being very helpful and giving quick and reasonable solutions when I needed not only for this study but for all academic issues.

I would like to thank Prof. Barış Tan and Dr. Utku Koç for kindly accepting to be in my thesis defense jury. Their motivation and attentive suggestions improve my view and the extent of this study.

I would like to thank Saim Oğuzülgen, Tuncay Çehreli, Dr.Yiğit Can Altan and Dr. Berk Orbay for providing information and never refusing my questions whenever I asked. Also, i would like to thank Assoc. Prof. Semra Ağralı for her guidance about my academic career and behaving always kindly and helpful to me.

I would also like to acknowledge my dear friends Semiha Erdoğan, Sevda Halaç, Buket Büyük for showing me real and endless friendship exists. The best sister and friend in my world, Narin, deserves the best of everything. She is my other half.

Lastly, I feel grateful towards my parents for their tolerance and helpfulness throughout my life. I lost my grandmother Zeliha Özlem while I was studying this thesis. She would be very happy to see my graduation. This thesis is dedicated to her, with a never ending longing.

I gratefully recognize the support of TÜBİTAK, the Scientific and Technological Research Council of Turkey, YURT İÇİ DOKTORA BURS PROGRAMI (2211) during my thesis period.

ABSTRACT

RISK ANALYSIS AND MODELING OF THE MARITIME TRAFFIC IN THE STRAIT OF ISTANBUL

The Istanbul Strait connecting Marmara and Black Sea is one of the narrowest waterways in the world with daily crowded local and transit vessel traffic. Other features such as currents, wind, fog and sharp turns in that narrow waterway lead to a high accident risk for transiting vessels. The most common accidents in the Istanbul Strait are collisions and groundings which have caused considerable amount of deaths and sea pollution so far. The main aim of this study is to measure the collision and grounding probabilities in Istanbul Strait based on mathematical models. A simulation model is built that mimicks the transit traffic pattern of the Istanbul Strait for seven years through a developed scheduling algorithm. The algorithm decides the entering vessel type and entrance times each day regarding past data and established maritime rules and regulations. In order to estimate the collision and grounding probabilities, the geometric probabilities (the vessel being on a collision or grounding course) and the causation probabilities (given that the vessel on a collision or grounding course, the inability to prevent accident) are multiplied. The geometric probability is estimated based on a physical model whereas the causation probability is estimated through created Bayesian networks. Effects of some vessel based and external factors on collision or grounding causation probability are investigated. The results show that having pilot service dramatically decreases the causation probability of collision and grounding. The number of accidents are estimated by integrating the probabilities with the simulation model and the results are compared with the actual number of accidents. Effects of some factors (such as sectors, season, day light, transiting vessel direction and type) on number of collisions are also investigated. For number of groundings, the factor analysis is also elaborated on transit traffic density, as well. The results show that most frequently dry cargo vessels collide and ground in the Istanbul Strait. Number of collisions and groundings increases at nights in model results and actual cases. Moreover, as the transit traffic density increases, number of groundings increases as well.

ÖZET

İSTANBUL BOĞAZI RİSK ANALİZİ VE GEMİ TRAFİĞİNİN MODELLENMESİ

Marmara Denizi ve Karadeniz'i birbirine bağlayan İstanbul Boğazı yoğun yerel ve transit gemi trafiğine sahip dünyanın en dar su yollarından biridir. Dahası, bu su yolundaki akıntı, rüzgar, sis ve keskin dönüş gibi özellikler buradan geçen gemiler için yüksek kaza riskine yol açmaktadır. İstanbul Boğazı'ndaki en yaygın gemi kazaları önemli sayıda ölüme ve deniz kirliliğne yol açan çarpışma ve karaya oturmadır. Bu çalışmanın asıl amacı, İstanbul Boğazı'ndaki çarpışma ve karaya oturma olasılıklarını matematiksel modeler yardımıyla hesaplamaktır. Geliştirilen bir çizelgeleme algoritması ile İstanbul Boğazı transit trafik yapısını yedi yıl boyunca simüle eden bir model kurulmuştur. Çizelgeleme algoritması giren geminin türüne ve giriş zamanına, geçmiş veriler ile kurallar ve yönetmelikleri dikkate alarak karar vermektedir. Çarpışma ve karaya oturma olasılıklarını hesaplamak için geometrik olasılıkları (geminin çarpışma veya karaya oturma rotasında olması) ve nedensellik olasılıkları (çarpışma veya karaya oturma rotasında olan geminin kazayı önleyememesi) birbiri ile çarpılmıştır. Geometrik çarpışma veya karaya oturma olasılığı fiziksel model ile hesaplanırken çarpışma veya karaya oturma nedensellik olasılığı geliştirilen Bayes ağları ile hesaplanmıştır. Bazı gemiye ait ve dışsal öğelerin çarpışma veya karaya oturma nedensellik olasılığı üzerindeki etkisi araltırılmıştır. Sonuçlar, kılavuz kaptan almanın nedensellik olasılığını önemli ölçüde azalttığını göstermiştir. Bu olasılıklar simülasyon modeline eklenmiş ve bir yılda beklenen çarpışma ve karaya oturma sayıları hesaplanmış ve sonuçlar gerçek çarpışma ve karaya oturma sayıları ile kıyaslanmıştır. Sektör, mevsim, gün ışığı, geçen geminin yönü ve türü gibi bazı öğelerin çarpışma üzerindeki etkisi araştırılmıştır. Karaya oturma sayıları için bu öğelerin analizi transit trafik yoğunluğu ile de derinleştirilmiştir. Sonuçlar, İstanbul Boğazı'nda daha fazla sıklıkta kuruyük gemilerinin çarpıştığını karaya oturduğunu göstermiştir. Model sonuçları ve gerçek duruma göre çarpışma ve karaya oturma geceleri artış göstermektedir. Dahası, transit trafik yoğunluğu arttıkça karaya oturma da artmaktadır.

TABLE OF CONTENTS

LIST OF FIGURES

LIST OF TABLES

LIST OF SYMBOLS

$N_{collision}$	Number of Collisions
$N_{grounding}$	Number of Groundings
P_{RC}	Probability of Collision
P_{RG}	Probability of Grounding
$P_{GeoColl}$	Geometric Collision Probability
$P_{CausColl}$	Collision Causation Probability
P_{GeoGrn}	Geometric Grounding Probability
$P_{CausGrn}$	Grounding Causation Probability

LIST OF ACRONYMS / ABBREVIATIONS

AIS	Automatic Identification System
BN	Bayesian Network
BRM	Bridge Resource Management
DAG	Directed Acyclic Graph
LNG	Liquefied natural gas
LPG	Liquid petroleum gas
NB	Northbound transiting vessel
PI	Prediction Interval
R&R	Istanbul Strait Traffic Rules and Regulations
SB	Southbound transiting vessel
SP-2	Sailing Plan 2
TSVTS	Turkish Straits Vessel Traffic Service Center
VTS	Vessel Traffic System

1. INTRODUCTION AND STUDY OBJECTIVES

Maritime transportation is of vital importance for world trade where globally approximately more than 80% of the goods are carried by sea [1]. The most vital reasons for this tendency are economic advantage, safety and environmentalist structure compared to other mass transports.

While having these upsides, sea freight has witnessed considerable amount of accidents all over the world in the past years. One of the best known maritime accidents in history is the British passenger vessel Titanic hitting an iceberg and sinking in 15 April 1912. Approximately 1,500 passengers died.

Another major maritime accident occurred on 29 May 1914, when a Canadian passenger liner sank after colliding with a cargo ship, killing 1,012 people.

On 3 March 1921, the Singapore passenger ship Hong Moh hit the rocks on an island and sank. 1,000 people died.

On 12 December 1939, the passenger ship Indigirka which was carrying prisoners, grounded in Japanese coast. Most of the prisoners were killed.

On 4 December 1948, the passenger ship Kiangya exploded and sank. More than 2,750 people died.

On 26 September 1954, the Japanese passenger ship Toya Maru travelling in bad weather conditions capsized and sank. It is known that more than 1,000 people were killed.

On 14 December 1970, The South Korean ferry Namyoung sank on 14 December 1970. Most of the passengers (323 of 338 people) died.

On 20 December 1987, the ferry (over weighted) Doña Paz collided with the tanker Vector in Philippines. A fire occurred and the vessel sank. The recorded number of deaths is more than 4,300 people [2].

On 28 September 1994, the RoRo ship Estonia sank in Baltic Sea due to capsizing in stormy weather.

The events stated above are some of the most disastrous maritime accidents in the world. However, on the whole, maritime transportation is not riskier than most of other transportation modes. Nevertheless, in narrow waterways (straits and channels) accident risk is considerably high due to intense vessel density and proximity. Additionally, many sea routes include narrow waterways which have encountered disastrous vessel accidents due to their geological features.

On 9 May 1980, the bulk carrier ship Summit Venture navigating in Tampa Bay, Florida collided with the Sunshine Skyway Bridge, 35 people died, while vehicles fell in the Bay.

On 15 February 1996, the oil tanker Sea Empress ran aground in the Milford Haven Channel in England and until she was floated again 72,000 tons of crude oil spilled in the Channel [3].

Istanbul Strait (the Strait) for instance, with 40 maritime accidents per 100000 passages is one of the riskiest channels in the world [4].

1.1. Istanbul Strait

The Strait of Istanbul (the Strait) is known as one the most strategic natural channels in the world; it separates the European continent from Asia and unites the Marmara and the Black Seas. The Strait is 31 kilometers (16.8 nm) in length and on average 1.5 km (1.8 nm) in width. The narrowest point is merely 660 meters, located between Rumelihisarı and Anadolu Hisarı. This width and depth, which varies between 30 and 120 meters, make the Strait one of the narrowest waterways in the world. (Figure 1.1).

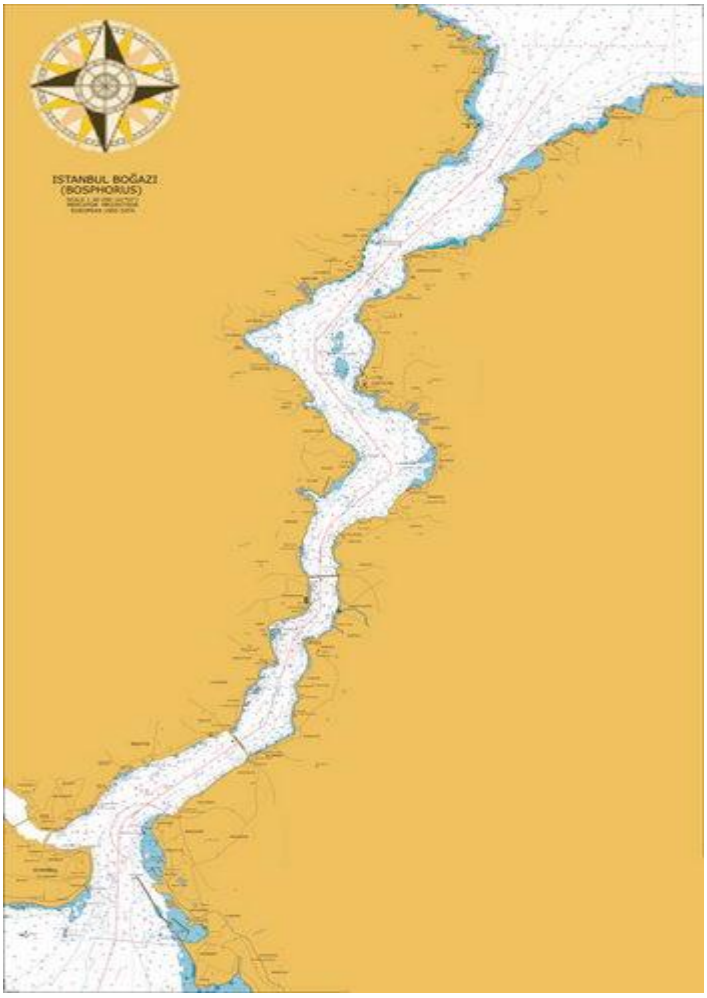

Figure 1.1 The Istanbul Strait [5].

The Strait features many sharp turns (even up to 80 degrees at Yeniköy) and vessels passing through the Strait change course more than 10 times.

The meteorological conditions are also peculiar to the Strait and have substantial impact on traffic volume and maritime accidents. The distinct current types are surface currents, deep currents, orkoz currents and eddies. Surface currents are the most dominant ones. Those currents occur due to the higher water level of the Black Sea (40 centimeters higher). The water flowing to the Marmara Sea with speeds reaching up to 8 knots (helped by strong northern winds) stops the transit traffic until current conditions improve. Deep currents are due to the higher salinity of the Marmara Sea water (1.8% saltier) and flow in the opposite (northbound) direction. Orkoz currents are due to strong southern winds reversing the flow direction of the surface currents. Eddies, on other hand, occur when

currents change direction when they hit the Channel shores and when they mix into one another. [6].

Moreover, other meteorological conditions (such as fog, rain and wind) also have significant negative impacts on navigation in the Strait. The fog and storms also affect the vessel traffic through the Strait. (In dense fog or adverse weather conditions, vessel traffic may be slowed down or even suspended until meteorological conditions improve).

Another distinctive feature of the Strait is the very high level of local vessel traffic, with a daily average of more than 2,500 trips [7]. The leading local transportation companies, Şehir Hatları, İDO, Dentur Avrasya Grup and Turyol carry a total of two million passengers between the two shores every day. In addition to the ferries, flybridges, naval vessels, tugboats, fishing boats, pleasure boats and surveyors form other important parts of local traffic. Most of the local ships generate east-west cross traffic, while some of them also move in the north south axis.

Transit traffic density is a major concern about the accident risk in the Strait. In 2008, more than 54,000 transit vessels passed through the Strait. However, in the last seven years there has been an almost 16% decrease in transit traffic. The main reasons for this decline are the increase in the number of high tonnage vessels, complementary activity of the Baku Ceyhan pipeline and the ongoing global economic slowdown [8] (Figure 1.2).

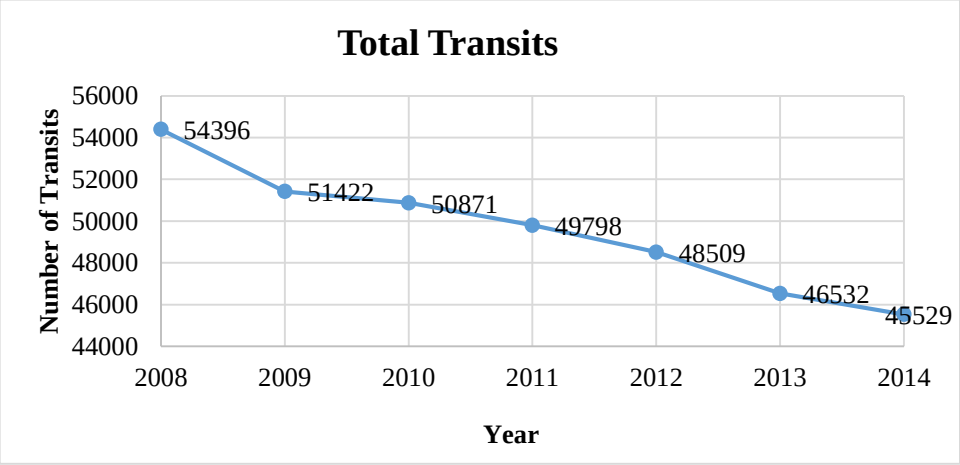

Figure 1.2. Total Number of Vessel Transits in the Strait [8].

The types of transit vessels passing through the Strait include dry cargo carrying vessels, passenger ships, hazardous material carrying vessels and tankers.

Considering all meteorological, oceanographic, morphological characteristics, notable dense local and transit traffic and being in the middle of a large metropolitan area, the Strait is prone to vessel accidents potentially having disastrous consequences not only for local and transit vessels, but also for the maritime environment and even for the more than 10 million people living around the Strait.

The Turkish Straits (including Çanakkale and Istanbul Straits and the Marmara Sea) have strategic importance for Turkey since ancient times. Flow of the most maritime exports and imports from Russia and other former Soviet Union republics including large quantities of oil exports can only be realized through these Straits. Actually, all maritime transportation of the States around the Black Sea and the connected States must pass through these Straits. In order to better define the legal status of the Straits, Montreux Convention was signed among Turkey, United Kingdom, France, Soviet Union, Japan, Greece and Yugoslavia in 1936. This agreement, while delegating all maritime traffic control decisions in the Strait to the Turkish Republic Government, also stipulates that all vessels have complete freedom to navigate in the Strait at both day and night during peacetime.

Turkish government adopted the Turkish Straits Maritime Traffic Regulations in 1994 to provide for safer navigation, while protecting lives, property and sea environment. The provisions were revised in 1998. The regulations comprise of monitoring vessels, organizing and controlling the transit vessel traffic and deciding upon the closure of the Strait traffic under adverse external conditions [9].

The Turkish Straits Vessel Traffic Service (TSVTS) is constituted for Turkish Straits in 2004 (which is under the General Directorate of Coastal Safety of the Ministry of Transport). The Vessel Traffic system (VTS) is established in order to provide service about necessary maritime traffic and meteorological information, technical and navigational guidance for vessels transiting the Strait and organization of vessel traffic before allowing the vessels to the Straits. The VTS also helps vessel operators in case of emergent risky situations. The main technical components of the VTS are radars, cameras, Doppler current

sensors, salinity and temperature profiles, automatic weather stations, record and replay units and Automatic Identification System (AIS) base stations. The VTS serves fully in accordance with national laws and special regulations which will be referred as “the Rules and Regulations: R&R” in this thesis.

Another important service provided by the VTS to vessels transiting the Strait is the provision of “pilot captains”, who are captains with extensive experience on the Strait navigation. Vessel captains unfamiliar to the Strait characteristics, large tankers and hazardous cargo carrying vessels may ask for and get assistance from these pilot captains. There are two pilot stations, the one for supporting southbound vessels, located at the northern entrance of the Strait, is called “the Rumeli Kavak station” and the one for northbound vessels, which is located at the southern entrance of the Strait, is called “the İstanbul station”. There are more than 60 pilots serving in the Strait.

Another service that the VTS renders is tugboat assistance to large/long vessels for their safe navigation in the Strait. VTS tugboats tow or push vessels in case of emergency, while maneuvering, clearing the anchorage or berth and at state of emergency. Vessels, based on their length and gross tonnage, may be obliged to take one or more tugboats during their transit in the Strait.

1.2. The Accidents in the Strait

The accidents in the Strait (and in most marine literature) might be generally categorized as collision, grounding, stranding, sinking and fire.

Collision or contact is the physical impact between two moving vessels, whereas grounding is the impacting of a ship to the seabed. Stranding is the running aground on the shore (included into grounding in this study). Sinking and fire generally occurs as a result of the above listed accident types.

Figure 1.3 depicts the locations of the geographical positions of the past accidents (collisions) documented in the Strait [10]. These locations are:

- Eminönü-Karaköy-Kadıköy
- Akıntıburnu
- İstinye
- Büyükdere
- Rumelikavağı
- Alburnu

The densest location is the Istanbul location which consists of Kadıköy, Sirkeci and Üsküdar. The least dense location is the Black Sea entrance.

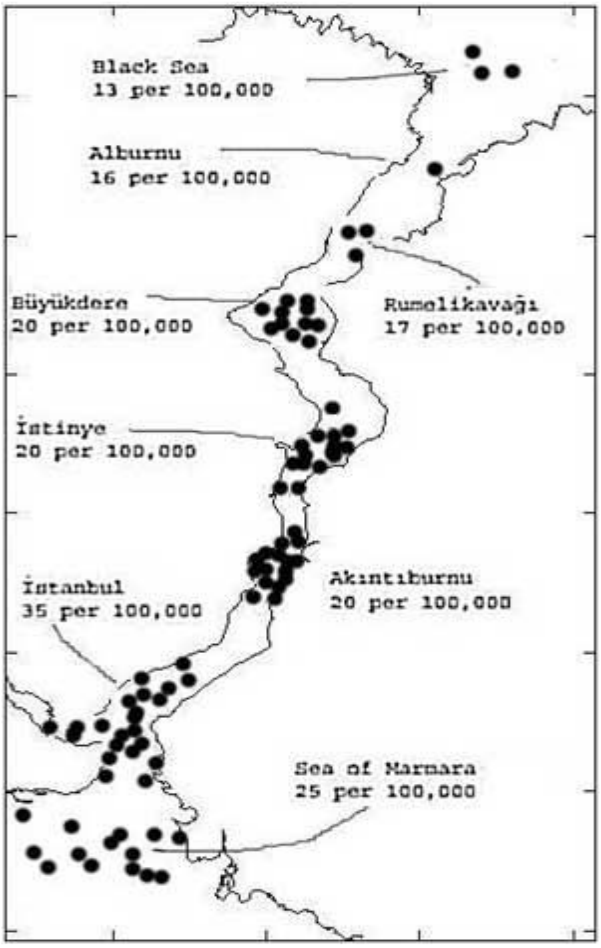

Figure 1.3. Accidents in the Strait [10].

There have been substantial numbers of accidents in the Strait, some of which with very unfortunate consequences [11].

On 14 December 1960, Greece flagged tanker M/T World Harmony collided with Yugoslavian flagged M/T Peter Zoranic. Including masters, 20 crew members died and thousands of oil spilled onto the Strait.

On 15 September 1964, Norwegian flagged Norborn hit the Peter Zoranic at Kanlica, caused a fire and oil spillage.

On 1 March 1966, Soviet flagged M/T Lutsk and Soviet flagged M/T Cransky Oktlabr collided at Kızkulesi point. Tons of oil spilled and two vessels burned due to the fire resulting from the collision.

On 3 July 1966, a Turkish passenger ferryboat collided with the Turkish coaster Aksaray causing 13 people to die.

On 18 November 1966, Bereket, a Turkish passenger ferry collided with the Romanian flagged Ploesti and 8 people passed away by drowning.

On 1 July 1970, Italian flagged Ancona grounded, causing a building under construction to collapse 5 people perished.

On 27 December 1972, the Turkish flagged passenger boat Turan Emeksiz collided with the Turkish flagged Cargo Vessel M/V Sönmezler and 5 people died.

On 21 April 1979, the Romanian flagged M/V Karpat collided with the Turkish flagged M/V Kefeli; 11 people passed away.

On 15 November 1979, the Romanian flagged, oil carrying M/T Independenta collided with the Greek flagged cargo vessel M/V Evriyali. Almost 94,600 tons of oil from Independeta spilled to the Sea of Marmara, 43 people died and the resulting fire lasted for weeks.

On 2 April 1980, the Greek flagged M/V Elsa collided with the Soviet flagged M/V Moskovosky, killing 2 people.

On 9 November 1980, the British flagged Nordic Faith collided with the Greek flagged Stravanda. The collision caused a fire.

On 29 October 1988, the Maltase flagged M/T Blue Star hit the Turkish flagged tanker M/T Gaziantep, while it was at the anchorage area. A thousand tone of chemical spilled in the sea.

On 25 March 1990, the Chinese flagged M/V Da Tung Shang collided with the Iraqi flagged tanker M/T Jampur. 2,600 tons of oil spillage caused a long lasting pollution.

On 14 November 1991, the Lebanese flagged livestock carrier M/V Rabunion XVIII collided with the Philippines flagged M/V Madonna, causing 5 people to die and 21,000 sheep to perish.

On 29 December 1999, the Russian flagged tanker Volganeft drifted stranded in the Strait. More than 1,000 tons of oil spilled in the Sea.

On 7 October 2002, the Maltase flagged Gotia rammed to the Emirgan Pier and 18 tons of fuel oil were released in the Strait.

On 10 November 2003, Georgian flagged dry cargo vessel Svyatoy Panteleymon grounded and broke into two. Around 500 tons of oil spilled in the Strait.

This study aims to assess the maritime risk in the Strait regarding vessel accident (collision and grounding) probabilities. We aim to categorize and analyze the factors leading to maritime accident in the Strait, based on accident modeling in narrow waterways. In order to assess the risk, first a simulation model is built which mimics the actual Istanbul Strait transit vessel flow. In this framework, interarrival times of each vessel class in both northbound and southbound directions, between years 2008 and 2014, are fitted into most appropriate probability distributions. Then a scheduling algorithm is designed to determine the most appropriate type of vessel (among the waiting vessels) to enter the Strait in the active direction, according to some randomness in interentrance times, while taking the R&R

into account. The algorithm also assigns the consecutive vessel type and its entrance time, until the end of the daytime and nighttime traffic for both traffic directions for seven years.

While deciding the entering type of vessel and its entrance time, the simulation model records the season, time of the day, traffic direction, the location (the sector) of the entering vessel and the pilot service usage in order to provide input for the accident probability estimation.

Vessel accident is intersection of two events; the event that the ship being on an accident (collision and grounding) course and the event that the ship does not make evasive maneuvers. In this study probability of accident P(A) is the multiplication of probability of the intersection of these two events. The probabaility of the event that the ship does not make evasive maneuvers is assumed to be independent of probability of the event that the ship being on an accident probability (marginally independent) In this study, P(A) is calculated for each vessel at each sector entrance while transiting through the Strait. In order to compute the accident probabilities, two separate models regarding these two events are formulated. One is the geometric probability model and the other one is the causation probability model. Geometric probability basically refers to the likelihood that a vessel on a blind navigation is on the accident route. On the other hand, the causation probability basically refers to the probability that the vessel does not make evasive maneuvers.

The developed accident probability models are integrated into the simulation model, so that at each sector in the Strait, the probability of accident, P(A) for each vessel type in each direction is found, based on the vessel characteristics and the environmental conditions at the time of transit (provided by the simulation model records).

After computing accident probabilities, P(A) which is the multiplication of geometric and causation probabilities, expected number of accidents per year and the expected number of accidents per 100,000 vessels are computed. To compute the number of accidents per year, P(A) is multiplied by the indicator function (which is equal to 1 if the vessel experiences an accident at the considered sector and 0 if the accident does not occur) and summed over all vessels entering the Strait and number of sectors (13) To compute the expected number of accidents per 100,000 vessels, expected number of accidents are divided

by the total number of transits at that year (the accident frequency is estimated) and then multiplied by 100,000.

In order to better observe the effect of transit traffic density on number of groundings, three years representing average, high and low transit traffic are selected and the expected number of groundings for these years are compared with the actual number of groundings occurred in the corresponding transit traffic density periods. Figure 1.4 explains this process in general terms.

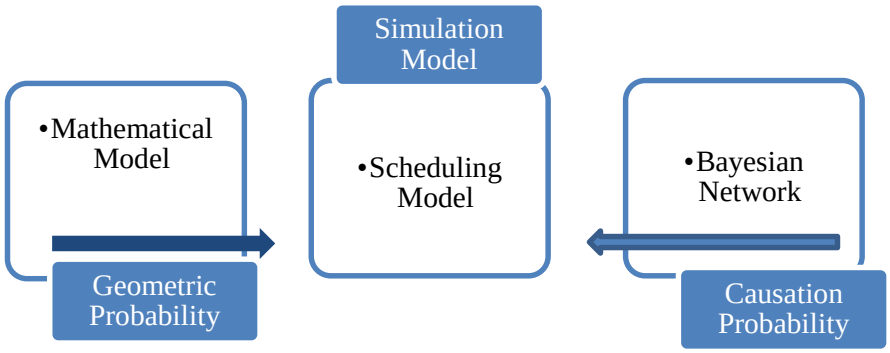

Figure 1.4. The main process of the study.

2. LITERATURE SURVEY

In this chapter several scientific studies related to contents and objectives of this study are summarized. This review covers basically the simulation models regarding maritime transportation analysis and the Bayesian Networks used for assessing the probability of global and local maritime accidents to make a risk analysis, respectively.

Petersen and Taylor [12] consider the problem of real time scheduling of vessels through the Welland Canal. The problem is formulated as a combination of a linear programming model and a heuristic, which is solved using a dynamic programming approach. The vessel scheduling obtained by the model is then calibrated through a greedy algorithm.

Golkar *et al*. [13] present the Panama Canal Simulation Model (PCSM) built by SABRE to assess the pilot working conditions and elaborates on different capacity issues. The model also includes various operational and environmental conditions such as vessel transit, locks operation, culvert assignment, tugboats operations and tide and fog conditions.

Or and Kahraman [14] utilize Bayesian inference to estimate the maritime accident probabilities in the Strait that are conditioned on several accident-contributing factors. The resulting probabilities are integrated into a simulation model which takes the vessel entrance rules into consideration and investigate the impact of transit and local vessel arrivals and environmental conditions on the number of vessel accidents in the Strait.

Franzese *et al*. [15] develop a simulation model with software Arena in order to mirror the operations in the Panama Canal, which is one of the most famous manmade waterways (having enormous locks systems) in the world. The study involves vessel arrival mix, Panama Canal traffic rules and vessel pre-sequencing (the daily routine of the Canal Scheduler) as inputs and evaluates and predicts the vessel and locks capacities for the Panama Canal up to year 2025.

Ulusçu *et al*. [16] focus on scheduling the transit vessel traffic in the Istanbul Strait by a mathematical model, which first decides how many large size hazardous vessels are planned to enter the Strait and then sequences them according to the daytime and nighttime plans. The other vessels are ordered in between those vessels and the vessels waiting in their queues are allowed to the Strait in the predetermined order as long as all meteorological conditions are satisfied.

Almaz *et al*. [17] develop a model to study the effect of meteorological conditions on vessel flows in the Istanbul Strait in detail. Year 2005 is used for arrival patterns of vessels; fog durations are assumed to be phase-type distributed, while current values are generated through an autoregressive model. The study also involves scenario analysis to reveal the effects of the vessel arrival process, resource (pilot and tugboat) usages, regulations and meteorological changes.

Cortes *et al*. [18] developed a simulation model for the operations in the Port of Seville such as freight transport throughout the estuary, vessel arrival, dock assignment, vessel departure, lorry arrival and container terminal. Vessel time in the system, vessel time in the dock and warehouse usages are the outputs of the model that provide important information about the logistic law at the Port of Seville.

Ozlem [19] developed a simulation model that represents the actual transit vessel traffic in the Strait of Istanbul for daytime and nighttime in year 2009. The study considers interarrival distributions for various vessel classes, which are categorized according to their length and cargo types. The model sequences ready to enter vessels based on minimum pursuit distance rules and regulations, pilot and tugboats availabilities and meteorological conditions and the active traffic direction. Moreover, the effects of some principal parameters, such as arrival rates, number of available pilots and minimum pursuit distances, on performance measures are investigated.

Candanoglu [20] developed an optimization model that minimizes the vessel waiting times, while scheduling the arrived vessels ready to enter the Istanbul Strait. The study also conducts scenario analysis. The effects of parameters such as minimum pursuit distances,

number of available pilots and arrival distribution of vessels on performance measures (total and average waiting times and number of vessels entering the Strait) are investigated.

Amrozowicz *et al*. [21] and Amrozowicz [22] focus on utilizing fault trees and event trees and incorporate the Human Error Rate Prediction data to quantify individual errors. The factors are identified in order to trigger the most effective and efficient use of resources to reduce the probability of grounding. The results show that the Electronic Chart Display and Information System with the International Safety Management Code might reduce the probability of grounding.

Merrick *et al*. [23] and Merrick *et al*. [24] present a detailed risk analysis of the oil transportation system in the Prince William Sound (PWS). As the methodology, they use system simulation, statistical data analysis on specific vessel arrivals, environmental conditions and accident data, and expert judgment for extension of data. The simulation model is designed to capture the dynamic environment of changing risk factors, such as traffic interactions, visibility or wind conditions. Moreover, an expert judgment elicitation method is proposed to integrate and combine the effects of multiple factors on the probability of an event.

Sotiralis *et al*. [25] aim to depict the importance of human factors in the evolution of the contemporary maritime world. This study describes and analyzes an original human-related questionnaire, which shows the current practice of human factors, through the implementation of the International Safety Management Code (ISMC). The questionnaire comprises of interviews to measure the effectiveness of ISMC implementation with regard to maritime accidents.

Itoh *et al*. [26] build a ship navigator's cognitive model based on cognitive task analysis of experimental navigation sessions using a maritime simulator. The model evaluates simple course-tracking tasks and reveals the dynamic interaction between the navigator's cognitive processes and the states during maneuvering. A navigator-error generating process is also integrated to the model. After examining the descriptive and predictive abilities of ship motion and navigator's behavior by means of the model, scenario analysis is performed in order to identify critical risks at sea.

Chauvin [27] describes the concepts and models developed in psychology, which help explain the significance of human factors in maritime casualties. He presents two concepts, active failures and latent failures and explains the Swiss Cheese Model. Moreover, this study examines the role of human factors in maritime casualties at three different levels: i) the level of cognitive factors, ii) the level of interpersonal factors and iii) the level of organizational factors.

In addition to scheduling of daytime and nighttime transit vessel traffic, Ulusçu *et al*. [28], also conduct maritime risk analysis in the Istanbul Strait. They investigate risk factors and build a mathematical risk model consisting of probabilistic arguments conditioned on instigators, situations, accidents, consequences, subject to historical data and expert opinions where data is incomplete. Scenario analysis is carried out to study the behavior of the accident risks, with respect to changes in the surrounding geographical, meteorological, and traffic conditions.

Otay and Özkan [29] developed a physics based model that mimics the random transit maritime traffic in the Istanbul Strait. They compute the probability distributions of the routes of vessels navigating through both sides of the Strait. The results indicate that the effect of pilotage on accident risk depends on vessel size and position in the waterway. They also present risk maps, which show the expected number of accidents in different sections of the Strait.

Otay and Tan [30] and Tan and Otay [31] design a casualty model for narrow waterways (like Bosporus) which combine the hydrodynamic model, drift probability model and the vessel traffic model in order to estimate the number of casualties due to tanker traffic. The hydrodynamic model measures the velocity of surface current while the drift probability model takes that velocity and vessel characteristics as inputs and estimates the drift probabilities. Vessel traffic model on the other hand incorporating arrival distributions and drifting probabilities with a Markov Chain model approach. Ultimately, intervessel collision and grounding probabilities for the considered area are estimated.

Merrick *et al*. [32] utilizes simulation methodology for oil transportation with tankers in The Prince William Sound (PWS). The study has two assumptions: risk is a dynamic

property of a system, and the judgment of experts who have a deep understanding of the system can be used to compensate for insufficient data. The objective of the study is to assess the current risk in the oil transportation system and to evaluate the efficiency of potential risk reduction measures. The simulation outcomes reveal that actions that diminish risk in one part of the system often increase risk in other parts. However, the identified interventions might increase the level of safety of oil transportation in the PWS.

Harrald *et al*. [33] investigates the impact of human error in the PWS. Due to insufficient data, the developed dynamic simulation model is based on some assumptions. Some of these assumptions are, i) that 80-20 rule applies, ii) that historical data may reveal human error causes, iii) that risk analysis based on human error data from other areas also apply to maritime accidents analysis. A detailed description of the current system is analyzed and afterwards the current system risk is defined and risk reduction measures are developed and evaluated.

Wheeler [34] studies the effectiveness of the safety of ocean-going vessels in U.S. The effectiveness of safety regulations is determined using risk-based metrics that link categories of root causes of accidents to particular inspection activities designed to reduce the risk of each root cause category. These metrics help to focus inspection resources.

Merrick and van Dorp [35] use an original Bayesian simulation model, which considers the probability distributions to determine the model parameters regarding the occurrence of risky situations. In order to find the conjugate prior probabilities, a Bayesian multivariate regression regarding the relationship between factors that cause these situations is used.

Li *et al*. [36] integrate logistic regression and Bayesian networks for estimating maritime risk. The study overcomes the problem of prior probability which is essential for Bayesian networks, by means of logistic regression. Expert opinion is used to build prior probabilities. Various types of vessels in different situations are analyzed to make a risk assessment.

Goerlandt and Montewka [37] analyze the oil spill in a ship to ship collision case. The study uses a Bayesian network to integrate the extent of damage in tank types with the oil outflow. The tank configuration data set is gathered through 219 product tanker designs navigating in the Baltic Sea. The tank arrangement is modelled in deference to tank volumes and location of bulkheads. In addition, various damage scenario analyzes are linked to the study to assess the uncertainty under very limited data.

In an another study, Goerlandt and Montewka [38] elaborate on the structure and content of risk analysis methods by first constructing a definition for risk and risk perspective (the way to define risk). Risk definitions (all based on uncertainty) are classified first. Second, the risk perspective is considered in aspects of measurement tools, scope of the analysis and the measurements for uncertainty and bias. Third, risk analysis approaches are classified and lastly applications for maritime transportation risk analysis are discussed.

Trucco *et al*. [39] analyze the effect of human and organizational factors at the design stage of High Speed Craft to quantify the risk at maritime transportation. A Fault Tree is developed and the dependencies among the basic events are provided by a Bayesian Belief Network, which updates the prior probabilities of basic events. The study aims to create an opportunity to mitigate risk at organizational and regulatory levels.

Akyuz and Celik [40] utilize the human factor analysis and classification system, which is derived from the Swiss cheese model for estimating human error causation factors in maritime accidents. The study integrates this analysis with cognitive mapping technique, which reveals the causal relationships between factors under consideration. Moreover, this hybrid method may be applied not only in marine accidents but also in ports, shipyards, terminals and even in the ship recycling industry.

Eliopoulou and Papanikolaou [41] discuss maritime accidents, vessel losses, fatalities and safety levels in detail by statistical analysis applied to their thirteen-year data. The results reveal that despite the obvious increase in vessel accident frequencies, the safety level remains the same and which is explained by underreporting. The study also investigates the relationship between ship age and accident rates. The results show that contrary to expectations, sometimes younger ships cause more maritime accidents.

Kum and Sahin [42] use Current Reality Tree as a tool for Root Cause Analysis, which investigates the factors of faults and failures resulting in collision and grounding incidents at the Arctic Region. In order to minimize the occurrence of accidents, minimal cut sets of top events for vessel accidents are identified. The results put emphasize on the importance of safety assessment in the Arctic region and highlight the effect of personnel training on ship safety.

Montewka *et al*. [43] provide an insight into maritime risk assessment with a proactive approach rather than the reactive approaches which are generally based on historical data. The study focuses on ship (RoPax) to ship collisions. A Bayesian Belief Network is designed for background knowledge about the events related to the vessel collisions. Morever, sensitivity analysis and value-of-information increase the credibility of the Bayesian Network results.

Macduff [44] makes use of the Buffon's needle problem in order to find the geometric probability of stranding and he also considers the causation factors for the generalized stranding probability. The study assumes random navigation, therefore random standing. Some causation factors included in the study are meteorological conditions such as fog and snow, technical factors like engine and steering failure and human-driven causes such as panic, ignorance and lack of attention.

Fujii [45] aggregates the concepts of grounding and stranding in his study. The objective is estimating the number of groundings in a specified waterway. The inputs of the equations used to estimate the number of grounding are, speed of the vessel, waterway traffic density, linear cross-section of the obstacle (place where the vessel hits) which is shallower than the vessel draught and vessel width. The number of groundings is assumed to fit a Poisson distribution.

Kite-Powell *et al*. [46] build a Bayesian model in order to estimate the grounding risk in 5 selected U.S. ports. Instead of showing causal relationships among factors in the model, the study intends to show associations among variables that lead to grounding risk. The factors considered are vessel type and size, wind speed, visibility, operator skill (flag

information is used when available data does not exist) and uncertainty in nautical chart surveys.

Fowler and Sørgård [47] split up the concept grounding into powered grounding and drift grounding. In powered grounding, clear visibility and reduced visibility turn up to be the are leading factors whereas in drift grounding; frequency of propulsion breakdown, drift track, wind speed, self-repairing and tow assistance frequencies become crucial. The study uses Fault Tree Analysis for calculating grounding probabilities.

Kristiansen [48] estimates the probability of grounding, collision, stranding or allusion for vessels navigating in the Japanese seaway, US fairways and ports and the Dover Strait. The study is the first one in the literature that distinguishes the terms grounding and stranding. The proposed accident model is the combination of Macduff [44] and Fujii [45] approaches which first presents a general framework for all accident types; afterwards provides a specific accident probability formula. Visibility and traffic separation scheme are two studied factors that are claimed to be dominant factors in considered maritime accident types.

Pedersen [49] studies ship to ship collisions, ship to platform collisions and ship groundings by building statistical models. Causation factor is computed by deploying a Fault tree method. Consequence (damage) investigation is also conducted through outer and inner dynamics and residual strength analysis.

Soares and Teixeira [50] re-examine several approaches to assess risk in maritime transportation starting with foundering and capsizing. Risk of structural failure is assessed through a failure equation borrowed from reliability analysis. Moreover, Formal Safety Analysis (FSA) methodology and some benefits such as decreasing lives lost or pollution are introduced.

Otto [51] observes a RoRo passenger ferry and determines the risk of collision and grounding based on statistical models. Collision probability is calculated through historical data for a specified route, whereas grounding probability is estimated for an artificial obstacle. Consequence analysis is also conducted where damage length and damage depth

are found. Costs due to capsizing and repairing are computed and compared for both collision and grounding.

Gucma and Goryczko [52] presents a method for calculating the risk of grounding for the entire waterway (instead of estimating risk only at critical points) by building real time simulation models. Normal distribution is assumed for the ship passage distribution and the estimated parameters of that distribution are used for calculating navigation reliability (including human factors). Technical reliability, on the other hand, is assumed to be independent of navigation reliability, so that navigational and technical reliability can be multiplied. Risk is estimated based on two factors; maximum energy of the vessel when the grounding occurs and permissible energy of a safe contact between the vessel and the bottom.

Hänninen [53] brings up the Bayesian network application issue in maritime accidents by presenting studies utilizing Bayesian networks in recent years. The study presents advantages and disadvantages of using Bayesian networks in maritime accidents. Some benefits emphasized are suitability of Bayesian networks for complex system modeling, managing uncertainty successfully, versatility, being able to add any kind of relevant factor to the model, dynamic modeling and usability in maritime safety decision making. On the other hand, the challenges of using Bayesian networks in maritime world are controversial definitions of accident and safety, insufficient data, data quality and expert judgement issues and validation data.

3. MODELING OF VESSEL TRAFFIC IN THE STRAIT OF ISTANBUL

3.1. Characteristics of Vessels Transiting the Strait

Vessels traveling in the Strait might be categorized according to their lengths, flags and cargo types as displayed in Figure 3.1.

<table>
<tr><td></td><td colspan="2">Tankers&Hazardous Material Carrying Vessels</td><td colspan="2">Other Cargo Vessels</td><td>Passenger Vessels</td></tr>
<tr><td>Length (m.)</td><td>Turkish Flagged Vessels</td><td>Other Flagged Vessels</td><td>Turkish Flagged Vessels</td><td>Other Flagged Vessels</td><td>Turkish & Other Flagged Vessels</td></tr>
<tr><td>75></td><td>F</td><td rowspan="2"></td><td>F</td><td rowspan="2"></td><td rowspan="5">P</td></tr>
<tr><td>75 - 100</td><td colspan="2">D</td></tr>
<tr><td>100 - 150</td><td colspan="2">C</td><td rowspan="3">C</td></tr>
<tr><td>150 - 200</td><td colspan="2">B</td></tr>
<tr><td>200 - 250</td><td colspan="2" rowspan="2">A</td></tr>
<tr><td>250 - 300</td><td colspan="2">E</td></tr>
<tr><td>> 300</td><td colspan="5">T6</td></tr>
</table>

Figure 3.1. Vessel classification [20].

Passenger vessels (Class P) have the highest transit priority among all classes and they are allowed to enter the Strait in both directions, while the R&R has allowed only uni-directional transit for all other types of vessel since 2005.

T6 vessels are the rarest class transiting through the Strait (at most 5 times in a year), therefore they are embedded in class A vessel (they have the similar entrance rules) in this study.

Class A vessels are the most important regarding perceived risk and accordingly they make up the backbone of the Strait vessel scheduling system. They carry hazardous materials, hence in order to diminish the risk, they may enter the Strait only during day time and with wide time/distance separation between two consecutive such vessels.

Class E vessels are the largest vessels carrying nonhazardous material.

Class B vessels also carry hazardous materials, but since they are shorter than Class A vessels, they are allowed to make nighttime transits. In other words, if there exists no class A vessel during day time, class B vessels may enter the Strait, otherwise they may pass the Strait at night time.

Class C vessels carry both hazardous and nonhazardous cargo varying by their lengths.

Class D vessels are the most numerous (59 % of all entrances) and have the least passage priority with class F vessels which are small Turkish flagged vessels.

This study gives consideration to all transit vessel traffic data compiled by the VTS system in the 2008 to 2014 period. Taking an overall look for these years, class C vessels show an increasing trend, whereas the number of class A and D vessels have decreased dramatically (Table 3.1).

Table 3.1. Number of vessel classes entered the Strait.

	Number of Vessels Entered the Strait in Each Year						
Vessel Class	2008	2009	2010	2011	2012	2013	2014
A	2070	2014	2058	1866	1805	1844	1819
B	2567	2739	2746	2667	2507	2627	2784
C	8709	9246	8392	9544	10674	10648	11326
D	33974	31792	31852	30169	27798	25844	23077
E	713	445	581	653	690	688	736
F	4613	3773	4118	3988	3808	3847	3662
P	1751	1323	1125	911	1047	1034	1262

3.2. Rules and Regulations for vessels transiting the Strait

Each vessel planning to enter the Strait has to submit an SP-1 report to the VTS at least 24 hours before her arrival. This report includes vessel characteristics, arrival time information and pilot and/tugboat requests. Every vessel approaching to the Strait also submits an SP-2 report, which supplies all the relevant information about the vessel, at least two hours or 20 nautical miles before her arrival.

Vessels providing their SP-2 reports and arriving at the Strait have to comply with the R&R. Every day and night, VTS planning officers schedule the vessel traffic based on the R&R. They then sequence the expected Strait entrance time vessels based on some priority rules and minimum pursuit distances between all consecutive vessels of same and different types.

Some of the critical R&R regarding vessels entering and sailing through the Strait (in either direction) are as follows:

- There should be a separation of at least 0.920 miles between two consecutive vessels entering the Strait from the same direction.
- Tankers and dangerous cargo carrying vessel longer than 200 meters should enter the Strait only during daytime.
- Tankers and vessels longer than 250 meters and carrying dangerous cargo or LNG-LPG should not come up against any type of vessel except passenger vessels, during their passage through the Istanbul Strait.
- Overtaking is discouraged unless vessel and environmental conditions are very favorable. Nevertheless, at the narrowest region between (Kanlıca and Vaniköy) overtaking is prohibited under any circumstance.
- Dangerous cargo carrying vessels longer than 200 meters, should not come across with dry cargo carrying vessels longer than 150 meters and vice versa.
- LNG-LPG or dangerous cargo carrying vessels should not come across with any other dangerous cargo or LNG-LPG carrying vessels regardless of their lengths.
- While transiting in the Strait, vessel speed should not exceed 10 nautical miles (except under extreme conditions).

However, these R&R are not rigidly applied at all times. Actual transits feature some deviations primarily triggered by meteorological conditions and vessel density, implemented through expert judgments. Therefore, in this study, instead of regarding vessel arrivals and entrances constant and fixed, the realized time intervals for all consecutive vessel pairs that enter the Strait are acquired from the actual VTS data and scheduling policy is assumed to be based on this data. Table 3.2. presents the successive vessel interentrance distributions

in northbound for 2011, while interentrance time distributions for successive vessels for the other years (2008 to 2014) period are displayed in the Appendix A.

Table 3.2. Successive northbound vessel entrance distributions based on 2011.

Direction	Vessel Pair	Fitted Distribution	Parameters
NB	AA	Wakeby	α=92.56 β=4.6333 γ=4.2284 δ=0.53332 ξ=64.754
NB	AC	Pearson 5 (3P)	α=2.8854 β=124.96 γ=-11.587
NB	AD	Log-Logistic	α=2.5154 β=8.9598
NB	AE	Burr	κ=0.58305 α=3.1117 β=31.804
NB	AF	Wakeby	α=41.972 β=4.1855 γ=32.151 δ=0.15969 ξ=-0.34706
NB	BB	Burr	k=0.34177 α=2.8025 β=20.475
NB	BC	Burr	k=1.2143 α=1.9479 β=25.491
NB	BD	Gen. Extreme Value	k=0.17178 σ=4.4099 μ=6.5525
NB	BE	Johnson SB	γ=1.5074 δ=0.78171 λ=313.48 ξ=7.003
NB	BF	Wakeby	α=0 β=0 γ=24.789 δ=0.10773 ξ=0.71018
NB	CA	Log-Logistic (3P)	α=2.308 β=46.33 γ=–0.04844
NB	CB	Log-Logistic	α=2.0819 β=25.623
NB	CC	Gen. Pareto	k=-0.09988 σ=83.827 μ=2.2786
NB	CD	Pearson 6	α_1=2.7171 α_2=7.581 β=26.781
NB	CE	Wakeby	α=91.263 β=0.16062 γ=0 δ=0 ξ=5.8981
NB	CF	Pareto 2	α=65.041 β=2876.1
NB	DA	Pearson 6 (4P)	α_1=4.9469 α_2=8.6738 β=28.16 γ=-1.7363
NB	DB	Burr	k=2.2047 α=2.0274 β=16.978
NB	DC	Gen. Extreme Value	k=0.1905 σ=5.8454 μ=8.2147
NB	DD	Gen. Gamma	k=0.59557 α=4.5977 β=0.98792
NB	DE	Gen. Extreme Value	k=0.17271 σ=6.6734 μ=9.7509
NB	DF	Wakeby	α=7.6211 β=3.0523 γ=7.3796 δ=0.09596 ξ=0.55522
NB	EA	Gen. Pareto	k=-0.14249 σ=41.779 μ=15.367
NB	EB	Wakeby	α=268.76 β=25.576 γ=35.649 δ=0.10288 ξ=-0.52703
NB	EC	Johnson SB	γ=1.1108 δ=0.56184 λ=317.93 ξ=6.4202
NB	ED	Pearson 6	α_1=3.2429 α_2=4.0948 β=11.629
NB	EE	Lognormal (3P)	σ=1.03 μ=4.0186 γ=5.581
NB	EF	Wakeby	α=3.6615 β=2.6522 γ=70.265 δ=-0.03919 ξ=-0.89743
NB	FA	Gen. Logistic	k=0.30061 σ=20.906 μ=47.297
NB	FB	Wakeby	α=21.686 β=4.3167 γ=24.849 δ=0.18439 ξ=1.2782
NB	FC	Wakeby	α=132.61 β=72.359 γ=46.072 δ=0.03898 ξ=0
NB	FD	Gen. Gamma	k=0.51455 α=5.3475 β=0.39439
NB	FE	Wakeby	α=-126.56 β=2.0124 γ=178.78 δ=-0.49374 ξ=2.8283
NB	FF	Dagum	k=0.37606 α=2.9179 β=99.845

3.3. The Simulation Model

3.3.1. The Arrival Process for the Simulation Model

Initial observations on the actual total arrival data of around 300,000 vessels between the 2008 and 2014 period considered in this study have indicated that all vessel types arriving at the Strait from either direction (North or South) have quite dissimilar interarrival patterns.

The simulation model starts with estimating the arrival distribution of each vessel classes in either direction and building a vessel arrival model for transit ship traffic in the Strait. Vessels entering the Strait from the south and traveling to the north are called northbound vessels (NB) and vessels entering the Strait from the north and traveling to the south are called southbound vessels (SB). In this study time of submitting SP-2 reports to the VTS is the input data used for determining interarrival distributions of vessel classes. Table 3.3 displays the fitted interarrival time distributions for each vessel class in either direction for 2008 and interarrival time distributions for the years 2009 to 2014 are displayed in Appendix A.

In this simulation model, Kolmogorov-Sminov (K-S) tests are deployed to measure whether the inerarrival data of vessel classes obtained for each year (from 2008 to 2014) follow a specified distribution or not. According to the K-S results, p-values of interarrival distributions for most vessel classes are higher than 0.05, which may be interpreted as “not rejecting the hypothesis that the specified interarrival distribution for the specified vessel class is an acceptable fitting distribution”. The statistical software EasyFit is used to find the best fitting interarrival time probability distributions, based on vessel classifications and directions.

In order to test the goodness of fitting of the specified distributions which are generated through EasyFit, instead of fitting whole year interarrival time data to the specified distributions for each vessel classes, 50% of the one year interarrival time data is chosen as training data set and the remaining part is chosen as the test data set. Afterwards, best fitted distributions of training data set for each vessel class is found and the random numbers generated from the fitted distributions are compared to the test data set using two sample

Kolmogorov-Smirnov test. The results show that except the specified distributions of NB_A, NB_C and SB_C vessels, all specified distributions are good fitting distributions at α=0.0001 (Table 3.4).

Table 3.3. Interarrival time distributions of vessel classes.

Vessel Type	Interarrival Distribution	Parameters	p-value
NB_A	Phased Bi-Weibull	α_1=0.97895 β_1=202.47 γ_1=1 α_2=0.38519 β_2=296.74 γ_2=158	<0.05
SB_A	Weibull (3P)	α=1.0696 β=568.64 γ=0.87475	0.925
NB_B	Log-Pearson 3	α=14.425 β=-0.40032 γ=10.89	<0.05
SB_B	Wakeby	α=98.724 β=8.1185 γ=393.73 δ=-0.01825 ξ=-5.0863	0.981
NB_C	Wakeby	α=-33.96 β=23.224 γ=105.33 δ=0.05185 ξ=0	0.617
SB_C	Gamma	α=0.93436 β=118.58	0.343
NB_D	Weibull	α=0.95676 β=34.732	<0.05
SB_D	Gen. Gamma	k=1.0442 α=0.86336 β=41.86	<0.05
NB_E	Gen. Pareto	k=-0.1623 σ=1871.7 μ=-6.6986	0.989
SB_E	Gen. Pareto	k=-0.05829 σ=1686.1 μ=5.0244	0.997
NB_F	Wakeby	α=-171.83 β=6.7453 γ=257.94 δ=0.0957 ξ=0	0.936
SB_F	Gamma	α=0.72738 β=363.0	0.550
NB_P	Gen. Pareto	k=0.12529 σ=1035.2 μ=-17.025	0.872
SB_P	Dagum	k=0.25082 α=2.6701 β=2020.6	0.927

3.3.2. The Scheduling Algorithm to Determine the Vessel Entrances

Vessels arriving at the Strait from either direction have to wait until they are allowed to enter. Every morning, the VTS planning specialists determine the starting traffic direction as “the active direction” and sequence all vessels throughout that day’s daytime and nighttime time windows.

Table 3.4. Comparison of training data set with the test data set for 2011.

Vessel Type	Interarrival Distribution	Parameters	p-value
NB_A	Log-Pearson 3	α=109.07 β=-0.15742 γ=22.43	<0.0001
SB_A	Wakeby	α=−348.32 β=0.99727 γ=869.29 δ=-0.20496 ξ=2.8277	0.220
NB_B	Log-Pearson 3	α=9.1774 β=-0.50984 γ=9.7633	0.098
SB_B	Wakeby	α=191.8 β=6.9601 γ=371.18 δ=−0.03011 ξ=−7.1503	0.454
NB_C	Burr	κ=70.498 α=0.95536β=10043.0	<0.0001
SB_C	Wakeby	α=9.1364 β=2.1676 γ=115.33 δ=0.04442 ξ=−0.75677	<0.0001
NB_D	Gen. Gamma	κ=1.0325 α=0.86702 β=41.192	0.040
SB_D	Kumaraswamy	a1=0.93957 a2=10553.0 b=6.6598E+5	0.01
NB_E	Gen. Pareto	k=-0.20911 s=2085.1 m=-38.446	0.145
SB_E	Wakeby	α=4298.5 β=17.253 γ=1680.0 δ=-0.07395 ξ=-124.31	0.003
NB_F	Wakeby	α=−143.93 β=3.6206 γ=251.42 δ=0.08498 ξ=−0.40694	0.0001
SB_F	Dagum	α=0.72738 β=363.0	0.002
NB_P	Pareto 2	a=3.8218 b=3817.0	0.399
SB_P	Dagum	k=0.2173 a=2.6212 b=2726.3	0.0003

The duration of the daytime traffic time window according to different seasons is displayed in Table 3.5.

Table 3.5. The daytime vessel traffic time window duration based on seasons.

Season	Start Time (t_s)	Maximum Duration (DT)
Winter	07:00	615
Spring	06:30	735
Summer	06:00	855
Autumn	06:30	735

The daily vessel scheduling accomplished by the VTS planners are expected to satisfy the R&R. On the other hand, as explained in the previous section, the R&R are not rigidly applied and some flexibility is allowed for expert judgement. In this study, the following algorithm is developed to mimic and represent the randomization in the actual scheduling of vessels originating from the "expert judgement" and "flexible" actions of the VTS planners.

The steps of the developed scheduling algorithm are displayed in Figure 3.2:

Step 1 Initialize first vessel entrance time t=0;

Set active direction d;

Set duration(d);

Set S(d)= {A, B, C, D, E, F}, class of selected vessels at direction d.

If (traffic==daytime traffic)

Set i=" A"; and set M=" B";

else

Set i=" B"; and set M=" A";

Step 2 Calculate $x_{ijd}(t) = \min_{j \in S(d) \setminus M} \{ t_{ij}, rnd_{ijd} \}$ and $j^* = \arg\min_{j \in S(d) \setminus M} \{x_{ijd}(t)\}$

Step 3 Set $t_{prev} = t$;

Step 4 $t = t_{prev} + x_{ijd}(t)$ and $i = j^*$; $i_{prev} = i$;

Step 5 Calculate $x_{ijd}(t) = \min_{j \in S(d) \setminus M} \{ t_{ij}, rnd_{ijd} \}$

Step 6 Update $x_{ijd}(t) = \min_{j \in S(d) \setminus M} \{ \max\{x_{i_{prev}jd}(t_{prev}), x_{ijd}(t)\} \}$

$j^* = \underset{j \in S(d) \setminus M}{argmin} \{ \max\{x_{i_{prev}jd}(t_{prev}), x_{ijd}(t)\} \}$;

Step 7 If t<=duration(d)

go to Step 3

else

go to Step 1.

Figure 3.2. The Scheduling Algorithm.

The explanation of the algorithm is as follows:

The proposed scheduling algorithm starts with randomly assigning the daily start time active direction (northbound or southbound). If current time is in the daytime vessel traffic time window, the algorithm searches for the class A vessel with the maximum waiting time at that direction. If current time is in the nighttime vessel traffic time window, the algorithm searches for the class B vessel with the maximum waiting time at that direction (Step 1). Next, the consecutive entering vessel and its entrance time is determined. To determine the next vessel to enter, minimum duration for each successive vessel pair candidates i.e. AA, AC, AD, AE, AF is found. Here, minimum duration is computed by picking the minimum of the random number generated by the interentrance time distribution of class i and j vessel entering the Strait successively at direction *d* (rnd_{ijd}) and the minimum pursuit time interval between vessel class i and j, determined by R&R (t_{ij},) given in Table 3.6. The vessel with such a value is assigned as the next vessel after the initial class A vessel (Step 2). previous time is taken as the current time (Step 3). Time is incremented as much as the minimum duration computed in Step 2 (Step 4). To determine the following consecutive vessels, minimum duration for maximum of minimum duration for each vessel pair is determined. For instance, if the recent vessel entering the Strait is class C, next vessel is determined by taking the minimum of maximum of minimum duration for vessel pairs, “AA and CA”, “AC and CC”, “AD and CD”, “AE and CE” and “AF and CF” (Step 5 and Step 6). The sequencing process for the active traffic direction ends when the preset time window for that direction expires (Step 7). Next, the opposite direction is designated as the active direction (Step 1). In a similar manner, the algorithm primarily searches for the class A vessel with the maximum waiting time at that direction and same steps are applied until the end of that direction’s time window (and end of daytime) (Steps 1 to 7). Nighttime traffic resumes with the latest daytime active direction, but, this time, instead of a class A vessel, the algorithm searches for class B vessels first and the same procedure is followed until the following day’s morning.

Table 3.6. Minimum pursuit time intervals indicated in R&R (in minutes).

Class	A	C	D	E	F
A	t_AA=75	t_AC=20	t_AD=10	t_AE=20	t_AF=5
C	t_CA=20	t_CC=20	t_CD=10	t_CE=20	t_CF=5
D	t_DA=10	t_DC=10	t_DD=10	t_DE=10	t_DF=5
E	t_EA=20	t_EC=20	t_ED=10	t_EE=20	t_EF=5
F	t_FA=5	t_FC=5	t_FD=5	t_FE=5	t_FF=60

3.3.3. Transit of Vessels in the Strait

The scheduling algorithm determines the vessel types in active direction and sequences the vessels based on the estimated interentrance durations. Northbound vessels enter the Strait at sector 1, proceed consecutively through sectors 2, 3, 4, 5, 6, 7, 8, 9, 10, 11, 12 and leaves the Strait from sector 13. Similarly, southbound vessels enter the Strait at sector 13, proceed consecutively through sectors 12, 11, 10, 9, 8, 7, 6, 5, 4, 3, 2 and leaves the Strait from sector 1. For each northbound (southbound) vessel, the simulation clock is initiated at sector 1 (13), then incremented at the vessel's passage to sector 2 (12), based on the average transit times displayed in Table 3.7.

Table 3.7. Average transit time at each sector.

Sector	Average Transit Time (minutes)
1	4.97
2	2.40
3	12.77
4	8.50
5	2.89
6	6.63
7	8.60
8	9.83
9	2.99
10	9.40
11	7.59
12	3.37
13	8.30

3.4. Simulation Model Results

The scheduling model is run in Matlab package through years 2008 to 2014, in one-year duration increments. Each year is replicated 20 times. The statistics tracked from the simulation model are the number of vessels transiting the Strait, average interarrival times for each vessel type in either direction, and interentrance time of vessels in either direction.

The first statistics is the interarrival times for each vessel type in northbound and southbound directions. The actual interarrival time for each vessel is obtained through VTS SP-2 reports.

Average interarrival time for all vessel types transiting the Strait in each simulation run and the actual interarrival time for all vessel types transiting the Strait for 2011 (base year for this study) are displayed in Table 3.8. The comparison for the years 2008 to 2014 are displayed in the Appendix B. The actual interarrival time for all vessel types in either direction is compared with average interarrival time for all vessel types obtained from simulation model (provided from 2011 data) by means of prediction interval. The results show that actual interarrival times for all vessel classes fall in the prediction interval of t distribution with $\alpha = 0.1$.

Table 3.8. Comparison of interarrival times from the simulation model and the actual case in 2011.

Vessel	RUN1	RUN2	RUN3	RUN4	RUN5	RUN6	RUN7	RUN8	RUN9	RUN10	RUN11	RUN12	RUN13	RUN14	RUN15	RUN16	RUN17	RUN18	RUN19	RUN20	Average	Actual Case	Std dev	PI left	PI right	all in rang
NB AA	559	576	585	569	591	536	558	541	520	596	567	554	574	594	596	592	561	576	577	567	569.4	570	20.9	485.3	653.6	TRUE
NB BB	407	414	416	395	420	433	417	427	405	427	396	397	418	390	403	433	421	412	404	415	412.5	413	12.6	361.7	463.3	TRUE
NB CC	110	109.4	111.8	109.5	109.9	109.5	109.6	111	111	108.5	110.2	110	109	108	112	110	109	108.7	110.8	110	109.8	110	1.1	105.4	114.3	TRUE
NB DD	35.5	35.44	35.41	35.11	35.44	35.59	35.65	35.56	35.9	35.61	35.45	35.5	35.5	35.2	35.1	35.7	35.4	35.08	35.04	35.48	35.4	35	0.2	34.5	36.4	TRUE
NB EE	1552	1547	1541	1551	1592	1554	1553	1532	1545	1556	1545	1528	1546	1529	1542	1539	1577	1520	1596	1544	1549.5	1550	19.5	1471.3	1627.6	TRUE
NB FF	260	260	252	265	251	265	265	277	278	269	263	268	274	270	269	259	262	253	274	259	264.7	265	7.9	232.9	296.4	TRUE
NB PP	1183	1208	1200	1159	1192	1167	1205	1234	1253	1168	1087	1197	1188	1132	1298	1142	1187	1139	1060	1182	1179.1	1179	53.2	965.3	1392.8	TRUE
SB AA	576	532	557	532	547	570	541	576	570	506	529	585	564	546	579	529	577	540	515	551	551.1	553	23.0	458.6	643.6	TRUE
SB BB	381	392	389	408	389	383	391	390	398	396	392	398	402	396	388	382	392	392	550	379	399.4	399	36.2	254.1	544.7	TRUE
SB CC	113	110	111	111	112	113	112	112	112	111	112	110	112	111	111	111	112	110	111	112	111.5	111	0.9	107.9	115.0	TRUE
SB DD	35.5	35.32	35.47	35.79	35.78	35.34	35.8	35.42	35.8	35.84	35.84	35.6	35.5	35.3	35.5	35.4	35.2	35.55	36.3	35.41	35.6	36	0.3	34.5	36.6	TRUE
SB EE	1689	1493	1502	1668	1645	1733	1573	1620	1586	1605	1672	1527	1657	1650	1588	1617	1531	1513	1578	1694	1607.1	1607	69.6	1327.4	1886.7	TRUE
SB FF	261	260	262	283	267	260	262	267	271	262	263	253	264	263	268	262	268	267	257	261	264.1	264	6.1	239.5	288.6	TRUE
SB PP	1093	1218	1082	1114	1149	1155	1233	1118	1134	1118	1245	1195	1150	1147	1168	1138	1155	1059	1163	1093	1146.4	1146	49.2	948.6	1344.1	TRUE

The second statistics is the number of vessels transiting the Strait in each year (from 2008 to 2014).

The number of vessels transiting the Strait in each simulation run and the actual number of vessels transiting the Strait for 2011 (base year for this study) are displayed in Table 3.9. The comparison for the years 2008 to 2014 are displayed in the Appendix C. The actual number of transits for each vessel type in either direction is compared with total number of transits for each vessel type in either direction obtained from simulation model (based on 2011 data) by means of prediction intervals. The results show that actual transits for all vessel classes fall in the prediction interval of t distribution with $\alpha = 0.1$.

Table 3.9. Comparison of vessel transits from the simulation model and the actual case in 2011.

Comparison of Number of transits in Northbound (NB) and Southbound (SB) Direction in 2011																									
Vessel type	Run 1	Run 2	Run 3	Run 4	Run 5	Run 6	Run 7	Run 8	Run 9	Run 10	Run 11	Run 12	Run 13	Run 14	Run 15	Run 16	Run 17	Run 18	Run 19	Run 20	Real Ca	Average	eviatio	PI left	PI righ	all in rang
NB_A	988	950	951	983	1027	1029	1057	948	977	1016	958	949	952	973	996	946	994	999	982	1008	920	920	31.93	791.8	1048	TRUE
NB_B	1213	1110	1217	1201	1186	1184	1213	1185	1256	1166	1273	1198	1194	1264	1266	1172	1216	1212	1249	1169	1332	1271	40.41	1109	1434	TRUE
NB_C	4849	4724	4826	4854	4843	4844	4784	4780	4888	4774	4820	4916	4916	4745	4795	4906	4780	4780	4805	4789	4795	4821	55.46	4598	5044	TRUE
NB_D	14872	14999	14949	14865	14798	14798	14866	15022	14789	14851	14851	14866	14866	15032	14733	15007	14985	14985	14973	14792	15130	14895	91.25	14528	15262	TRUE
NB_E	346	348	334	330	342	342	342	346	352	348	362	358	358	350	349	338	329	329	334	340	326	344	9.708	304.8	382.9	TRUE
NB_F	2123	2165	2078	2068	2088	2065	1988	1979	2058	2071	2064	2032	2026	2046	2117	2088	1968	1963	2113	2146	1998	2062	57.22	1832	2292	TRUE
NB_P	414	419	418	461	444	445	422	406	459	483	434	436	448	409	455	438	519	519	402	458	447	444	33.19	311.1	577.8	TRUE
SB_A	1014	990	975	964	996	996	933	954	1055	1018	923	931	931	1018	943	1014	1007	1009	977	955	946	980	37.15	830.9	1129	TRUE
SB_B	1328	1300	1254	1356	1327	1327	1322	1301	1279	1301	1285	1288	1288	1331	1339	1301	930	928	1373	1271	1335	1271	120.6	786.6	1756	TRUE
SB_C	4770	4736	4738	4665	4397	4398	4714	4703	4699	4710	4751	4750	4750	4730	4722	4701	4733	4733	4684	4584	4749	4683	105.5	4259	5107	TRUE
SB_D	14861	14871	14731	14753	14730	14730	14852	14698	14660	14723	14848	14889	14889	14832	14882	14972	14585	14585	14824	14780	15039	14785	104.7	14364	15206	TRUE
SB_E	366	350	313	324	324	324	357	343	325	310	362	321	321	338	324	346	337	337	309	323	327	333	16.86	265	400.4	TRUE
SB_F	1984	2047	1841	2021	2000	2000	1994	1912	2040	2016	2081	1995	1995	1965	2037	1986	2017	2017	2023	1908	1990	1994	54.32	1776	2212	TRUE
SB_P	436	474	474	437	470	470	452	483	501	414	428	442	452	446	445	462	444	444	486	472	464	457	21.79	369	544.2	TRUE

In this study, year 2008 transit traffic is chosen as the high intensity vessel traffic scenario. Average interarrival times of vessels transiting the Strait in the simulation model with 20 random replications and the actual interarrival times transiting the Strait at high intensity vessel traffic case (year 2008) are displayed in Figure 3.2. The results show that actual interarrival times for most vessel classes (except class F vessels in either direction and southbound class D vessels) fall in the prediction interval of t distribution with $\alpha = 0.1$.

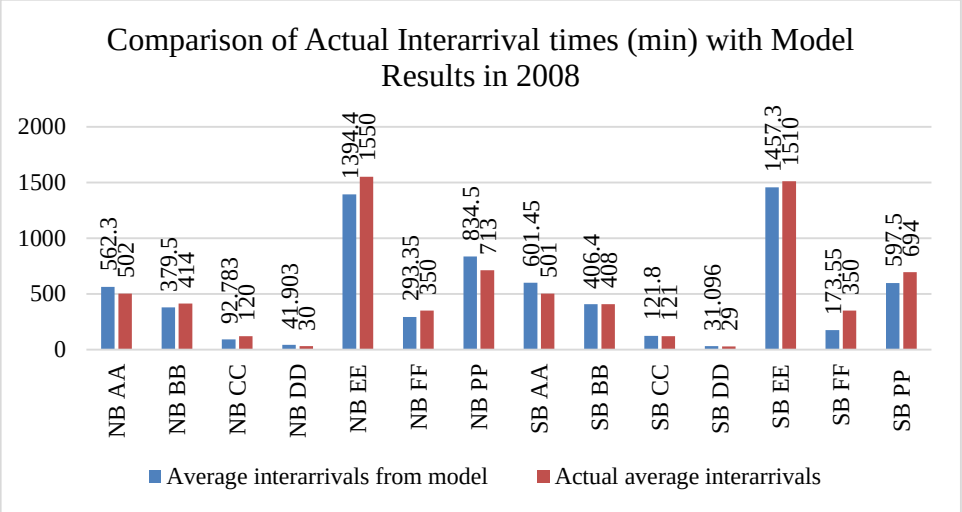

Figure 3.3. Vessel interarrival time comparison for 2008.

Average number of vessels transiting the Strait in the simulation model with 20 random replications and the actual number of vessels transiting the Strait at high intensity vessel traffic case (year 2008) are displayed in Figure 3.3. The results show that actual transits for all vessel classes (except southbound A class and class F) fall in the prediction interval of t distribution with $\alpha = 0.1$.

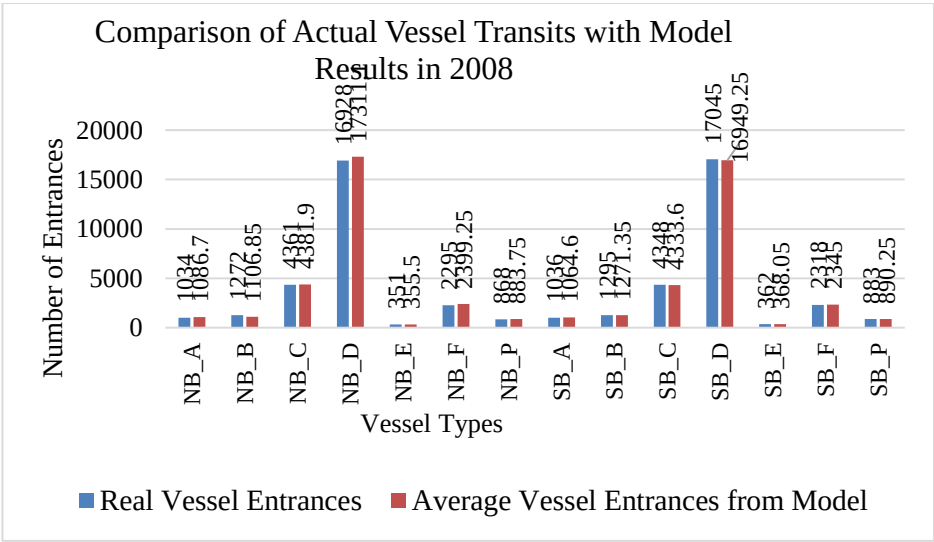

Figure 3.4. Vessel transits comparison for 2008.

In this study, year 2014 transit traffic is chosen as the low intensity vessel traffic scenario. Average interarrival times of vessels transiting the Strait in the simulation model with 20 random replications and the actual interarrival times of vessels transiting the Strait at low intensity vessel traffic case (year 2014) are displayed in Figure 3.4. The results show that actual interarrival times for all vessel classes fall in the prediction interval of t distribution with α= 0.1.

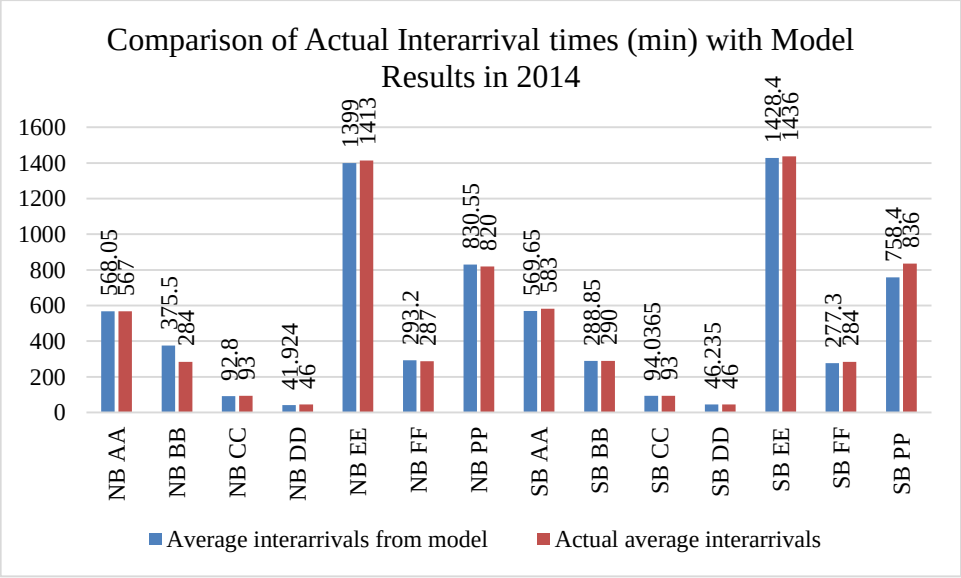

Figure 3.5. Vessel interarrival time comparison in 2014.

Average number of vessels transiting the Strait in the simulation model with 20 random replications and the actual number of vessels transiting the Strait at low intensity vessel traffic case (year 2014) are displayed in Figure 3.5. The results are close enough to deduce that scheduling algorithm sufficiently represents the real transit traffic pattern in 2014. The results show that actual transits for most of the vessel classes (except northbound class D, southbound class A and class D) fall in the prediction interval of t distribution with α= 0.1.

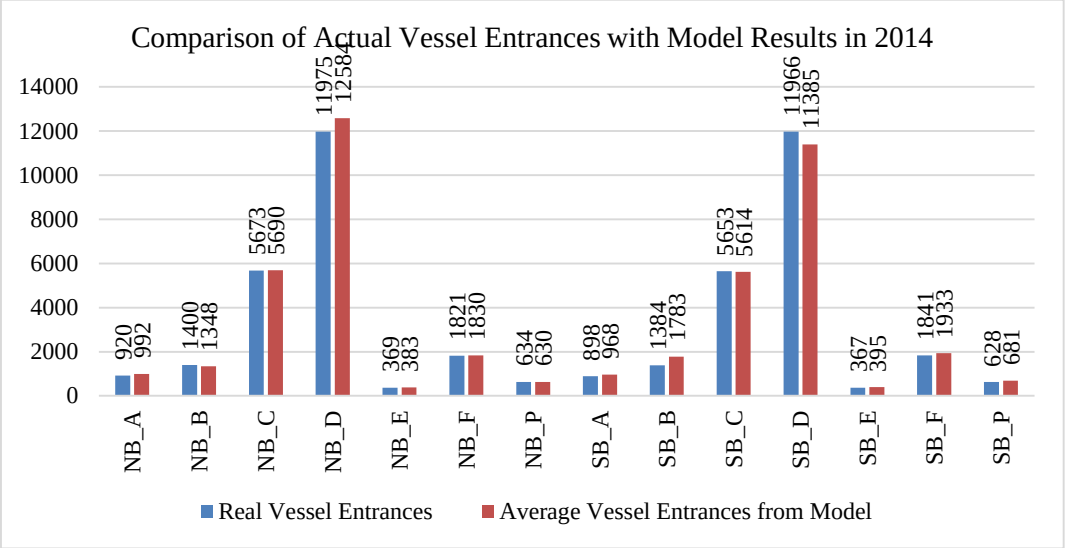

Figure 3.6. Vessel entrances comparison for 2014.

Average number of vessels transiting the Strait in the simulation model for all considered years (2008 to 2014) follow closely the average number of real vessel transits in the same period. The deviation for total number of vessels is 1.16%. The percentage deviation for each vessel class is displayed in Table 3.10.

Table 3.10. Average number of vessel transits.

Vessel types	Model average Passages/Year	Actual case average	Difference (%)	Weighted % difference
NB_A	1016	971	4.7	1.16
NB_B	1200	1331	9.8	
NB_C	4905	4900	0.1	
NB_D	14741	14663	0.5	
NB_E	327	320	2.3	
NB_F	2029	1984	2.3	
NB_P	609	604	1.0	
SB_A	1002	993	1.0	
SB_B	1361	1332	2.2	
SB_C	4860	4892	0.7	
SB_D	14822	14675	1.0	
SB_E	330	323	2.1	
SB_F	2022	1989	1.7	
SB_P	613	604	1.5	

The last statistics investigated is the average interentrance time of each vessel type transiting from either direction at the Strait.

Average interentrance time intervals for consecutive vessels (class A enters the Strait and afterwards the other vessel classes follow class A vessel) in each direction resulting in the simulation model with 20 replications based on the 2008 data and the actual results for 2008 are displayed in Figure 3.6. The results are close to each other except the average interentrance time between northbound class A vessels followed by class C vessels (9 minutes difference on the average).

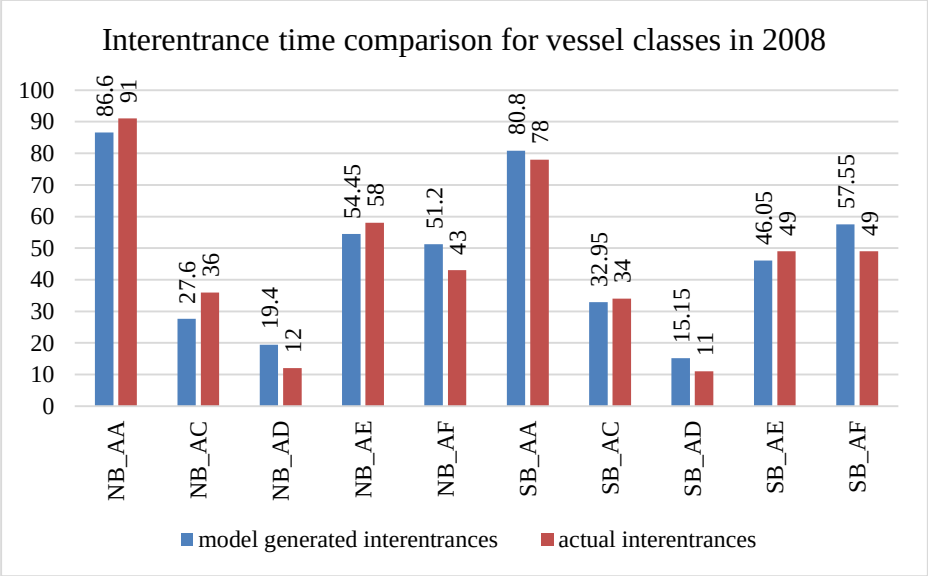

Figure 3.7. Vessel interentrance time comparison for class A and successive classes in 2008.

Average interentrance time intervals for consecutive vessels (class A and the following vessels) in each direction resulting in the simulation model with 20 replications based on the 2011 data and the actual results for 2011 are displayed in Figure 3.7. The results are close to each other except the average interentrance time between northbound class A vessels and the following class C vessels (25 minutes difference on the average).

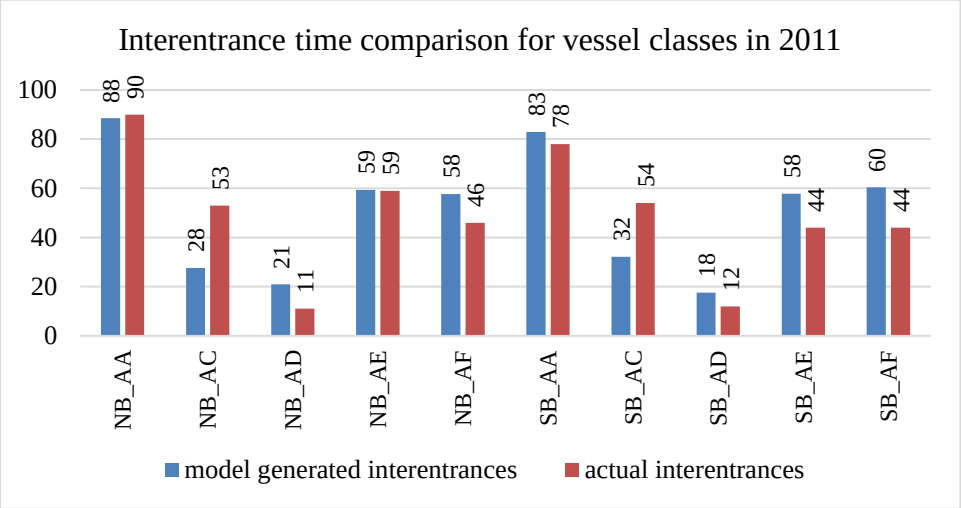

Figure 3.8. Vessel interentrance time comparison for class A and successive classes in 2011.

Average interentrance time intervals for consecutive vessels (class A and the following vessels) in each direction resulting in simulation model with 20 replications based on the 2014 data and the actual results for 2014 are displayed in Figure 3.8. The results are close to each other except the interentrance time between southbound class A vessels and the following class F vessels (17 minutes difference on the average).

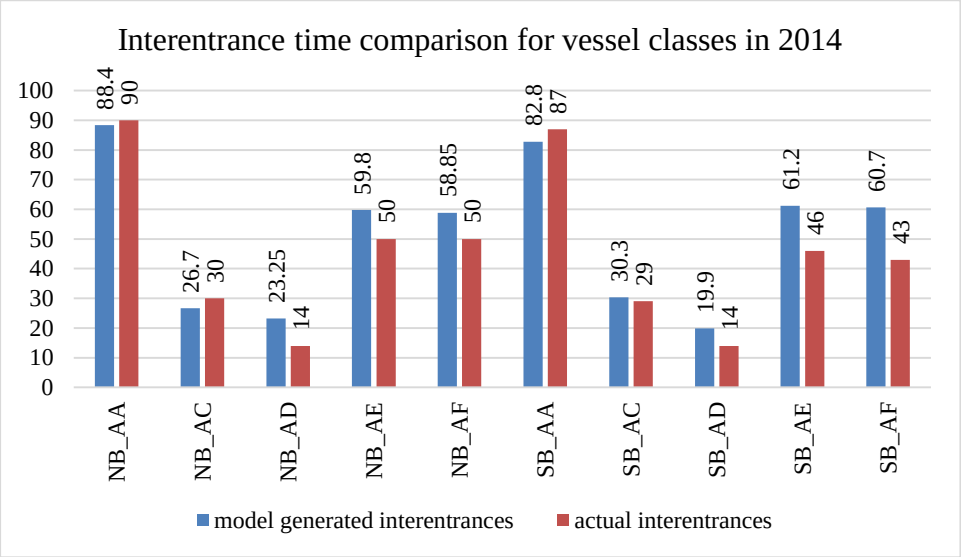

Figure 3.9. Vessel interentrance time comparison for class A and successive classes in 2014.

Average interentrance time intervals for consecutive vessels (class B and the following vessels) in each direction resulting in simulation model with 20 replications based on the 2008 data and the actual results for 2008 are displayed in Figure 3.9. The results are close to each other except the interentrance time between northbound class B vessels and the following class F vessels (15 minutes difference on the average) and interentrance time between southbound class B vessels and the following class E vessels (21 minutes difference on the average).

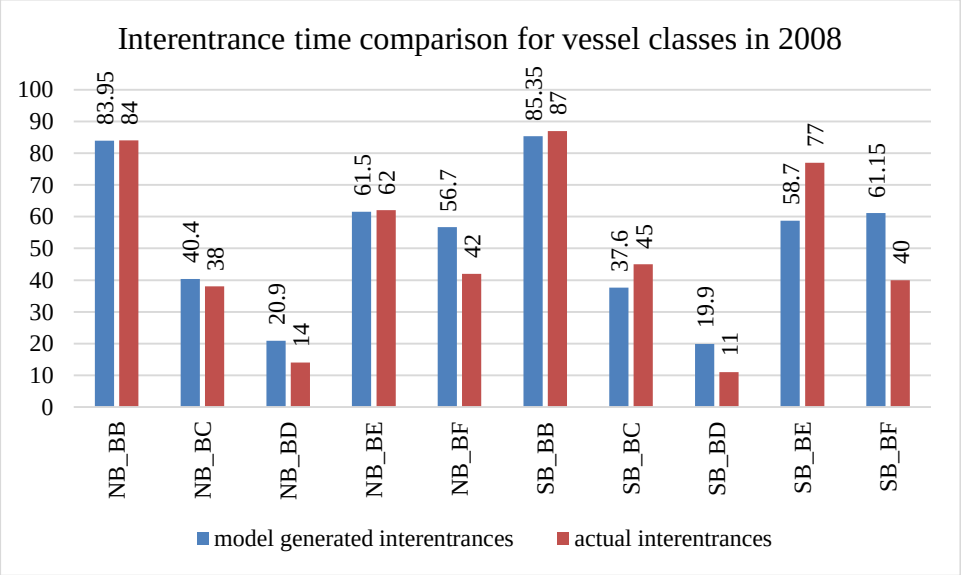

Figure 3.10. Vessel interentrance time comparison for class B and successive classes in 2008.

Average interentrance time intervals for consecutive vessels (class B and the following vessels) in each direction resulting in simulation model with 20 replications based on the 2011 data and the actual results for 2011 are displayed in Figure 3.10. The results are close to each other except the interentrance time between two class B vessels in both directions and interentrance time between class B vessels and the following class F vessels in both directions (34 minutes on the average).

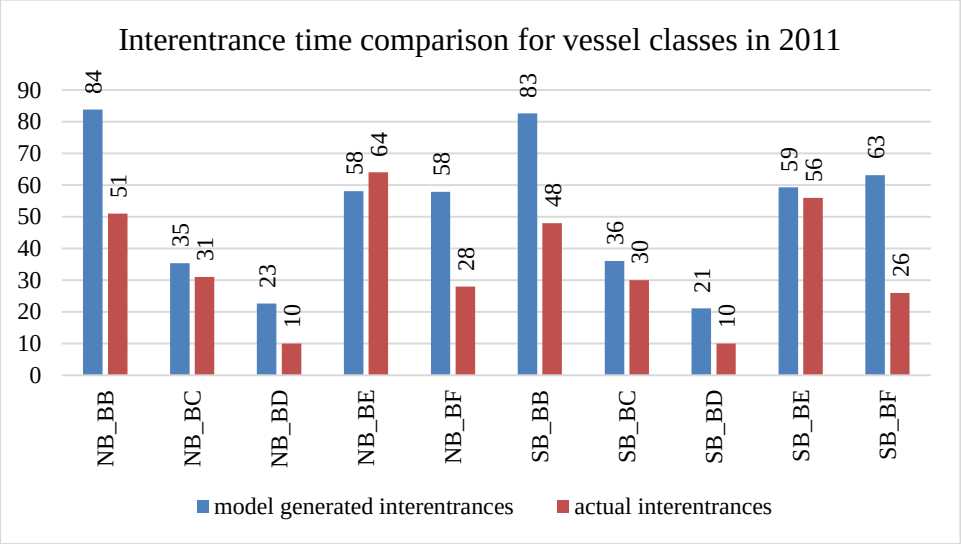

Figure 3.11. Vessel interentrance time comparison for class B and successive classes in 2011.

Average interentrance time intervals for consecutive vessels (class B and the following vessels) in each direction resulting in simulation model with 20 replications based on the 2014 data and the actual results for 2014 are displayed in Figure 3.11. The results are close to each other except the interentrance time between class B vessels and the following class E vessels in both directions (38 minutes on the average).

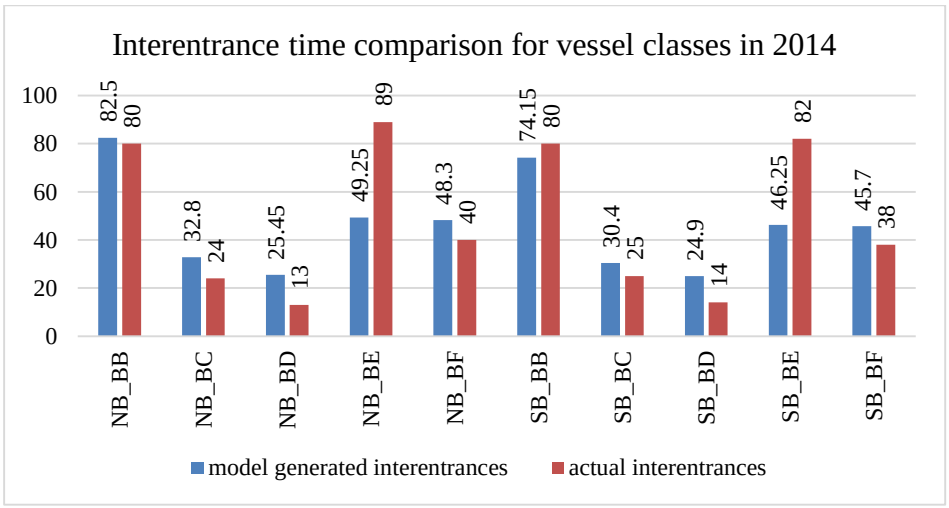

Figure 3.12. Vessel interentrance time comparison for class B and successive classes in 2014.

Average interentrance time intervals for consecutive vessels (class C and the following vessels) in each direction resulting in simulation model with 20 replications based on the 2008 data and the actual results for 2008 are displayed in Figure 3.12. The results are close to each other except the interentrance time between class C vessels and the following class F vessels in both directions (23 minutes on the average).

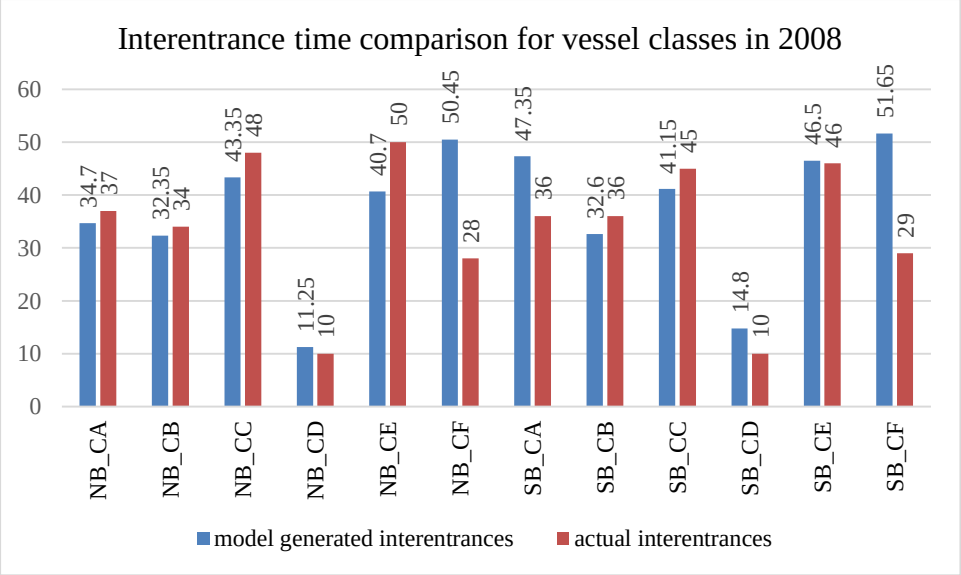

Figure 3.13. Vessel interentrance time comparison for class C and successive classes in 2008.

Average interentrance time intervals for consecutive vessels (class C and the following vessels) in each direction resulting in simulation model with 20 replications based on the 2011 data and the actual results for 2011 are displayed in Figure 3.13. The results are close to each other except the interentrance time between class C vessels and the following class F vessels in both directions (26 minutes on the average).

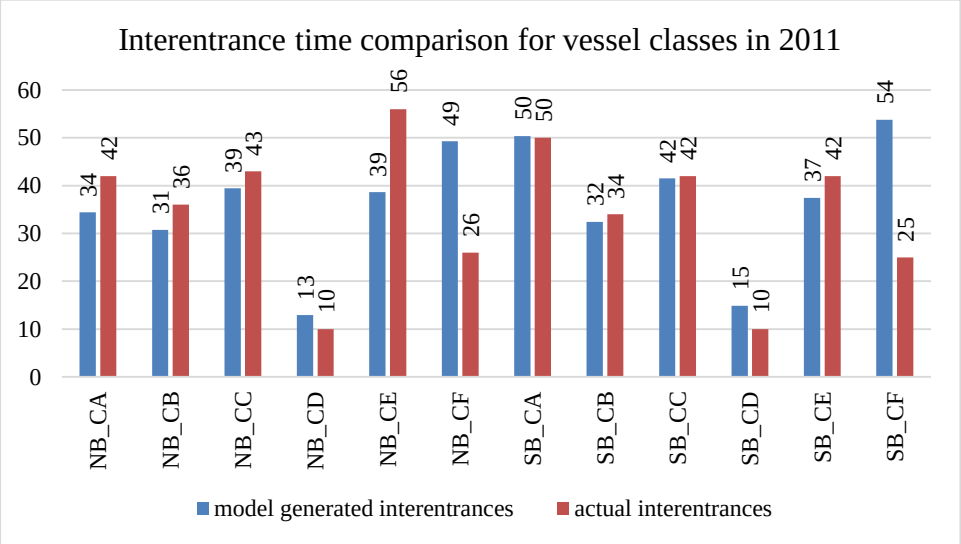

Figure 3.14. Vessel interentrance time comparison for class C and successive classes in 2011.

Average interentrance time intervals for consecutive vessels (class C and the following vessels) in each direction resulting in simulation model with 20 replications based on the 2014 data and the actual results for 2014 are displayed in Figure 3.14. The results are close to each other except the interentrance time between class C vessels and the following class F vessels in both directions (25 minutes on the average).

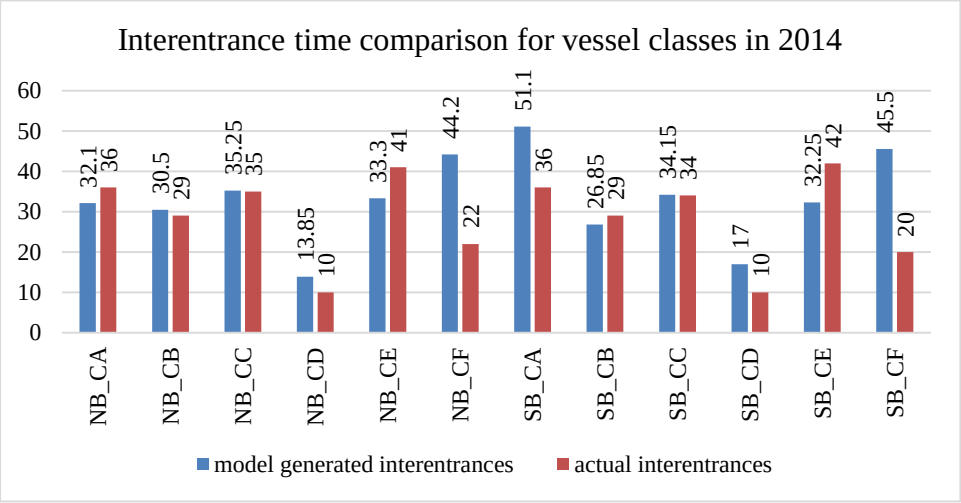

Figure 3.15. Vessel interentrance time comparison for class C and successive classes in 2014.

Average interentrance time intervals for consecutive vessels (class D and the following vessels) in each direction resulting in simulation model with 20 replications based on the 2008 data and the actual results for 2008 are displayed in Figure 3.15. The results are close to each other except the interentrance time between class D vessels and the following class F vessels in both directions (7 minutes on the average).

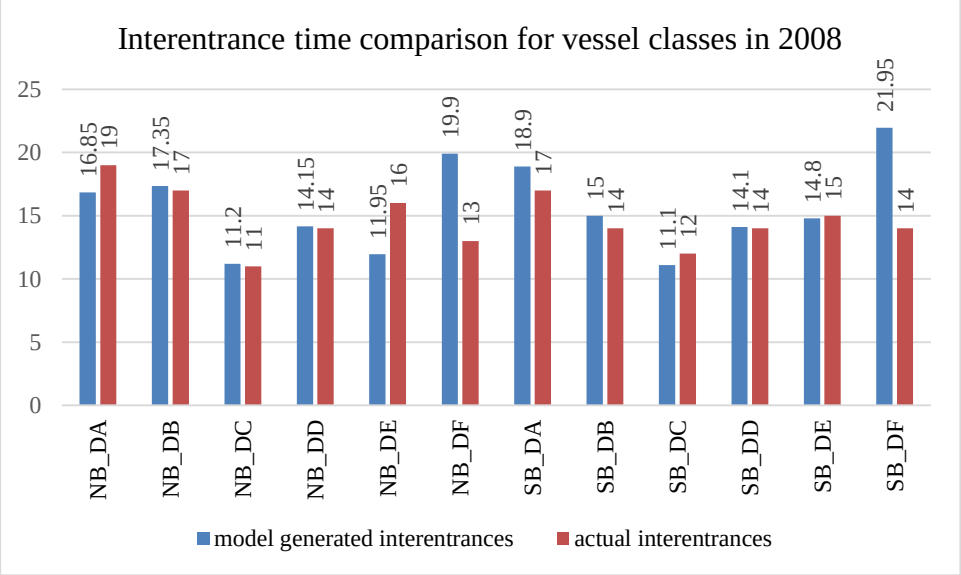

Figure 3.16. Vessel interentrance time comparison for class D and successive classes in 2008.

Average interentrance time intervals for consecutive vessels (class D and the following vessels) in each direction resulting in simulation model data with 20 replications based on the 2011 and the actual results for 2011 are displayed in Figure 3.16. The results are close to each other except the interentrance time between class D vessels and the following class F vessels in both directions (13 minutes on the average).

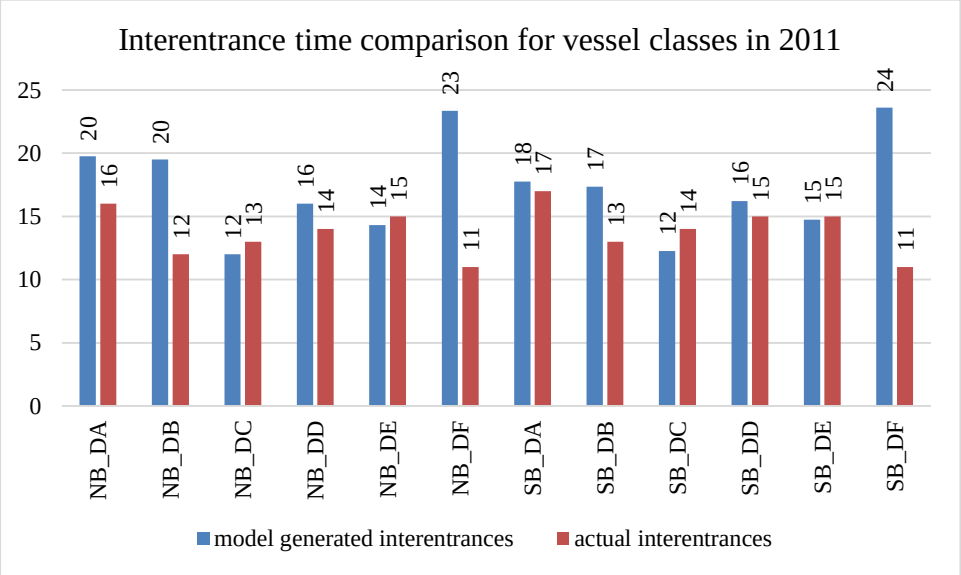

Figure 3.17. Vessel interentrance time comparison for class D and successive classes in 2011.

Average interentrance time intervals for consecutive vessels (class D and the following vessels) in each direction resulting in simulation model with 20 replications based on the 2014 data and the actual results for 2014 are displayed in Figure 3.17. The results are close to each other except the interentrance time between class D vessels and the following class F vessels in both directions (15 minutes on the average).

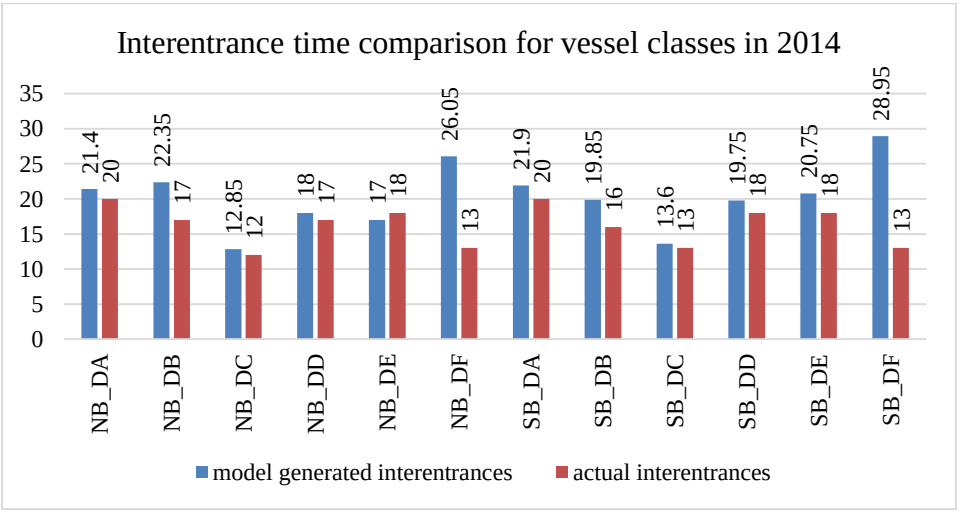

Figure 3.18. Vessel interentrance time comparison for class D and successive classes in 2014.

Average interentrance time intervals for consecutive vessels (class E and the following vessels) in each direction resulting in simulation model with 20 replications based on the 2008 data and the actual results for 2008 are displayed in Figure 3.18. The results are close to each other except the interentrance time between class E vessels and the following class F vessels in both directions (41 minutes difference).

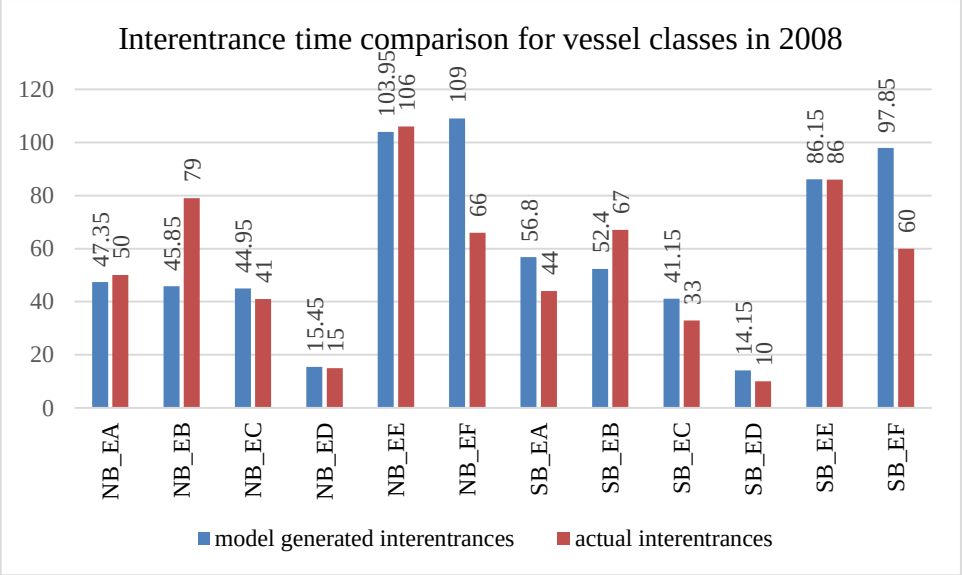

Figure 3.19. Vessel interentrance time comparison for class E and successive classes in 2008.

Average interentrance time intervals for consecutive vessels (class E and the following vessels) in each direction resulting in simulation model with 20 replications based on the 2011 data and the actual results for 2011 are displayed in Figure 3.19. The results are close to each other except the interentrance time between class E vessels and the following class F vessels in both directions (42 minutes on the average).

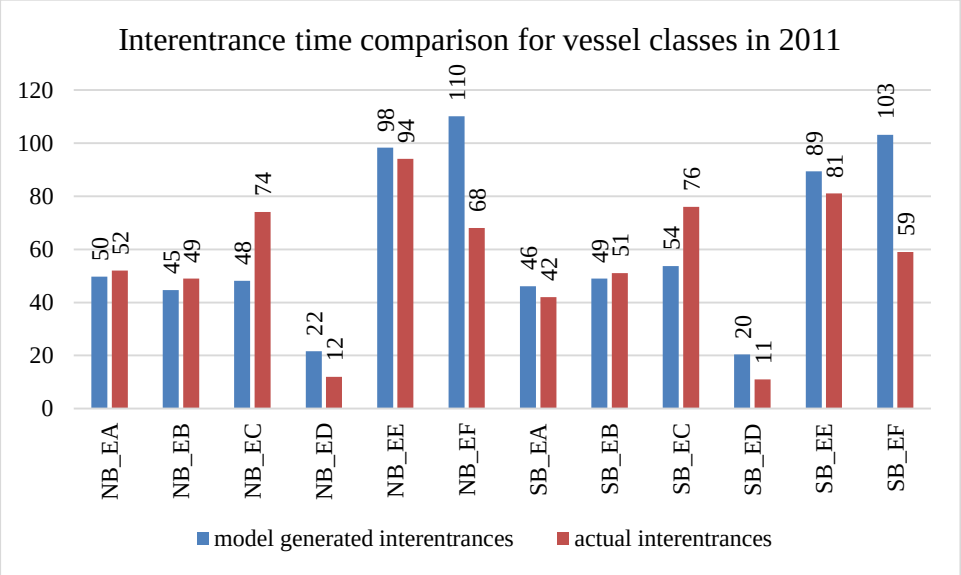

Figure 3.20. Vessel interentrance time comparison for class E and successive classes in 2011.

Average interentrance time intervals for consecutive vessels (class E and the following vessels) in each direction resulting in simulation model with 20 replications based on the 2014 data and the actual results for 2014 are displayed in Figure 3.20. The results are close to each other except the interentrance time between class E vessels and the following class F vessels in both directions (50 minutes on the average).

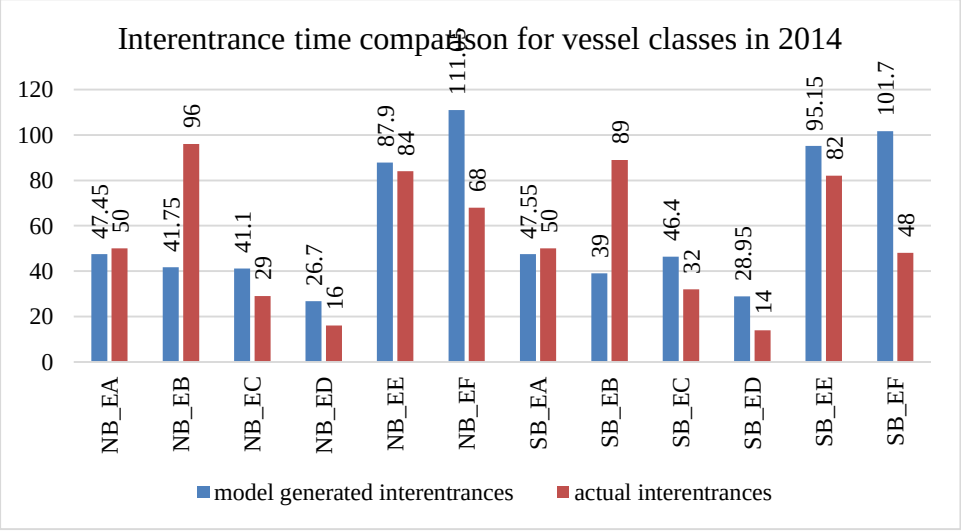

Figure 3.21. Vessel interentrance time comparison for class E and successive classes in 2014.

Average interentrance time intervals for consecutive vessels (class F and the following vessels) in each direction resulting in simulation model with 20 replications based on the 2008 data and the actual results for 2008 are displayed in Figure 3.21. The results are close to each other except the interentrance time between successive southbound class F vessels (22 minutes on the average).

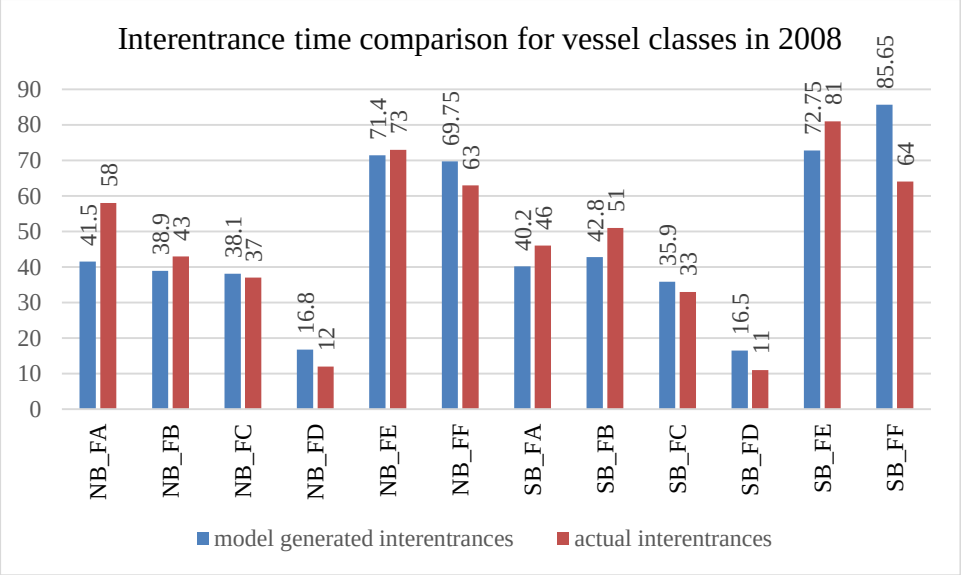

Figure 3.22. Vessel interentrance time comparison for class F and successive classes in 2008.

Average interentrance time intervals for consecutive vessels (class F and the following vessels) in each direction resulting in simulation model with 20 replications based on the 2011 data and the actual results for 2011 are displayed in Figure 3.22. The results are close to each other except the interentrance time between southbound class F vessels and the following class B vessels (22 minutes on the average).

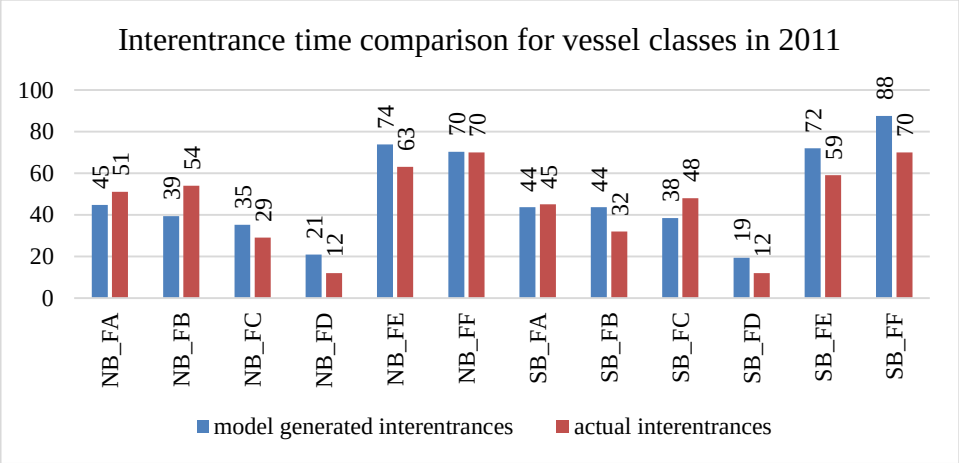

Figure 3.23. Vessel interentrance time comparison for class F and successive classes in 2011.

Average interentrance time intervals for consecutive vessels (class F and the following vessels) in each direction resulting in simulation model with 20 replications based on the 2014 data and the actual results for 2014 are displayed in Figure 3.23. The results are close to each other except the interentrance time between southbound class F vessels and the following class E vessels (18 minutes on the average).

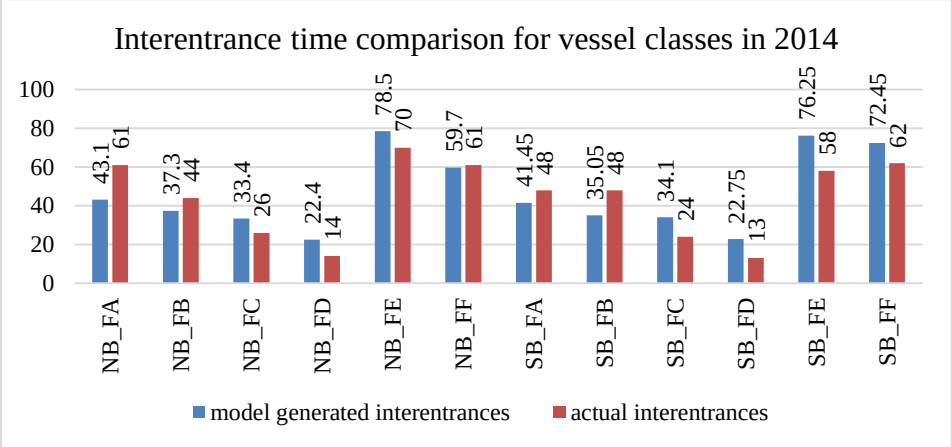

Figure 3.24. Vessel interentrance time comparison for class F and successive classes in 2014.

Average interentrance time intervals for consecutive vessels (in each direction resulted in the simulation model with 20 replications based on 2009, 2010, 2012 and 2013 data and the actual results for 2009, 2010, 2012 and 2013 are displayed in Appendix D.

Table 3.11 displays the comparisons of average interentrance times of two consecutive northbound vessels from the model output (aggregated outputs of seven years) and actual case (aggregated outputs of seven years). The results are close to each other when taking the difference of two average time. There is only 2.5 minutes difference between two northbound class A vessels entering the Strait, 6.4 minutes difference between two northbound class B vessel entering the Strait, 4.5 minutes between two northbound class C vessels entering the Strait, 1.4 minutes difference between two northbound class D vessels entering the Strait, 0.4 minutes difference between two northbound class E vessels entering the Strait, 1.1 minutes between two northbound class F vessels entering the Strait.

Table 3.11. Comparison of northbound vessel entrances.

Northbound (NB) Vessel Pair	Model Average Time(min)	Real Case Average Time(min)	Difference (min)	Percent Difference
NB_AA	87.19	89.7	2.52	-3%
NB_AC	25.12	36.1	11.02	-30%
NB_AD	20.60	12.3	8.31	68%
NB_AE	54.21	55.4	1.22	-2%
NB_AF	55.01	48.0	7.01	15%
NB_BB	83.70	77.3	6.41	8%
NB_BC	34.64	29.7	4.92	17%
NB_BD	23.79	12.1	11.65	96%
NB_BE	55.60	103.9	48.26	-46%
NB_BF	55.76	41.3	14.47	35%
NB_CA	34.92	38.6	3.65	-9%
NB_CB	32.42	33.0	0.58	-2%
NB_CC	37.26	41.7	4.45	-11%
NB_CD	13.28	10.0	3.28	33%
NB_CE	34.25	49.0	14.75	-30%
NB_CF	46.21	25.6	20.64	81%
NB_DA	21.62	18.3	3.34	18%
NB_DB	21.55	15.3	6.26	41%
NB_DC	14.21	12.0	2.21	18%
NB_DD	16.23	14.9	1.37	9%
NB_DE	15.74	16.6	0.84	-5%
NB_DF	24.34	11.6	12.76	110%
NB_EA	51.44	53.0	1.56	-3%
NB_EB	47.90	95.9	47.96	-50%
NB_EC	46.38	42.1	4.24	10%
NB_ED	23.31	13.9	9.46	68%
NB_EE	95.31	95.7	0.40	0%
NB_EF	111.54	69.4	42.11	61%
NB_FA	43.84	57.0	13.16	-23%
NB_FB	39.64	45.6	5.94	-13%
NB_FC	37.29	34.0	3.29	10%
NB_FD	21.30	13.3	8.01	60%
NB_FE	77.95	75.4	2.52	3%
NB_FF	66.10	65.0	1.10	2%

Table 3.12 displays the comparison of average interentrance time of two consecutive southbound vessels from the model output (aggregated outputs of seven years) and actual case (aggregated outputs of seven years). The results are close to each other when taking the difference of two average time. There is only 0.8 minutes difference between two southbound class A vessels entering the Strait, 2.3 minutes difference between two southbound class B vessels entering the Strait, 1.6 minutes difference between two southbound class C vessels entering the Strait, 0.8 minutes difference between two southbound class D vessels entering the Strait, 9.8 minutes diference between two southbound class E vessels entering the Strait, 17.1 minutes difference between two southbound class F vessels entering the Strait.

Table 3.12. Comparison of southbound vessel entrances.

Southbound (SB) Vessel Pair	Model Average Time(min)	Real Case Average Time(min)	Difference(min)	Percent Difference
SB_AA	81.9	81.1	0.8	1%
SB_AC	30.2	34.6	4.3	-13%
SB_AD	16.8	12.3	4.5	36%
SB_AE	52.6	45.7	6.9	15%
SB_AF	58.9	47.1	11.8	25%
SB_BB	81.9	79.6	2.3	3%
SB_BC	35.9	30.1	5.8	19%
SB_BD	22.0	11.6	10.5	90%
SB_BE	56.1	92.3	36.2	-39%
SB_BF	59.0	39.7	19.3	49%
SB_CA	53.6	37.7	15.9	42%
SB_CB	32.9	33.1	0.3	-1%
SB_CC	39.0	40.6	1.6	-4%
SB_CD	15.4	9.7	5.7	58%
SB_CE	37.0	42.7	5.7	-13%
SB_CF	51.0	25.1	25.9	103%
SB_DA	21.0	17.4	3.6	21%
SB_DB	18.9	14.9	4.0	27%
SB_DC	14.2	12.4	1.8	15%
SB_DD	15.9	15.1	0.8	5%
SB_DE	16.2	15.6	0.7	4%
SB_DF	24.7	11.6	13.1	113%
SB_EA	52.6	51.1	1.4	3%
SB_EB	50.3	101.9	51.6	-51%
SB_EC	52.9	39.9	13.0	33%
SB_ED	21.4	11.4	9.9	87%
SB_EE	90.5	80.7	9.8	12%
SB_EF	104.2	62.3	41.9	67%
SB_FA	42.9	47.0	4.1	-9%
SB_FB	43.0	50.9	7.8	-15%
SB_FC	39.5	32.1	7.4	23%
SB_FD	20.0	12.1	7.9	65%
SB_FE	75.1	62.4	12.6	20%
SB_FF	82.8	65.7	17.1	26%

4. COLLISION AND GROUNDING PROBABILITIES FOR VESSELS TRANSITING THE STRAIT

While being used in a wide variety of areas such as economy, finance, health, safety, engineering, insurance, business, psychology and maintenance, the definition and assessment of "risk" is still not unique [54]. The discussions have started with distinguishing the terms "risk" and "uncertainty". [55] defines "risk" as the computable uncertainty, whereas in "uncertainty" the probability of outcome is not exactly known. [56] asserts that in order for risk to exist, uncertainty is a prerequisite. [57] claims that uncertainty is the indispensable element for our unknown world. [58] on the other hand, argues that uncertainty about the potential outcomes and the importance of these outcomes in terms of providing utility or disutility are two essential components of risk.

Risk is generally defined as the product of the probability of an undesired event and its consequences to human life, health, possessions or the environment. Risk analysis on the other side is the set of systematic activities to discern the attributes of risk and to reveal the risk with the information gathered [59].

This study aims to estimate the probability of transit vessel accidents (collision and grounding) in the Strait rather than estimating the consequences of these accidents. One reason to confine the study to the probability (of undesirable events) is that there are insufficient data regarding the consequences of the Strait maritime accidents. The other reason is that the Strait Traffic authorities cannot control the nature of the cargo carried by the vessels, which is the main factor influencing accident consequences. Moreover, most of the other related studies on maritime accidents also focus on probabilities.

Vessel accident (event "A" is intersection of two events; the event that the ship being on an accident (collision and grounding) course (event "Geo") and the event that the ship does not make evasive maneuvers (event "Caus") as displayed in Figure 4.1:

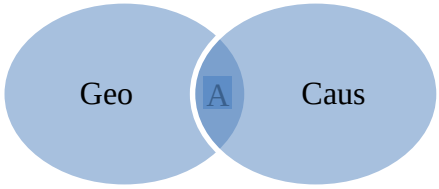

Figure 4.1. Representation of vessel accident as intersection of two events.

Accordingly, P(A) is calculated by:

$$P(A) = P(Geo \cap Caus) = P(Geo, Caus) \tag{4.1}$$

where A is either a collision or a grounding event and

$$P(A) = P(Geo) * P(Caus|Geo) \tag{4.2}$$

In this study, discussion with various experts (pilot captains and VTS officials) have lead to the assumption that the event that the vessel does not make evasive maneuvers is marginally independent of the event that the vessel is on the accident course, therefore;

$$P(A) = P(Geo) * P(Caus) \tag{4.3}$$

for both accident types elaborated in this study (collision and grounding).

The collision probabability is the multiplication of geometric collision probability and the conditional probability of collision causation probability.The geometric collision probability is provided by [60] while the causation probability is computed by the designed Bayesian network where some of the nodes (such as season, day light, sector and vessel type) are observed (preset) through the simulation model described in Chapter 3. Therefore similar to [44,45] the probability of collision (P_{RC}) can be expressed as,

$$P_{RC} = P_{GeoColl} * P_{CausColl} \tag{4.4}$$

where $P_{GeoColl}$ is the geometric probability of being in a course of collision while navigating blindly (taking no evasive actions) and $P_{CausColl}$ is the causation probability of being incapable of doing evasive action in order to prevent collision [44,45].

In order to compute the grounding probabilities, two separate models are formulated, as well. One is the geometric grounding probability model and the other one is the grounding causation probability model. Geometric grounding probability basically refers to the likelihood that a vessel on a blind navigation is on the grounding route by considering the stopping distance of the vessel and the sector length. On the other hand, the grounding causation probability basically refers to the probability that the vessel does not make evasive maneuvers. Unlike geometric collision probability estimation the geometric grounding probability is estimated regarding a proposed analytical model and the grounding causation probability is computed by the designed Bayesian network where some of the nodes (such as season, day light, sector and vessel type) are observed (preset) through the simulation model described in Chapter 3.The grounding probability is the multiplication of geometric grounding probability and the conditional probability of grounding causation probability just as [44, 45] expressed:

$$P_{RG} = P_{GeoGrn} * P_{CausGrn} \tag{4.5}$$

where P_{GeoGrn} is the geometric probability of being in a course of grounding while navigating blindly (taking no evasive actions) and $P_{CausGrn}$ is the causation probability of being incapable of doing evasive action in order to prevent grounding.

One main objective of this study is to estimate the collision and grounding probabilities of vessels sailing in the Strait based on the above defined multiplication of geometric collision (and grounding) probability and the collision (and grounding) causation probability.

4.1. Geometric Collision Probability

Most of the researches to evaluate the geometric collision probability P_{Geo} is based on molecular collision theory. This theory asserts that, gas-phase chemical reactions occur when molecules collide with sufficient kinetic energy and these molecular collisions are called successful collisions. The rate of these collisions is directly proportional to overall collision frequency multiplied by probability of successful collisions.

[61] aligned this theory with maritime accidents and estimated the number of vessel collisions (N_C) in a given time period (T) through the equation:

$$N_C = \rho_1 \rho_2 D |\overrightarrow{V_1} - \overrightarrow{V_2}| ST \tag{4.6}$$

where,

- ρ_1 is the traffic density of type 1 vessel,
- ρ_2 is the traffic density of type 2 vessel,
- V_1 is the velocity of type 1 vessel which is sailing on a random course
- V_2 is the velocity of type 2 vessel which is sailing on a random course
- D is the geometrical collision diameter which is the projection length of the chained area perpendicular to the direction of relative velocity $|\overrightarrow{V_1} - \overrightarrow{V_2}|$ (Figure 4.2) and
- S is the area of the considered waterway.

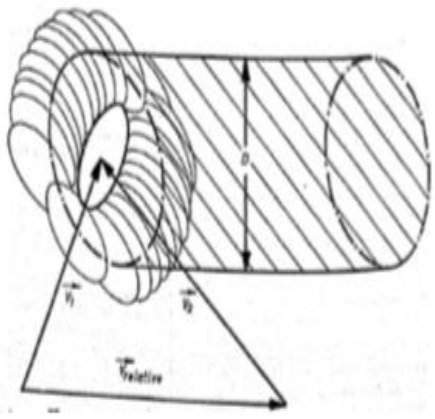

Figure 4.2. Representation of collision diameter [61].

Since this approach assumes random navigation for either vessel types, the researchers rewrote the equation as:

$$N_C = \int_0^T \iint_S \frac{1}{2} (\rho_1 + \rho_2)^2 / 2PD |\overrightarrow{V_1} - \overrightarrow{V_2}| dSdt \tag{4.7}$$

where, PD is the collision diameter, which is a function of vessel size and angle between courses. In order to get the collision dimeter, [48] utilized the equation:

$$D_{ij} = \frac{L_i^1 V_j^2 + L_j^2 V_i^1}{V_{ij}} sin\theta + B_j^2 \left\{1 - \left(sin\theta \frac{V_i^1}{V_{ij}}\right)^2\right\}^{\frac{1}{2}} + B_i^1 \left\{1 - \left(sin\theta \frac{V_j^2}{V_{ij}}\right)^2\right\}^{\frac{1}{2}} \quad (4.8)$$

where,

- L_i^1 is the length of type *i* vessel in waterway (course) 1,
- L_j^2 is the length of type *j* vessel in waterway (course) 2,
- B_i^1 is the width of type *i* vessel in waterway (course) 1,
- B_j^2 is the width of type *j* vessel in waterway (course) 2,
- V_i^1 is the velocity of type *i* vessel in waterway (course) 1,
- V_j^2 is the velocity of type *j* vessel in waterway (course) 2,
- V_{ij} is the relative velocity of vessel type *i* and vessel type *j* and
- θ is the approaching angle of vessels.

Relative velocity of vessels is calculated by the equation:

$$\left|V_{ij}\right| = \sqrt{V_i^1 + v_j^2 - V_i V_j cos\theta} \quad (4.9)$$

In order to obtain the geometric collision probabilities, the results of [60] were used. [60] utilized the equation for calculating geometric collision probability for a given time period in the Strait as,

$$P_G = \sum_s \sum_i \sum_j \sum_{ik} (s)\rho_i(ik(s), s)\rho_j(jk(s), s)v_{ij}(s)D_{ij}(s)\Delta l(ik, s)\Delta l(jk, s)\Delta t \quad (4.10)$$

where,

- *s* is the sector,
- *i* and *j* are the entrance direction (N, S, E, W)
- *ik* and *jk* are the cells inside the sector based on entrance,
- ρ_i is the vessel density in the i^{th} direction,
- ρ_j is the vessel density in the j^{th} direction,

- Δl is the travelling distance,
- Δt is the time in consideration,
- D_{ij} is the collision diameter of the vessels on the i^{th} and j^{th} direction
- v_{ij} is the relative velocity of the vessels on the i^{th} and j^{th} direction.

[60] subdivided the Strait into 13 sectors according to the coordinates given in Table 4.1.

Table 4.1. Coordinates of the sectors in the Strait.

East Border			West Border		
Point No	Longitude Degree	Latitude Degree	Point No	Longitude Degree	Latitude Degree
1	41.000	29.010	1	41.005	28.990
2	41.018	29.001	2	41.022	28.990
3	41.025	29.003	3	41.029	28.996
4	41.052	29.049	4	41.049	29.035
5	41.075	29.056	5	41.076	29.049
6	41.083	29.065	6	41.082	29.057
7	41.101	29.064	7	41.104	29.058
8	41.287	29.090	8	41.125	29.077
9	41.123	29.089	9	41.151	29.055
10	41.148	29.065	10	41.159	29.055
11	41.158	29.064	11	41.175	29.075
12	41.180	29.087	12	41.200	29.100
13	41.195	29.113	13	41.205	29.111
14	41.220	29.143	14	41.230	29.125

The coordinates and size of the sectors are based on the regions, environmental, geographic and navigational conditions. Accordingly, conditions such as speed and course over ground, heading, ship dimensions (Length overall called as LOA and beam) and number of vessels in the considered sailing directions are assumed not to change throughout the sector [60].

[60] obtained the geometric collision probabilities for each sector and for each vessel type at each sector. Related results, displayed in Table 4.2, show that Sector 10 has the highest geometric collision probability and Sector 3 has the lowest geometric collision probability. The average geometric collision probability in the Strait is 0.026559 (the geometric collision frequency per vessel per year).

Table 4.2. Geometric probability for collision in each sector.

Sectors	Geometric Probability
Sector 1 (S1)	0.0113
Sector 2 (S2)	0.0152
Sector 3 (S3)	0.0049
Sector 4 (S4)	0.0346
Sector 5 (S5)	0.0367
Sector 6 (S6)	0.0139
Sector 7 (S7)	0.0124
Sector 8 (S8)	0.0233
Sector 9 (S9)	0.0292
Sector 10 (S10)	0.0724
Sector 11 (S11)	0.0497
Sector 12 (S12)	0.0192
Sector 13 (S13)	0.0224

Geometric probability of collisions in terms of vessel classes is given in Table 4.3. The highest geometric collision probability is observed for class D. According to LOA, the highest collision probability is observed for vessels with length 100-150 m.

Table 4.3. Geometric collision probability of vessels in each sector.

	Geometric Collision Probability						
	Vessel Class						
Sector	A	B	C	D	E	F	P
1	0.0108	0.0344	0.0381	0.0388	0.0108	0.0275	0.0223
2	0.0179	0.0478	0.0548	0.0603	0.0179	0.0436	0.0346
3	0.0191	0.0482	0.0612	0.0734	0.0191	0.0451	0.0388
4	0.0109	0.0313	0.0431	0.0527	0.0109	0.0254	0.0254
5	0.0213	0.0448	0.0572	0.0669	0.0213	0.0374	0.0377
6	0.0084	0.0218	0.0279	0.0331	0.0084	0.0192	0.0173
7	0.0070	0.0237	0.0267	0.0271	0.0071	0.0170	0.0153
8	0.0069	0.0237	0.0308	0.0368	0.0069	0.0209	0.0181
9	0.0073	0.0258	0.0327	0.0378	0.0073	0.0213	0.0191
10	0.0056	0.0309	0.0407	0.0468	0.0056	0.0212	0.0216
11	0.0087	0.0326	0.0411	0.0467	0.0087	0.0248	0.0233
12	0.0038	0.0133	0.0179	0.0218	0.0038	0.0110	0.0104
13	0.0581	0.0926	0.1125	0.1231	0.0581	0.0696	0.0765
Average	0.0142	0.0362	0.0450	0.0512	0.0143	0.0295	0.0277

[60] also investigated the effect of season on geometric collision probability. According to Table 4.4, the highest geometric collision probability is in the winter season and the lowest geometric collision probability is in the spring season.

Table 4.4. Geometric collision probability of vessels in each season.

Season	Geometric Collision
Winter	0.1074
Spring	0.0887
Summer	0.0935
Autumn	0.1029

These results concerns only the first part (geometric collision probability) for collision probability estimation in the Strait. The second part is the collision causation probability, which regards the factors affecting the captain's and the vessel's ability/potential to make evasive maneuvers given the condition that the vessel is in a collision course.

4.2. Collision Causation Probability

Geometric collision probability regards the physical features (width, length, and velocity) of vessels and traffic patterns in the Strait (vessel densities and position of vessels). However, using just geometric collision probability and the number of vessels passed, the result would be above 1000 collisions/year, whereas the actual frequency is around 0.8 collisions/year. Therefore, another factor is obviously impacting the true collision probabilities. This additional factor in almost all maritime environment is the efforts made by the approaching vessels to avoid a potential accident.

As stated in Equation (3.1), causation probability $P_{caus}(\text{collision})$ is the probability of being incapable of doing evasive action in order to prevent collision. In other words, $P_{caus}(\text{collision})$ is the probability that in the vessels which are approaching a collision, the captains make no moves and/or are unable to avoid the accident. [44], instead of estimating $P_{caus}(\text{collision})$, directly utilized the real collision statistics in the Dover Strait and extracted

$P_{caus}(\text{collision})$ via dividing the vessel collision frequency by the geometric collision probability.

This study on the other hand, aspires to estimate the $P_{caus}(\text{collision})$) for transiting vessels in the Strait directly. For this purpose, a Bayesian network model is built and then solved through the Matlab package. Figure 4.3, which is designed through the software Genie©, will help visualizing the resulting Bayesian Network

4.2.1. Bayesian Networks

While modeling many systems for real world applications, it is inevitable to confront uncertainty. Probability theory mathematically quantifies the uncertainty via probabilistic models. In this general context, Bayesian networks are directed acyclic graphs (DAG) that are used in reasoning for uncertainty. Bayesian networks are easy to understand tools consisting of a set of variables (nodes) and a set of directed arcs among the nodes. These graphical models indicate the conditional independencies between nodes, whose states are mutually exclusive.

In a Bayesian network,

$$P(X_1, \dots, X_n) = P(X_1 = x_1, \dots, X_n = x_n) \tag{4.11}$$

which shows the joint probability distribution of *n* variables, X_i being in state x_i, for i=1,…n.

The joint probability distribution might also be written as:

$$P(X_1, \dots, X_n) = \prod_{i=1}^{n} P(x_i | x_{parents(i)}) \tag{4.12}$$

where $x_{parents(i)}$ are the parents of *i* (the nodes directly affecting the node *i*).

Since Bayesian networks are DAG,

$$P(X_1, \dots, X_n) = \prod_{i=1}^{n} P(x_i | x_{i-1}, \dots, x_1) \tag{4.13}$$

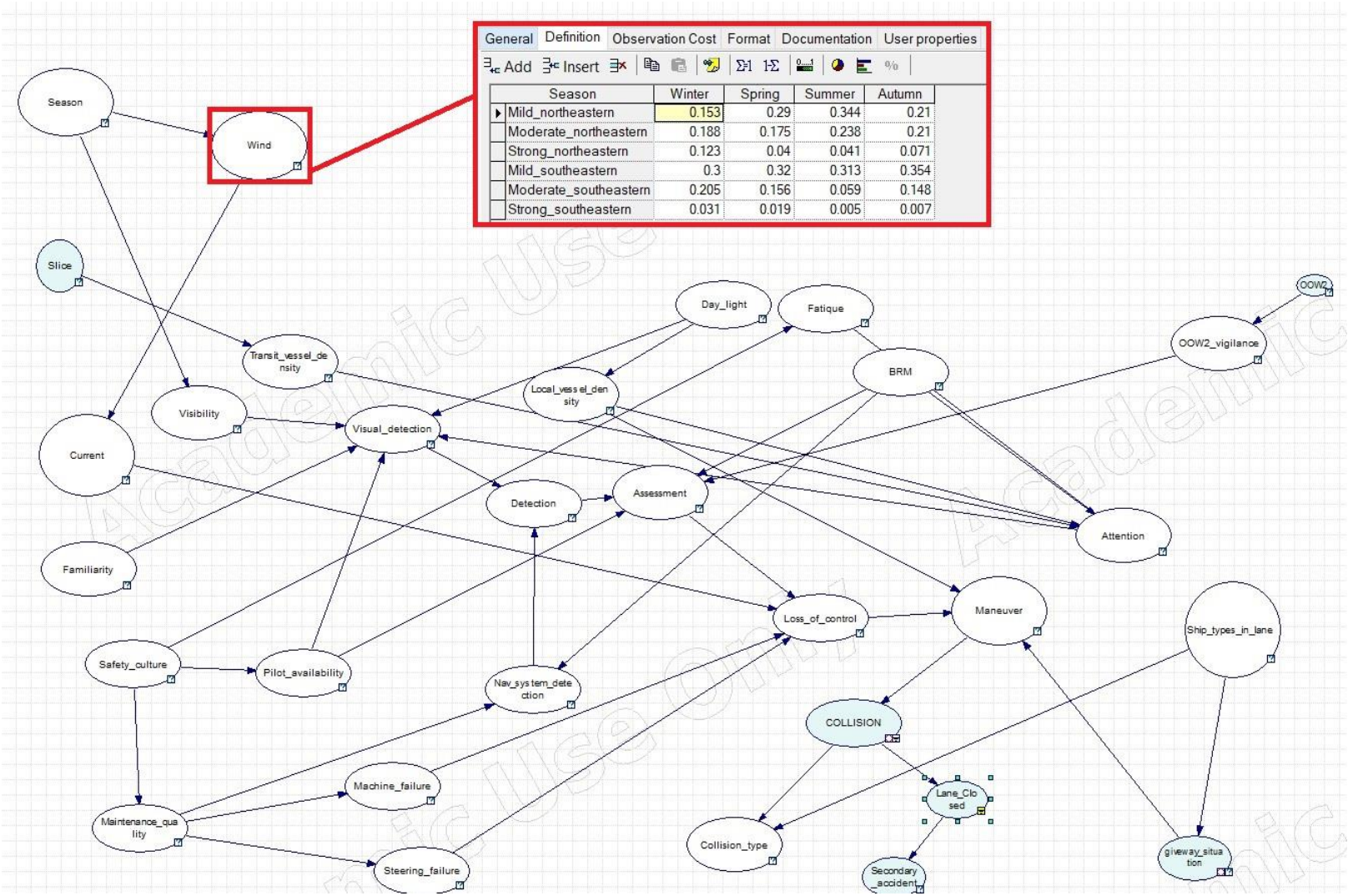

Figure 4.3. Bayesian Network designed for estimating Collision Causation Probability.

The marginal distribution of a node in a Bayesian network is computed as:

$$P(X_i) = \sum_{X_1} \dots \sum_{X_{i-1}} \sum_{X_{i+1}} \dots \sum_{X_N} P(X_1, \dots, X_n) \tag{4.14}$$

The conditional distribution of a variable in a Bayesian network is computed as:

$$P(X_i|X_j = \frac{P(X_i X_j)}{P(X_j)} \tag{4.15}$$

The important steps to build a Bayesian network are:

(i) The nodes and the arcs among these nodes (relations) are defined.
(ii) A sensible DAG model is designed.
(iii) Conditional probabilities for the states of the nodes in the designed network are computed.
(iv) Inference algorithms are applied to estimate the conditional probabilities given some observed (preset) nodes [62].

4.2.2. Bayesian Network for Calculating Collision Causation Probability

One might categorize the Bayesian network for (P_{Caus}(collision)) into three groups of factors as displayed in Figure 4.4:

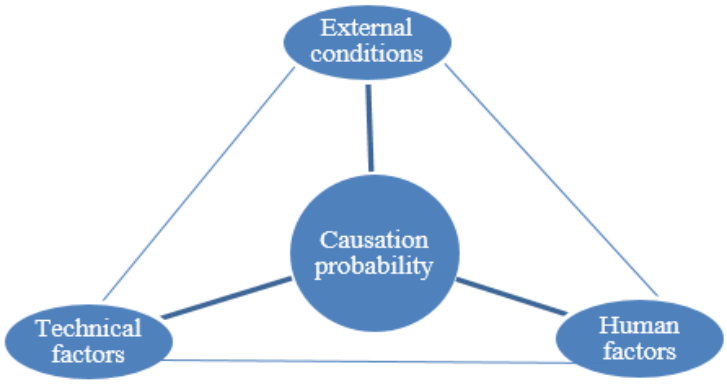

Figure 4.4. The Bayesian network model of "Collision Causation Probabilities".

These factor groups are discussed below.

4.2.2.1. External Conditions. These conditions, which are individually explained below, are those factors that affect the captain's maneuvering ability externally (i.e. the captain has no control over them).

- Season: This node includes all seasons affecting the vessel traffic and navigation. The states of "the Season" node are:

  (i) Winter
  (ii) Spring
  (iii) Summer
  (iv) Autumn

If a specific time period is not indicated (or predefined), the probabilities for these states are assumed to be equally likely.

"The Season" node directly affects "the Wind" and "the Visibility" nodes.

- Wind: This node contains the active wind types and strengths in the Strait. The conditional probabilities for the states of this node are estimated through the wind data of the "Devlet Meteoroloji İşleri" (DMI) for the previous 10-year period [62]. The DMI actually measures the speed and the direction of the wind at every 10 meters throughout a day. The speed of the wind is then categorized as mild, moderate and strong by means of the Beaufort wind scale. Accordingly, the states of this node are:

  (i) Mild northeastern
  (ii) Moderate northeastern
  (iii) Strong northeastern
  (iv) Mild southwestern
  (v) Moderate southwestern
  (vi) Strong southwestern

In the developed Bayesian Network, “the Season” node directly affects “the Wind” node” and “the Wind” node directly affects “the Current” node. For instance, according to Figure 4.3, the probability that there exists mild northeastern given that season is winter is 0.153.

- Day light: This node is designed to give consideration to the effects of “time of day” on daytime/nighttime vision and vessel density. The day is divided into three periods (which are the states of this node) as:

    (i) Morning
    (ii) Afternoon
    (iii) Night

“The Day light” node directly affects” the Local vessel density” and “the Visual Detection” nodes.

- Current: This node features three types of currents based on intensities. However, since there is not sufficient data to obtain the conditional probabilities for the states of this node, conditional probability of wind types, conditioned on “the Wind” and “the Slice” nodes, are associated with current states. For example, the probability of strong current given that strong southwestern (northeastern) wind is prevailing is assumed to be 1 and the probability of mild current given that mild southwestern (northeastern) wind is prevailing is assumed to be 1. The states of this node are:

    (i) Mild current
    (ii) Moderate current
    (iii) Strong current

“The Slice” and “the Wind” nodes directly affect the Current node and “the Current” node directly affects the “Loss of control” node.

- Slice: This node represents the 13 sectors which are defined by [60] in order to calculate the geometric collision probabilities. The division is based upon the navigational and geographic differences. The states of this node are:

  (i) Sector 1
  (ii) Sector 2
  (iii) Sector 3
  (iv) Sector 4
  (v) Sector 5
  (vi) Sector 6
  (vii) Sector 7
  (viii) Sector 8
  (ix) Sector 9
  (x) Sector 10
  (xi) Sector 11
  (xii) Sector 12
  (xiii) Sector 13

  "The Slice node directly affects the "Current" and "the Transit vessel density" nodes.

- Local Vessel Density: This node gives consideration to the density of local traffic in the Strait. The conditional probabilities for the states of this node are estimated based on the data collected through active local traffic companies (such as Şehir Hatları, İDO and Turyol) timetables. Private vessel traffic and fishing boats are not considered. The states of this node are:

  (i) Low density local traffic
  (ii) Moderate density local traffic
  (iii) Dense local traffic

"The Day light" node directly affects "the Local vessel density" node and "the Local vessel density" node directly affects "the Attention" and "the Maneuver" nodes.

- Transit Vessel Density: This node groups the density of transit traffic in the Strait. The conditional probabilities for the states of this node are based on [60]. The states of this node are:

    (i) Low density transit traffic
    (ii) Moderate density transit traffic
    (iii)Dense transit traffic

"The Slice" node directly affects "the Transit vessel density" node and "the Transit vessel density" node directly affects "the Attention" node.

- Visibility: This node reflects the visibility conditions in the Strait. Due to fog, the Strait is closed when visibility is less than 0.5 nm. The conditional probabilities for the states of this node (conditioned regarding "the Season" node) are compiled through the DMI. The states of this node are:

    (i) Visibility more than 1 nm
    (ii) Visibility less than 1 nm

"The Season" node directly affects "the Visibility" node and "the Visibility" node directly affects "the Visual Detection" node.

- Ship types in lane: The Strait maritime traffic has been primarily uni-directional since 2005. However, small vessels (class D and F) and (rarely) passenger vessels (class P) may enter the Strait against the active direction. The conditional probabilities for the states of this node are estimated based on the VTS traffic data. The states of this node are:

    (i) Class D
    (ii) Class F
    (iii)Class P
    (iv)No oncoming ship

"The Ship types in lane" node directly affects "the Collision Type" and "the Give way situation" nodes.

4.2.2.2. Technical Factors. These factors, which are individually explained below, are those that affect the captain's maneuvering ability, while the captains are assumed to have some control over their vessels' status.

- Bridge Resource Management (BRM): According to the International Maritime Organization (IMO), BRM is the effective management tool that best enables the bridge team to use all available vessel resources with the aim that the voyage of vessel is safely completed [63]. The probabilities for the states of this node are gathered through expert opinion. The states of this node are:

    (i) Available
    (ii) Not available

"The BRM" node directly affects "the Assessment", "the Attention" and "the Navigational System Detection" nodes.

- Safety Culture: This node reflects the safety comprehension of the vessel crew. The probabilities for the states of this node are obtained through expert opinions. The states of this node are:

    (i) Perfect
    (ii) Standard

"The Safety Culture" node directly affects "the Fatigue", "the Maintenance quality" and "the Pilot Availability" nodes.

- Maintenance Quality: This node reflects the technical maintenance frequency and level of the vessel under consideration. The conditional probabilities for the states of this node are obtained via expert opinions. The states of this node are:

(i) Perfect
(ii) Standard

"The Safety culture" node directly affects" the Maintenance quality" node and "the Maintenance quality" node directly affects "the Machine failure", "the Steering failure" and "the Navigational System Detection" nodes.

- Machine Failure (Power Loss): This node provides for the engine failures of vessels in the Strait. The conditional probabilities for the states of this node are derived from previous accidents reported by the VTS. The states of this node are:

(i) Failure occurs
(ii) Failure does not occur

"The Maintenance quality" node directly affects "the Machine failure" node and "the Machine failure" node directly affects "the Loss of Control" node.

- Steering Failure: This node provides for the steerage failures of vessels in the Strait. The conditional probabilities for the states of this node are derived from previous accidents reported by the VTS. The states of this node are:

(i) Failure occurs
(ii) Failure does not occur

"The Maintenance quality" node directly affects "the Steering failure" node and "the Steering failure" node directly affects "the Loss of Control" node.

- Navigational System Detection: This node covers the interoperability of navigational tools such as radar, charts and GPS. The conditional probabilities for the states of this node are obtained through expert opinions. The states of this node are:

(i) May detect
(ii) May not detect

"The Maintenance quality" and "the BRM" nodes directly affect "the Navigational system detection" node and "the Navigational system detection" node directly affects "the Detection" node.

- Pilot Availability: According to the R&R, tankers and large, hazardous cargo carrying vessels have to take pilot captains during their transit in the Strait. This service is also recommended to other vessels, but they are not obliged to get this service. The conditional probabilities for the states of this node are obtained from the VTS statistics. The states of this node are:

    (i) Available
    (ii) Not available

"The Safety" culture node directly affects "the Pilot availability" node and "the Pilot availability" node directly affects "the Assessment" and "the Visual Detection" nodes.

- Officer on watch 2 (OOW2): While keeping a watch on the bridge, an officer on watch (OOW) is the representative of the ship's master and has the total responsibility of safe and smooth navigation of the ship. OOW is also in charge of the bridge team, which is there to support him in the navigation process. The probabilities for the states oh this node are obtained via expert opinion. The states of this node are:

    (i) Available
    (ii) Not available

"The OOW2" node directly affects "the OOW2 vigilance" node.

4.2.2.3. Human Factors. These factors, which are individually explained below, are those that affect the captain's maneuvering ability, while the captain is assumed to have full control over them.

- Fatigue: Vessel crew are assumed to have clear and well planned working schedules. However, occasionally, they may work overtime which causes fatigue. The conditional

probabilities for the states of this node are obtained from expert opinions. The states of this node are:

(i) Regular work hours
(ii) Overtime work

"The Safety culture" node directly affects "the Fatigue" node and "the Fatigue" node directly affects "the Attention" node.

- Familiarity: Being acquainted with the Strait makes the master of the ship navigate easily. The conditional probabilities for the states of this node are obtained from expert opinion. The states of this node are:

(i) Entirely familiar
(ii) Familiar
(iii) Unfamiliar

"The Familiarity" node directly affects "the Visual detection" node.

- OOW2 vigilance: This node measures the effect of availability of the second officer on watch (other than the navigator). The conditional probabilities for the states of this node are obtained via expert opinion. The states of this node are:

(i) OOW2 vigilant
(ii) OOW2 reckless

"The OOW2" node directly affects" the OOW2 vigilance" node and "the OOW2 vigilance" node directly affects "the Assessment" node.

- Attention: This node indicates the caution capability of the captain. The conditional probabilities for the states of this node are obtained via expert opinion. The states of this node are:

(i) Attentive
(ii) Inattentive

"The BRM", "the Fatigue" and "the Transit vessel density" nodes directly affect "the Attention" node and "the Attention" node directly affects "the Visual detection" node.

- Assessment: This node points out the judgement accuracy in case of being in a collision course. The conditional probabilities for the states of this node are obtained via expert opinion. The states of this node are:

(i) Correct assessment
(ii) Incorrect assessment

"The BRM", "the Detection", "the OOW2 vigilance" and "the Pilot availability" nodes directly affect "the Assessment" node and "the Assessment" node directly affects "the Loss of control" node.

- Detection: This node shows whether the captain recognizes an approaching danger by means of navigational equipment and visually. The conditional probabilities for the states of this node are obtained via expert opinions. The states of this node are:

(i) May detect
(ii) May not detect

"The Navigation system detection" and "the visual detection" nodes directly affect "the Detection" node and "the Detection" node directly affects" the Assessment" node.

- Loss of Control: This node indicates the inability to take control of the vessel. The conditional probabilities for the states of this node are obtained from expert opinions. The states of this node are:

(i) Exists
(ii) Does not exist

"The Assessment", "the Current", "the Machine failure" and "the Steering failure" nodes directly affect "the Loss of control" node and "the Loss of control" node directly affects "the Maneuver" node.

- Maneuver: This node is essential to prevent a potential collision by means of the captain's and/or oncoming vessel captain's abilities**.** The conditional probabilities for the states of this node are obtained via expert opinions. The states of this node are:

    (i) Vessel give way: This state corresponds to changing its course and giving the way to the other vessel.
    (ii) Other vessel give way: This state corresponds to the other vessel changing its course and giving the way to the vessel in consideration.
    (iii) Both give way: This state corresponds to both vessels changing their courses to avoid the approaching collision.
    (iv) None give way: This state corresponds to none of the vessels changing their courses in order to avoid the approaching collision.

"The Local vessel density", "the Loss of control" and "the Giveway situation" nodes directly affect "the Maneuver" node and "the Maneuver" node directly affects the "Collision Causation Factor" node.

- Collision Causation Factor: This is the target (final) node in order to estimate the collision causation probability, which is the probability of being unable to prevent collision for the collision candidate vessel. The conditional probabilities for the states of this node are obtained from expert opinions. The results of this node gives the collision causation probabilities. The states of this node are:

    (i) Occurs
    (ii) Does not occur

The Maneuver node directly affects the Collision Causation Factor node.

4.2.3. Collision Causation Probability (Factor) Results

As explained in Section 4.2.1, the Bayesian network model developed is deployed to estimate the Collision Causation Probabilities associated with vessels entering the Strait. In the most generic case, this probability is estimated regarding only the sailing direction of the vessel (northbound or southbound). This result reveals that probability of not taking evasive actions is higher in southbound traffic (4.7091% more probable than northbound traffic) (Table 4.5). This result is obtained under the assumption that no observed (preset) node exists.

Table 4.5. Collision causation probabilities in each direction.

Preset state of "the Direction" node	$P_{Caus}(\text{collision})$(*E-5)
Northbound	3.5896
Southbound	3.6619

Additionally, Collision Causation Probabilities are also estimated under some "preset node status" conditions, as explained below.

Class A and B vessels are obliged to get the pilotage service during their transit. Additionally, safety culture for these two classes are also almost always top notch. Therefore, for class A and B vessels, the states of the "Pilot Availability" and the "Safety Culture" nodes are preset as follows:

$$P(Availability = Available) = 1$$
$$P(Safety\ Culture = Perfect) = 1$$

The results show that, such setting of the Pilot Availability and the Safety Culture nodes decreases the collision causation probabilities as follows (Table 4.6):

Table 4.6. Collision causation probabilities for Class A (B) vessels.

Preset state of "the Vessel class" node	$P_{Caus}(\text{collision})$(*E-5)	% Decrease from the reference case
Northbound Class A (B)	3.5895	-0.0028%
Southbound Class A (B)	3.6618	-0.0027%

Next, the effect of season on causation probability is investigated by presetting “the season” node. Results are displayed in Table 4.7, which show that, captains’ ability/potential to avoid an oncoming collision is lowest in the winter season and highest in the summer season.

Table 4.7. Collision causation probabilities for vessels in each season.

Preset state of “the Season” node	P_{Caus}(collision)(*E-5)	% Change from the yearly average displayed in the reference case
Winter	3.6032	0.6219%
Spring	3.5850	1.1239%
Summer	3.5807	1.2425%
Autumn	3.5897	0.9943%

The collision causation probability in different time periods are given in Table 4.8. The results show that the causation probability is highest in the morning period and is lowest at nighttime. This result is in line with the fact that local traffic density increases the collision causation probability.

Table 4.8. Collision causation probabilities for vessels in different times of the day.

Preset state of "the Day light” node	P_{Caus}(collision)(*E-5) Northbound vessel	% Change from the yearly average displayed in the reference case	P_{Caus}(collision)(*E-5) Southbound vessel	% Change from the yearly average displayed in the reference case
Morning	4.1361	-15%	4.2121	-15%
Afternoon	3.7268	-4%	3.7958	-4%
Night	3.1706	12%	3.2424	11%

The effect of pilotage services on causation probability is shown in Table 4.9. Taking pilot during Strait transit dramatically increases the accident avoidance potential in both directions.

Table 4.9. Collision causation probabilities for vessels taking pilot service.

Preset state of "the Pilot service" node	P_{Caus}(collision)(*E-5) Northbound vessel	% Change from the yearly average	P_{Caus}(collision)(*E-5) Southbound vessel	% Change from the yearly average
Yes	3.5896	0.00%	3.6619	0.00%
No	3.5991	-0.26%	3.6714	-0.26%

The collision causation probability changes at different transit traffic densities as given in Table 4.10. The causation probability increases as intensity of transit traffic increases in both directions.

Table 4.10. Collision causation probabilities for vessels at different transit traffic densities.

Preset state of "the Transit Traffic	P_{Caus}(collision)(*E-5) Northbound vessel	% Change from the yearly average displayed in the	P_{Caus}(collision)(*E-5) Southbound vessel	% Change from the yearly average displayed in the
Low	3.589652	-0.00145%	3.661982	-0.00224%
Moderate	3.589653	-0.00148%	3.619834	1.14875%
High	3.589655	-0.00153%	3.661985	-0.00232%

The collision causation probability changes at several local traffic densities as given in Table 4.11. As expected, the probability increases as intensity of local traffic goes up in both directions.

Table 4.11. Collision causation probabilities for vessels at different local traffic densities.

Preset state of "the Local Traffic Density" node	P_{Caus}(collision)(*E-5) Northbound vessel	% Change from the yearly average displayed in the reference case	P_{Caus}(collision)(*E-5) Southbound vessel	% Change from the yearly average displayed in the reference case
Low	2.8409	21%	2.9209	20%
Moderate	3.4055	5%	3.4482	6%
High	4.7268	-32%	4.8181	-32%

The impact of machine failure on collision causation probability is presented in Table 4.12. As suspected, machine failure notably increases the maneuvering incapability.

Table 4.12. Collision causation probabilities for vessels experiencing machine failures.

Preset state of "the Machine failure" node	P_{Caus}(collision)(*E-5) Northbound vessel	% Change from the yearly average	P_{Caus}(collision)(*E-5) Southbound vessel	% Change from the yearly average
Occurs	4.1316	-15.10%	4.2040	-14.80%
Does not Occur	3.5892	0.01%	3.6614	0.01%

The effect of fatigue on collision causation probability is shown in Table 4.13. As suspected, overtime work increases the collision causation probability.

Table 4.13. Collision causation probabilities for vessels whose captains are in a state of fatigue.

Preset state of "the Fatigue" node	P_{Caus}(collision)(*E-5) Northbound vessel	% Change from the yearly average	P_{Caus}(collision)(*E-5) Southbound vessel	% Change from the yearly average
Regular	3.5896	1.87%	3.6619	1.56%
Overtime	3.5899	-7.20%	3.6622	-7.06%

The effect of attention on collision causation probability is given in Table 4.14. As expected, having "attentive" captains decreases the causation probability in both directions.

Table 4.14. Collision causation probabilities for vessels regarding "attention levels "of the captains.

Preset state of "the Attention"	P_{Caus}(collision)(*E-5) Northbound vessel	% Change from the yearly average	P_{Caus}(collision)(*E-5) Southbound vessel	% Change from the yearly average displayed in
Attentive	3.5223	-0.00%	3.6046	-1.9744%
Inattentive	3.8481	0.01%	3.9203	1.9662%

The effect of multiple preset nodes on collision causation probability is given in Table 4.15. As expected, causation probability significantly increases given that traffic direction, season, day light, current, transit and local traffic density, pilot availability and fatigue of the navigator are at their "most negative/undesirable" states.

Table 4.15. Collision causation probabilities for vessels with multiple nodes preset at their "most negative" states.

Node	Preset state of Node	P_{Caus}(collision) (*E-5)	% Change from the yearly average displayed in the reference case
Direction	Southbound	5.3747	47%
Season	Winter		
Day light	Morning		
Current	High		
Transit Vessel Density	Dense		
Local Vessel Density	Dense		
Pilot Availability	Not available		
Fatigue	Overtime		

4.3. Modeling and Analysis of Geometric Grounding Probability

Most studies on vessel grounding probabilities are also inspired by the research of [43]. The researcher estimated the grounding probability of a vessel (P_{RG}) as,

$$P_{RG} = P_{GeoGrn} * P_{CausGrn} \tag{4.16}$$

where: P_{Geo} is the probability of being in a "grounding course. P_{Caus} is the probability of failing to take evasive actions in order to avoid grounding.

The researcher also asserted that the geometrical probability of random grounding (assuming random navigation through a waterway) can be estimated as:

$$P_{GeoGrn} = \frac{4 * T}{\pi * C} \tag{4.17}$$

where, T is the track length (or stopping distance) of the vessel. T is also a function of the size and speed of the ship, which is estimated to be roughly equal to 20 times of the length of the ship [3]. C is the width of the waterway. However, [43] applied this equation in the Dover Strait, which is almost 20 times wider than Istanbul Strait. The VTS experts and pilots claim that estimation for track length (20*L) does not account for narrow waterway conditions. Therefore, a new formula becomes necessary.

On the other hand**,** [64] considered the importance of dynamic situation of vessels and modified the [43] formula as:

$$P_{Geo} = \frac{4 * T}{\pi C} = \frac{4 * (V * \alpha)}{\pi C} \tag{4.18}$$

where:

- V: is the speed of the vessel under consideration
- α: is the average duration between two consecutive position checks (or course alterations) of the vessel

Just like [43], the formula of [64] does not give sufficient consideration to the "extreme narrowness "of the waterway which effects the geometric likelihood of grounding. Moreover, both studies consider the geometric probability of hitting the shores of almost wide open seas, whereas in the Strait, it is essential to estimate the probability of running aground at the turning points.

4.3.1. A New Proposal for Estimating the Geometric Grounding Probability in Narrow Waterways

Based on the discussions in the previous section, we propose to estimate the geometric grounding probability $P_{Geo(ij)}$ for a vessel *i* navigating along a narrow waterway at sector *j:*

$$P_{Geo(ij)} = \begin{cases} \frac{T_i}{L_j} = \frac{V_{ij*\alpha}}{L_j} & if \quad \frac{T_i}{L_j} < 1 \\ 1 & if \quad \frac{T_i}{L_j} \geq 1 \end{cases} \tag{4.19}$$

where:

- T_i is the track length (stopping distance) of ship class i
- L_j is the length of sector j (of the waterway)
- V_{ij} is the speed of vessel i at sector j (of the waterway)
- α is the average time interval for successive position checks.

There are 12 major turning points in the Istanbul Strait where captains adjust/reset their course. The approximate transiting time in the Strait is 90 minutes, therefore the value of α is estimated as follows:

$$\alpha = \frac{90}{12} = 7.5 \text{ minutes} = \frac{1}{8} hours$$

In this study, the Strait is divided into 13 sectors. The geometric grounding probability in the Strait is basically the probability that the vessel will hit the shore at the turning points (endpoints) of the sectors while transiting in the Strait.

In order to estimate the geometric grounding probability for each vessel (i) at each sector (j), the average velocity V_{ij} and the length of each sector L_j are found for each of those sectors whereas α is considered constant (7.5 minutes). The length of each sector is given in Figure 4.5. Sector 3 is the longest and Sector 2 is the shortest sectors respectively and average sector length is 1.27 nm.

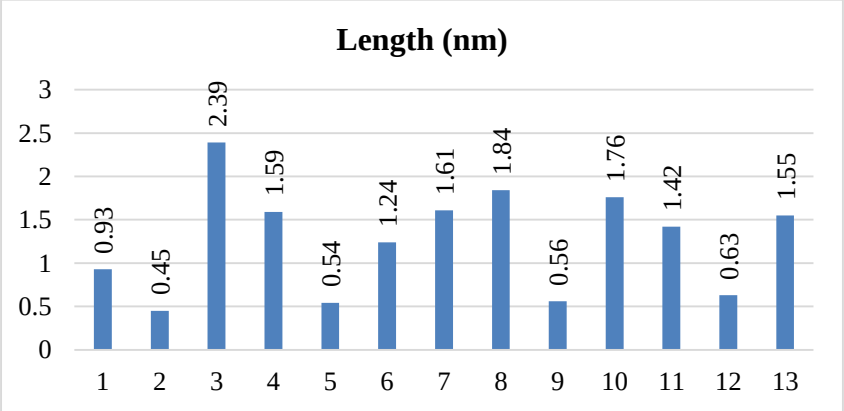

Figure 4.5. Lengths of sectors in the Strait.

Speed of vessels vary according to their vessel class, direction and the sector they are transiting. According to Figure 4.6, southbound vessels in all classes have higher speed than

that of northbound classes. The slowest vessels are class F vessels (small, Turkish flagged vessels) navigating in both directions and the fastest vessels are southbound class B vessels.

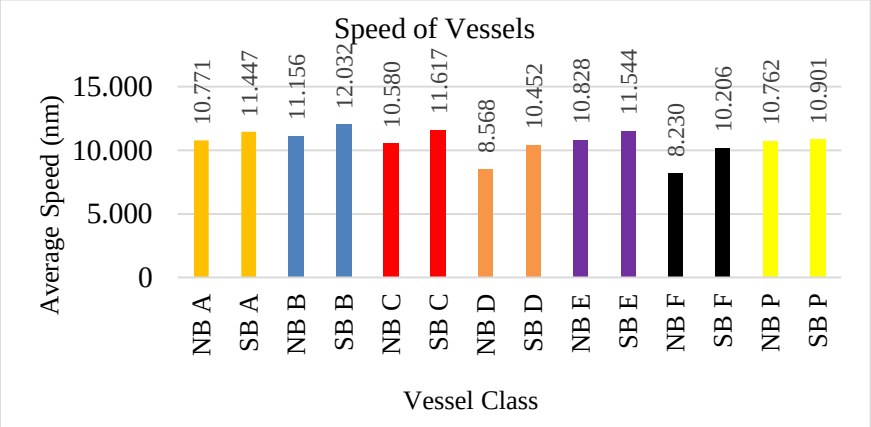

Figure 4.6. Average speed of vessels in the Strait.

According to [60], the speeds of vessels differ in each sector with respect to the vessel class. The speed of each vessel class in either direction is shown in Table 4.16 and Table 4.17, respectively. The results show that in sectors 1,2,3 and 13 vessels move slower than average in the northbound direction. Each vessel class reaches its highest speed in sector 9.

Table 4.16. Average speed of northbound vessels at each sector.

Speed of Vessel Classes (knots)							
Sector	North-bound_A	North-bound_B	North-bound_C	North-bound_D	North-bound_E	North-bound_F	North-bound_P
1	9.92	10.27	9.74	7.89	9.97	7.58	9.91
2	10.68	11.07	10.49	8.49	10.74	8.16	10.68
3	10.09	10.45	9.91	8.03	10.15	7.71	10.08
4	10.94	11.33	10.75	8.71	11.00	8.36	10.93
5	11.07	11.47	10.88	8.81	11.13	8.46	11.06
6	10.72	11.10	10.53	8.53	10.77	8.19	10.71
7	11.35	11.76	11.15	9.03	11.41	8.67	11.34
8	11.23	11.64	11.03	8.94	11.29	8.58	11.22
9	11.99	12.43	11.79	9.54	12.06	9.17	11.99
10	11.05	11.45	10.86	8.79	11.11	8.44	11.04
11	11.18	11.58	10.98	8.89	11.24	8.54	11.17
12	11.44	11.85	11.24	9.09	11.20	8.74	11.43
13	10.92	11.31	10.73	8.69	10.98	8.35	10.91

The results in Table 4.17 show that in sectors 11, 12 and 13 vessels move slower than average in the southbound direction. Each vessel class reaches its highest speed in sector 3.

Table 4.17. Average speed of southbound vessels at each sector.

Speed of Vessel Classes (knots)							
Sector	South-bound A	South-bound B	South-bound C	South-bound D	South-bound E	South-bound F	South-bound P
1	11.89	12.50	12.07	10.86	9.97	10.60	10.03
2	12.29	12.92	12.48	11.23	10.74	10.96	10.81
3	12.89	13.55	13.08	11.77	10.15	11.49	10.21
4	12.40	13.03	12.58	11.32	11.00	11.05	11.08
5	12.03	12.65	12.21	10.99	11.13	10.73	11.21
6	11.58	12.18	11.76	10.58	10.77	10.33	10.85
7	11.41	11.99	11.58	10.42	11.41	10.18	11.49
8	11.29	11.88	11.47	10.32	11.29	10.07	11.37
9	11.78	12.38	11.95	10.76	12.062	10.50	12.14
10	11.73	12.33	11.91	10.71	11.11	10.46	11.18
11	10.49	11.03	10.65	9.58	11.25	9.36	11.32
12	9.81	10.31	9.96	8.96	11.50	8.75	11.58
13	9.20	9.67	9.34	8.40	10.98	8.21	11.05

When formula 3.15 is applied to the data presented in Tables 3.16 and 3.17, the results (as summarized in Table 4.18) show that regarding the northbound vessels in the Strait, the geometric grounding probability is generally high, which implies that, a vessel navigating blindly in the Strait, most probably grounds at or close to the endpoints of the sections. On the other hand, since Sector 3 is the longest sector, in this sector, the grounding geometric probabilities for all vessel types are less than geometric probabilities of other vessels at other sectors. Additionally, northbound class D and class F are small vessels having lower tracking lengths (they are slower than other vessels); therefore, geometric grounding probability of these vessel types are lower in various sectors.

Table 4.18. Geometric grounding probability of northbound vessels.

Geometric Grounding Probability							
Vessel Class							
Sector	North-bound A	North-bound B	North-bound C	North-bound D	North-bound E	North-bound F	North-bound P
1	1.00	1.00	1.00	1.00	1.00	1.00	1.00
2	1.00	1.00	1.00	1.00	1.00	1.00	1.00
3	0.53	0.55	0.52	0.42	0.53	0.40	0.53
4	0.86	0.89	0.85	0.68	0.86	0.66	0.86
5	1.00	1.00	1.00	1.00	1.00	1.00	1.00
6	1.00	1.00	1.00	0.86	1.00	0.83	1.00
7	0.88	0.91	0.87	0.70	0.89	0.67	0.88
8	0.76	0.79	0.75	0.61	0.77	0.58	0.76
9	1.00	1.00	1.00	1.00	1.00	1.00	1.00
10	0.81	0.84	0.80	0.65	0.82	0.62	0.81
11	0.98	1.00	0.97	0.78	0.99	0.75	0.98
12	1.00	1.00	1.00	1.00	1.00	1.00	1.00
13	0.88	0.91	0.87	0.70	0.89	0.67	0.88

In a similar fashion, the results in Table 4.19 show that, regarding the southbound traffic in the Strait, the geometric grounding probability is generally high, which implies that, a vessel navigating blindly in the Strait, most probably grounds at the endpoints of the sections. On the other hand, since Sector 3 is the longest sector, the grounding geometric probabilities for all vessel types are less than geometric probabilities of other southbound vessels at other sectors. Additionally, southbound class D and class F are small vessels which have lower tracking length (slower than other vessels) therefore; on average geometric grounding probability of these vessel types are lower.

Table 4.19. Geometric grounding probability of southbound vessels.

Geometric Grounding Probability							
	Vessel Class						
Sector	South-bound A	South-bound B	South-bound C	South-bound D	South-bound E	South-bound F	South-bound P
1	1.00	1.00	1.00	1.00	1.00	1.00	1.00
2	1.00	1.00	1.00	1.00	1.00	1.00	1.00
3	0.67	0.71	0.68	0.62	0.53	0.60	0.53
4	0.97	1.00	0.99	0.89	0.86	0.87	0.87
5	1.00	1.00	1.00	1.00	1.00	1.00	1.00
6	1.00	1.00	1.00	1.00	1.00	1.00	1.00
7	0.89	0.93	0.90	0.81	0.89	0.79	0.89
8	0.77	0.81	0.78	0.70	0.77	0.68	0.77
9	1.00	1.00	1.00	1.00	1.00	1.00	1.00
10	0.86	0.91	0.88	0.79	0.82	0.77	0.82
11	0.92	0.97	0.94	0.84	0.99	0.82	1.00
12	1.00	1.00	1.00	1.00	1.00	1.00	1.00
13	0.74	0.78	0.75	0.68	0.89	0.66	0.89

The results displayed in Table 4.18 and 4.19 show that geometric grounding probability for a class A vessel in either direction is lowest in sector 3 (the longest sector), and sector 13 at southbound traffic (the lowest speed). Geometric grounding probability for Class B vessels in either direction are high. Geometric grounding probability for Class C vessels in either direction are more than 0.9 except sector 3. Since speed of Class D vessels are low, geometric grounding probability is less than 1 at sectors 3, 4, 6, 7, 8, 10, 11 and 13. However, southbound vessels are faster than northbound vessels therefore; geometric grounding probability is less than 1 at sectors 3, 8, 10 and 13. Similar to class A vessel, geometric grounding probability for class E vessel in either direction are 1 except sector 3 (the longest sector) and sector 13 at southbound traffic (the lowest speed). Similar to class D vessel, geometric grounding probability is less than 1 at sectors 3, 4, 8, 10 and 13. However, southbound vessels are faster than northbound vessels therefore; geometric grounding probability is less than 1 at sectors 3, 8 and 13. Geometric grounding probability for Class P vessels in either direction are 1 except sector 3.

Since geometric grounding probability for all vessel classes are generally high, the grounding causation probability (which estimates the capability of the captain to prevent grounding when navigating blindly) become important.

4.4. Grounding Causation Probability

As explained in Section 4.3, causation probability ($P_{Caus}(\text{grounding})$) is the probability of being incapable of doing evasive action in order to prevent grounding. In other words, $P_{Caus}(\text{grounding})$ is the probability that in a vessel, which is on a grounding course, the captain makes no move or is unable to avoid grounding accident.

In this study, a Bayesian network is built and solved through the Matlab package in order to estimate grounding probabilities ($P_{Caus}(\text{grounding})$) of vessel classes in different sectors. In order to visualize the network Figure 4.7 is developed through the software Genie. For instance, according to Figure 4.7, the probability that vessel having machine failure given that maintenance quality being perfect is 0.001.

The grounding causation probability Bayesian Network resembles collision causation probability network in many nodes. However, some nodes and the related (inflow and outflow) arcs specific to collision accidents are omitted in the grounding accidents network. These are:

- Ship types in lane
- Maneuver
- Collision causation factor

On the other hand, two new nodes are added in building the grounding causation probability network. These are explained below.

- Action: This node is essential to prevent the grounding by means of the captain's abilities**.** The conditional probabilities for the states of this node are obtained via expert opinion. The states of the node are:

  (i) Correct
  (ii) Incorrect

"The Action" node directly affects "the Grounding Causation Factor" node.

- Grounding Causation Factor: This is the target (final) node in order to estimate the grounding causation probability, which is the probability of being unable to prevent grounding for the grounding candidate vessel. The conditional probabilities for the states of this node are derived from expert opinion. The results of this node gives the grounding causation probabilities. The states of the node are:

  (i) Occurs
  (ii) Does not occur

4.4.1. Grounding Causation Probability (Factor) Results:

The Bayesian Network designed and explained in the previous section is used to individually estimate the Grounding Causation Probabilities regarding the direction of vessels entering the Strait. The results reveal that taking evasive actions is more probable in northbound traffic (6.639 %). This result is obtained under the assumption that no evidence node exists (Table 4.20).

Table 4.20. Grounding causation probabilities in each direction.

Preset state of "the Direction" node	$P_{Caus}(\text{grounding})(E-6)$
Northbound	4.8915
Southbound	5.2192

Class A and B vessels are obliged to get the pilotage service during their transit. Therefore, for class A and B vessels in the Bayesian network for grounding,

$$P(Availability = Available) = 1$$
$$P(Safety\ Culture = Perfect) = 1$$

The results show that such setting of the Pilot Availability and Safety Culture decreases the grounding causation probability in either direction (Table 4.21).

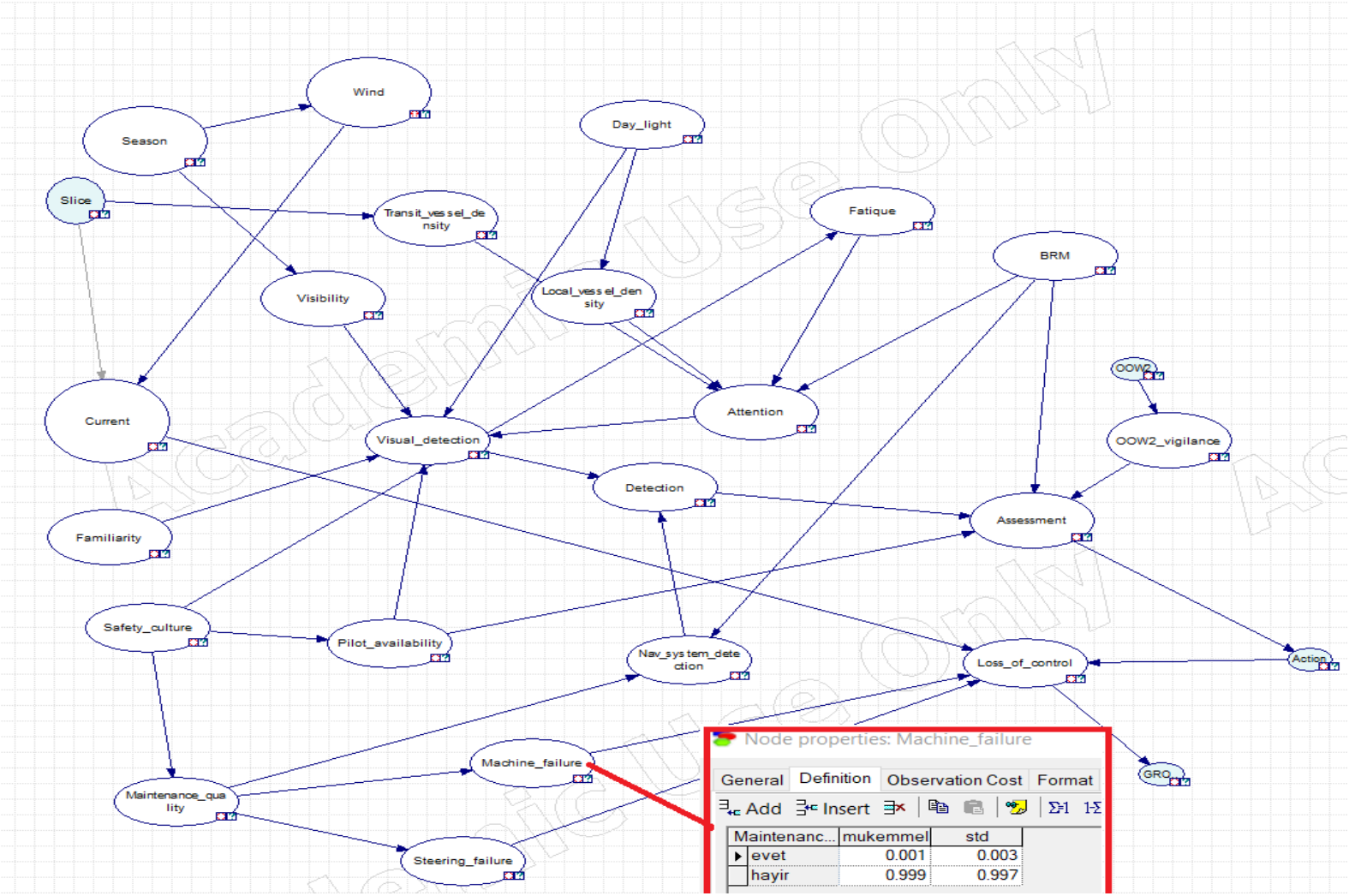

Figure 4.7. Bayesian Network designed for estimating Grounding Causation Probabilities.

Table 4.21. Grounding causation probabilities for Class A (B) vessels.

Preset state of "the Vessel class" node	P_{Caus}(grounding)(*E-6)	% Decrease from the reference case
Northbound Class A (B)	4.3019	-12.05%
Southbound Class A (B)	4.5883	-12.09%

The grounding causation probability for each slice is represented in Table 4.22. High transit vessel density at sectors 4, 5 and 9 in northbound traffic and sectors 5 and 9 in southbound traffic make maneuvering more difficult therefore; grounding causation probabilities are higher at those sectors.

Table 4.22. Grounding causation probabilities for vessels at each sector.

Preset state of "the Slice" node	P_{Caus}(grounding)(*E-6) Northbound	% Change from Strait average in the reference case	P_{Caus}(grounding)(*E-6) Southbound	% Change from Strait average in the reference case
1	4.8915	-0.001%	5.2149	0.082%
2	4.8915	-0.001%	5.2163	0.056%
3	4.8902	0.026%	5.2163	0.056%
4	4.8902	0.026%	5.2163	0.056%
5	4.8902	0.026%	5.2176	0.030%
6	4.8915	-0.001%	5.2163	0.056%
7	4.8915	-0.001%	5.2163	0.056%
8	4.8915	-0.001%	5.2163	0.056%
9	4.8902	0.026%	5.2177	0.030%
10	4.8915	-0.001%	5.2149	0.082%
11	4.8915	-0.001%	5.2163	0.056%
12	4.8915	-0.001%	5.2163	0.056%
13	4.8903	0.025%	5.2163	0.056%

The effect of season on causation probability is given in Table 4.23. Regarding the results, in winter captains are not vigilant enough to take control of the grounding candidate vessel whereas in summer undesired meteorological conditions such as fog are rare. Therefore, evasive actions are easier to take.

Table 4.23. Grounding causation probabilities for vessels in each season.

Preset state of "the Season" node	P_{Caus}(grounding)(*E-6)	% Change from the yearly average displayed in the reference case
Winter	5.5691	13.85%
Spring	4.6629	-4.67%
Summer	4.4297	-9.44%
Autumn	4.9041	-0.26%

The grounding causation probability at several time periods are given in Table 4.24. The results show that since visual detection is more difficult at night, identifying the danger at the grounding area is harder and day light enables the captain detecting the danger in the morning.

Table 4.24. Grounding causation probabilities for vessels in different times of the day.

Preset state of "the Day light" node	P_{Caus}(grounding)(*E-6) Northbound vessel	% Change from the yearly average displayed in the reference case	P_{Caus}(grounding)(*E-6) Southbound vessel	% Change from the yearly average displayed in the reference case
Morning	4.8808	-0.22%	5.2048	-0.28%
Afternoon	4.8873	-0.09%	5.2118	-0.14%
Night	4.9004	0.18%	5.2258	0.13%

The effect of pilotage services on grounding causation probability is shown in Table 4.25. In both directions, taking pilot during transiting the Strait dramatically increases the accident avoiding likelihood.

Table 4.25. Grounding causation probabilities for vessels taking pilot service.

Preset state of "the Pilot service" node	P_{Caus}(grounding)(*E-6) Northbound vessel	% Change from the yearly average displayed in the reference case	P_{Caus}(grounding)(*E-6) Southbound vessel	% Change from the yearly average displayed in the reference case
Yes	4.3840	-10%	4.6757	-10%
No	50.414	931%	50.766	873%

The grounding causation probability changes at several transit traffic densities as given in Table 4.26. As expected, the probability increases as intensity of transit traffic goes up in both directions.

Table 4.26. Grounding causation probabilities for vessels at different transit traffic densities.

Preset state of "the Transit Traffic Density" node	P_{Caus}(grounding)(*E-6) Northbound vessel	% Change from the yearly average displayed in the reference case	P_{Caus}(grounding)(*E-6) Southbound vessel	% Change from the yearly average displayed in the reference case
Low	4.8903	-0.00145%	5.2149	-0.00224%
Moderate	4.8915	-0.00148%	5.2163	1.14875%
High	4.8928	-0.00153%	5.2177	-0.00232%

The grounding causation probability changes at several current intensities as given in Table 4.27. As expected, the causation probability increases as current gets more violent at both directions.

Table 4.27. Grounding causation probabilities for vessels at different current intensities.

Preset state of "the Current" node	P_{Caus}(grounding)(*E-6) Northbound vessel	% Change from the yearly average displayed in the reference case	P_{Caus}(grounding)(*E-6) Southbound vessel	% Change from the yearly average displayed in the reference case
Mild	2.8853	-41%	3.2100	-38%
Moderate	7.0285	44%	7.3506	41%
Strong	9.7436	99%	10.007	-92%

The impact of machine failure on grounding causation probability is presented in Table 4.28. As proposed, machine failure notably increases the loss of control at both directions.

Table 4.28. Grounding causation probabilities for vessels at machine failure condition.

Preset state of "the Machine failure" node	P_{Caus}(grounding)(*E-6) Northbound vessel	% Change from the yearly average displayed in the reference case	P_{Caus}(grounding)(*E-6) Southbound vessel	% Change from the yearly average displayed in the reference case
Occurs	424.99	8588%	424.99	8588%
Does not	0.72	-85%	0.72	-85%

The effect of fatigue on grounding causation probability is shown in Table 4.29. Overtime work increases the grounding causation probability.

Table 4.29. Grounding causation probabilities for vessels with fatigue state of the captain.

Preset state of "the Fatigue" node	P_{Caus}(grounding)(*E-6) Northbound vessel	% Change from the yearly average displayed in the reference case	P_{Caus}(grounding)(*E-6) Southbound vessel	% Change from the yearly average displayed in the reference case
Regular	4.9972	-2%	4.9972	-2%
Overtime	6.4008	31%	6.4008	31%

The effect of attention on grounding causation probability is given in Table 4.30. As expected, paying attention decreases the causation probability in both directions.

Table 4.30. Grounding causation probabilities for vessels with attention capability of the captain.

Preset state of "the Attention" node	P_{Caus}(grounding)(*E-6) Northbound vessel	% Change from the yearly average displayed in the reference case	P_{Caus}(grounding)(*E-6) Southbound vessel	% Change from the yearly average displayed in the reference case
Attentive	5.2004	6%	5.2004	6%
Inattentive	5.2880	-1%	5.2880	-1%

Another scenario analysis is conducted when vessel arrival rate is increased by 10 per cent and the visibility factor is added. Results of 24 scenarios show that visibility is the most critical factor for performance measures and its interaction with minimum pursuit distance at different levels is also significant for performance measures such as average waiting time of vessels, number of vessels passed and pilot utilization.

The results of the study reveal that increase in vessel demand or long lasting fog conditions on the Strait lead to very dense vessel traffic, which may cause high risk on the Strait may be somewhat eased by reducing pursuit distances and / or deploying higher number of pilots. However, the risk impacts of such decision effecting vessel waiting times, pursuit distances, pilot utilization and vessel density are beyond the scope of this study.

5. NUMBER OF VESSEL COLLISIONS AND GROUNDINGS IN THE STRAIT OF ISTANBUL BASED ON THE DEVELOPED MODEL

In this study the probabilistic risk analysis in the Strait is conducted through integrating the physical conditions that lead to collisions and grounding and technical, environmental and personal factors that strengthen the ability to prevent vessel accidents.

Let $P_{RC}(i, sec)$ be the probability of vessel *i* colliding at sector *sec* and as described in equation (4.4):

$$P_{RC}(i, sec) = P_{GeoColl}(S(i), sec) * P_{CausColl}(i, sec) \quad (5.1)$$

where,

- $P_{GeoColl}(S(i), sec)$ is the geometric collision probability for vessel *i* (member of class *S*) at sector *sec* (i.e. probability of vessel *i* being on a collision course),
- $P_{CausColl}(i, sec)$ is the collision causation probability for vessel i at sector sec,
- S is the class of all vessels entering the Strait.

Let $X_{collision}$ be the random variable representing the number of vessels which collides in a collision accident for n vessels and 13 sectors and $x_{(i,sec)}$ be the specific states indicating whether there is a collision ($x_{(i,sec)} = 1$) or no collision ($x_{(i,sec)} = 0$) for a specific vessel, *i*, at a specific sector, *sec*.

Then the expected number of collisions is computed by the formulas:

$$N_{collision} = E[X_{collision}] \quad (5.2)$$

$$N_{collision} = \sum_{i=1}^{n} \sum_{sec=1}^{13} x_{(i,sec)} * P_{RC}(i, sec) \quad (5.3)$$

where,

- $N_{collision}$ is the expected number of collisions,
- n is the number of all vessels entering the Strait at the considered time period (one year in this study).

Accordingly,

$$N_{collision/_{100,000}} = \frac{N_{collision}}{n} * 100{,}000 \tag{5.4}$$

where, $N_{collision/_{100,000}}$ is the expected number of collisions per 100,000 transiting vessels.

Let $\mathrm{P_{RG}}(i, sec)$ be the probability of vessel *i* grounding at sector *sec* and as described in equation (4.5):

$$\mathrm{P_{RG}}(i, sec) = P_{GeoGrn}(S(i), sec) * P_{CausGrn}(i, sec) \tag{5.5}$$

where,

- $P_{GeoGrn}(S(i), sec)$ is the geometric groundibg probability for vessel *i* (member of class S) at sector *sec* (i.e. probability of vessel *i* being on a grounding course),
- $P_{CausGrn}(i, sec)$ is the grounding causation probability for vessel i at sector sec,
- S is the class of all vessels entering the Strait,

Let $X_{grounding}$ be the random variable representing the number of vessels which grounds for n vessels and 13 sectors and $x_{(i,sec)}$ be the specific states indicating whether there is a grounding($x_{(i,sec)} = 1$) or no grounding ($x_{(i,sec)} = 0$) for a specific vessel, *i*, at a specific sector, *sec*.

Then the expected number of groundings is computed by the formulas:

$$N_{grounding} = E\left[X_{grounding}\right] \tag{5.6}$$

$$N_{grounding} = \sum_{i=1}^{n} \sum_{sec=1}^{13} x_{(i,sec)} * \mathrm{P_{RG}}(i, sec) \quad (5.7)$$

where,

- $N_{grounding}$ is the expected number of groundings,
- n is the number of all vessels entering the Strait at the considered time period (one year in this study).

Accordingly,

$$N_{grounding_{/100,000}} = \frac{N_{grounding}}{n} * 100{,}000 \quad (5.8)$$

where, $N_{grounding_{/100,000}}$ is the expected number of groundings per 100,000 transiting vessels.

In order to estimate the number of collisions and groundings per year, the simulation model (replicated 20 times), which mimics the Strait transit vessel traffic is utilized. At each simulation run, the vessel class, length, entrance direction, entrance date and time to each sector are recorded. This information provide input for geometric and causation probability estimations of the transiting vessels.

5.1. Analysis of Model Generated Collisions

Regarding the comparison of the collision probabilities and estimated number of collisions generated by the model with the actual number of collisions in the study period, first the study period is taken as 2005-2016 (since one-way traffic started on 01 August 2005). Since the number of actual collisions is quite small, even in 12-year duration, the whole study period data is considered, while the overall average vessel arrival rates are assumed as the model inputs.

As the main scenario, the results of an average one year simulation run is taken into consideration, as displayed in Table 5.1. According to the results, on the average 0.825 collisions per year are predicted by the mathematical model (with the left and right prediction

interval (PI) limits at α=0.025). Although the actual number of collisions is out of that range, the predicted number of collisions is close to the recorded number of collisions per year.

Table 5.1. Collisions in the main scenario.

Number of Collisions in the Main Scenario	
average	0.83
standard deviation	0.01
PI_left	0.80
PI_right	0.86

On the other hand, actually there have been 9 collisions inside the Strait between 2005 and 2016, which result in 0.79 collisions per year [65]. While this actual annual average value is out of the prediction interval range predicted by the model, the predicted average number (0.8252 collisions/year) is not way off the actual average number (0.79 collisions/year): an overestimation of the annual number of collision by 3.8%. Additionally, as displayed in Table 5.2, the predicted number of collisions per 100,000 vessels are even close to the actual number of collisions per 100,000 vessels: The model overestimates the number of collisions per 100,000 vessels by only 2.5%.

Table 5.2. Comparison of number of collisions in the main scenario.

Collisions	Number of Collision	Number of Years Observed	Total Vessel Entrances	Collisions /year	Collisions /100,000 vessels	Impacted Vessels per 100,000 vessels
Actual Number of Collisions	9	11.4	556834	0.79	1.62	3.23
Collision Resulting from the	0.825	1	49798	0.83	1.66	3.31

Next, the annual number of collisions predicted by the model and the actual annual average of the 2005-2016 period are compared with respect to season and time of day (daylight versus nighttime).

Figure 5.1 displays the effect of season on the estimated and actual number of collisions. In the observed time period (2005-2016), collisions occur more often in summer and in winter, while the least number of collisions are in autumn. In the mathematical model collision frequency is also higher in summer, then in winter and lowest in autumn. Therefore, the model is quite successful in mimicking the season effect on number of collisions (even though the low number of actual collision cases do not allow a reliable comparison).

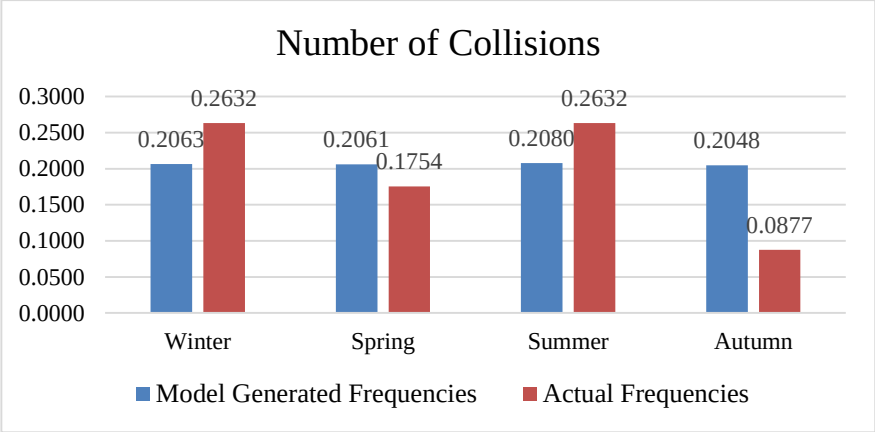

Figure 5.1. Collisions at each season in the main scenario.

Figure 5.2 displays the effect of day light on the estimated and actual number of collisions. In the observed data, most collisions occur at night, while least collisions occur in the morning hours. The model, on the other hand, predicts highest collision frequency for nighttime and the lowest frequency for the afternoon hours.

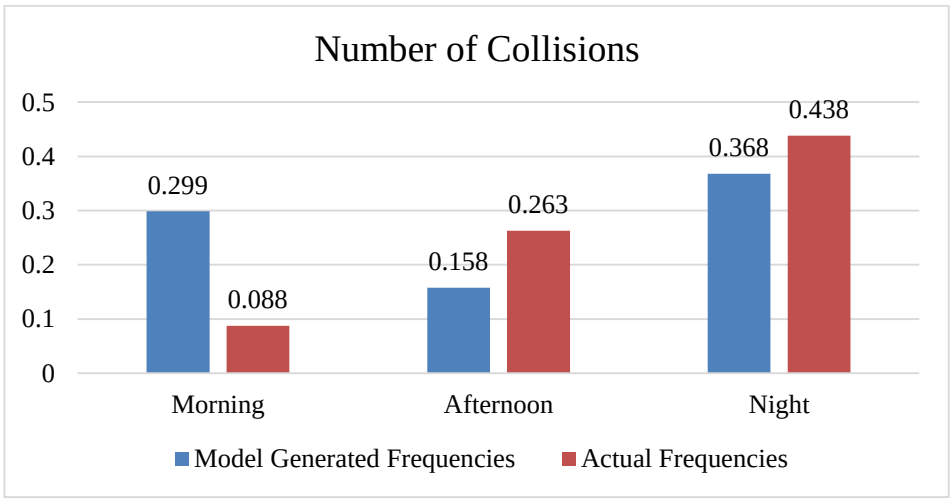

Figure 5.2. Collisions at different times of day in the main scenario.

The effect of traffic direction on the estimated and actual number of collisions is also analyzed in this study. In the observed data, 55.6 % of collisions involve northbound vessels, whereas in the model generated results, 50.25 of the collisions involve northbound vessels.

Table 5.3 displays the effect of northbound vessel classes on the estimated and actual number of collisions. In the observed data, most such collisions involve northbound short dry cargo vessels (which are classified as NB D in this study) followed by long dry cargo vessels (which are classified as NB C in this study); while the same two class of northbound vessels feature the highest frequency of collisions (and in the same order) in the model generated results as well. Still the low number of actual cases per vessel class do not allow for a reliable comparison

Table 5.3. Number of collisions involving northbound vessels.

Vessel Type	Number of Collisions	
	Model Generated Frequencies	Actual Frequencies
NB_A	0.01	0.00
NB_B	0.02	0.00
NB_C	0.08	0.09
NB_D	0.28	0.26
NB_E	0.00	0.00
NB_F	0.02	0.09
NB_P	0.01	0.00

Table 5.4 displays the effect of southbound vessel classes on the estimated and actual number of collisions. In observed data, most such collisions involve southbound long dry cargo vessels (which are classified as SB D in this study) followed by short dry cargo vessels (which are classified as SB C in this study); southbound D vessels feature the highest frequency of collisions in the model generated results as well. Still the low number of actual cases per vessel class do not allow for a reliable comparison.

Table 5.4. Number of collisions involving southbound vessels.

Vessel Type	Number of Collisions	
	Model Generated Frequencies	Actual Frequencies
SB_A	0.01	0.00
SB_B	0.02	0.00
SB_C	0.07	0.00
SB_D	0.28	0.26
SB_E	0.000	0.00
SB_F	0.020	0.09
SB_P	0.005	0.00

5.2. Analysis of Model Generated Groundings

Regarding the comparison of the grounding probabilities and estimated number of groundings generated by the model with the actual number of groundings in the study period, first the study period is taken as 2001-2016 to make use of a larger data set. In this regard, the experts interviewed expressed that one-way/two-way traffic separation schemes have negligible effect on groundings.

As the main scenario, the results of an average one year simulation runs is taken into consideration, as displayed in Table 5.5. According to the results, on the average 2.34 groundings per year are predicted by the mathematical model (with the left and right prediction interval (PI) limits at α=0.025). Although the actual number of groundings is out of that range, the predicted number of groundings is close to the recorded number of groundings per year.

Table 5.5. Groundings in the main scenario.

Number of Groundings in the Main Scenario	
average	2.34
standard deviation	0.04
PI_left	2.25
PI_right	2.43

On the other hand, actually there have been 34 groundings inside the Strait between 2001 and 2016 which results in 2.13 groundings per year [65]. While this actual annual average value is out of the prediction interval range predicted by the model, the predicted average number (2.34 groundings/year) is not way off the actual average number (2.13 groundings/year): an overestimation of the annual number of groundings by 9%. Additionally, as displayed in Table 5.6, the predicted number of groundings per 100,000 vessels are even close to the actual number of groundings per 100,000 vessels: The model overestimates the number of groundings per 100,000 vessels by only 3.4%.

Table 5.6. Comparison of number of groundings in the main scenario.

Comparison for Main Scenario	Number of Groundings	Number of Years Observed	Total Vessel Entrances	Groundings /year	Groundings /100,000 vessels
Actual Number of Groundings	34	16	748257	2.13	4.54
Grounding Resulting from the Model	2.34	1	49798	2.34	4.70

Next the annual number of groundings predicted by the model and the actual annual average of the 2001-2016 period are compared with respect to sectors.

The low number of actual groundings in the study period do not really permit for a reliable sectoral analysis. Nevertheless, Table 5.7 displays the frequency of groundings at each sector, as estimated by the model and the actual case (for the years 2001 to 2016). According to the model results, groundings most frequently occur at sector 5. In the actual case, groundings most frequently occur in sector 8. So, as pointed out, the model does not correctly mimick the actual groundings in 13 sectors, primarily because of the very low level of actual cases per sector.

Table 5.7. Groundings at each sector in the main scenario.

Sector	Number of Groundings	
	Model Generated Frequencies	Actual Frequencies
1	0.077	0.125
2	0.08	0.000
3	0.065	0.188
4	0.078	0.000
5	0.08	0.063
6	0.078	0.063
7	0.078	0.563
8	0.075	0.875
9	0.08	0.063
10	0.075	0.063
11	0.074	0.063
12	0.08	0.000
13	0.078	0.063

Next the annual number of groundings predicted by the model and the actual annual average of the 2001-2016 period are compared with respect to season and time of day (daylight versus nighttime).

Figure 5.3 displays the effect of season on the estimated and actual number of groundings. In the observed time period (2001-2016), groundings occur more often in summer, while the least number of groundings are in spring. In the mathematical model, grounding frequency is higher in winter and lowest in summer. Therefore, the model is not successful in mimicking the season effect on number of groundings. The model predictions regarding seasonal variations is not good, since the number of actual groundings per season is low for a reliable comparison.

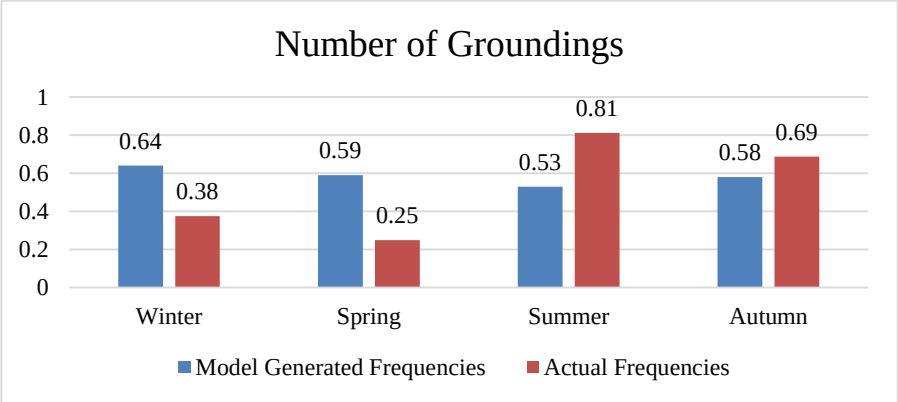

Figure 5.3. Groundings at each season in the main scenario.

Figure 5.4 displays the effect of day light on the estimated and actual number of groundings. In the observed data, most groundings occur at night, while least groundings occur in the afternoon hours. Accordingly, the model predicts highest grounding frequency for nighttime and the lowest frequency for the afternoon hours. Therefore, the model is successful in mimicking the day light effect on number of groundings.

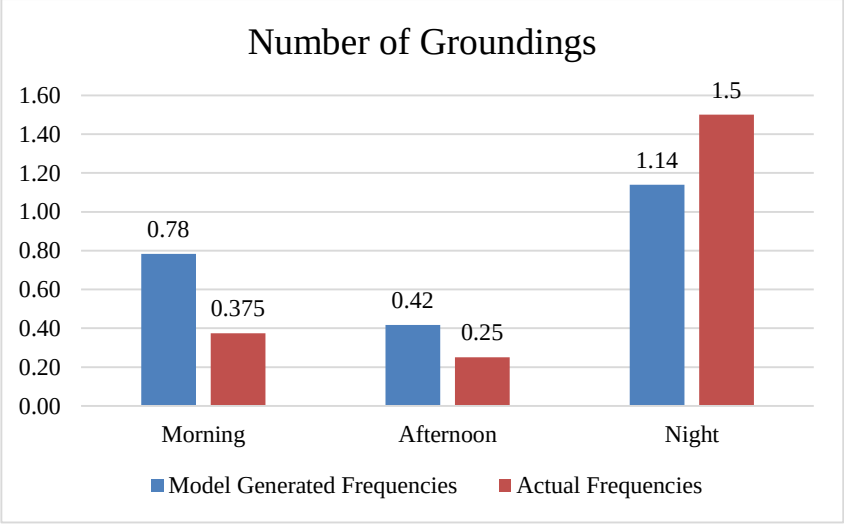

Figure 5.4. Groundings at different times of day in the main scenario.

The effect of traffic direction on the estimated and actual number of groundings is also analyzed in this study. In the observed data, 52.9 % of the groundings involved southbound vessels, whereas in the generated model, 52.4% of the groundings involved southbound vessels

Table 5.8 displays the effect of northbound vessel classes on the estimated and actual number of groundings. In the observed data, most such groundings involve northbound short dry cargo vessels (which are classified as NB D in this study) followed by long dry cargo vessels (which are classified as NB C in this study); while the same two class of northbound vessels feature the highest frequency of groundings (and in the same order) in the model generated results as well. Still the low number of actual cases per vessel class do not allow for a reliable comparison.

Table 5.8. Number of groundings involving northbound vessels.

Vessel Type	Number of Groundings	
	Model Generated Frequencies	Actual Frequencies
NB_A	0.048	0.06
NB_B	0.056	0.00
NB_C	0.232	0.19
NB_D	0.704	0.69
NB_E	0.016	0.00
NB_F	0.096	0.06
NB_P	0.024	0.00

Table 5.9 displays the effect of southbound vessel classes on the estimated and actual number of groundings. In the observed data, most such groundings involve southbound short dry cargo vessels (which are classified as SB D in this study) followed by long dry cargo vessels (which are classified as SB C in this study); while the same two class of southbound vessels feature the highest frequency of groundings (and in the same order) in the model generated results as well. Still the low number of actual cases per vessel class do not allow for a reliable comparison

Table 5.9. Number of groundings involving southbound vessels.

Vessel Type	Number of Groundings	
	Model Generated Frequencies	Actual Frequencies
SB_A	0.096	0.00
SB_B	0.072	0.00
SB_C	0.224	0.33
SB_D	0.76	0.61
SB_E	0.016	0.00
SB_F	0.104	0.00
SB_P	0.024	0.06

Next, in order to better observe the effects of transit traffic density on groundings, the overall period is divided into three segments (scenarios) representing,

(i) 2002, 2009-2012 period as the “average transit traffic density” period,
(ii) 2001, 2003, 2013-2016 period as the “lower transit traffic density” period,
(iii)The 2004-2008 period as the “higher transit traffic density” period.

5.2.1. Groundings Comparisons Based on the Average Transit Traffic Density Scenario

In order to analyze the effect of average traffic density on the number of groundings, the estimated number of groundings in the average traffic density case (based on 2011 data) are compared with the actual number of groundings in “average traffic density” period. As displayed in Table 5.10, the model results are close to the actual results (the model overestimates the annual grounding by 6% and overestimates the number of groundings per 100,000 vessels by 8%).

Table 5.10. Comparison of number of groundings in the average transit traffic density scenario.

Groundings	Number of Groundings	Number of Years Observed	Total Vessel Entrances	Groundings/ year	Groundings/ 100,000 vessels
Actual Number of Groundings	11	5	247883	2.2	4.44
Grounding Resulting from the Model	2.34	1	49261	2.34	4.75

The low number of actual groundings in the study period do not really permit for a reliable sectoral analysis. Nevertheless, Table 5.11 displays the relative frequency of groundings at each sector, as estimated by the model and the actual case (for 5 years). According to the model results, groundings more frequently occur in sectors 2, 5, 9 and 12. In the actual case, groundings occur more frequently in sector 8. So, as pointed out, the model does not correctly mimick the actual groundings in 13 sectors, primarily because of the very low level of actual cases per sector.

Table 5.11. Groundings at each sector in the average transit traffic density scenario.

Sector	Number of Groundings	
	Model Generated Frequencies	Actual Frequencies
1	0.18	0.20
2	0.19	0.00
3	0.15	0.40
4	0.18	0.00
5	0.19	0.00
6	0.18	0.20
7	0.18	0.40
8	0.18	0.80
9	0.19	0.00
10	0.18	0.00
11	0.17	0.20
12	0.19	0.00
13	0.18	0.00

Figure 5.5 displays the effect of season on the estimated and actual number of groundings under average transit traffic conditions. In the observed time period, groundings occur more often in summer, while the least number of groundings are in spring. In the mathematical model grounding frequency is higher in winter and lowest in autumn. Therefore, the model is not successful in mimicking the season effect on number of groundings. Again the models predictions regarding seasonal variations is not good in the average transit traffic period, primarily because the number of actual realization per season is low for a reliable comparison.

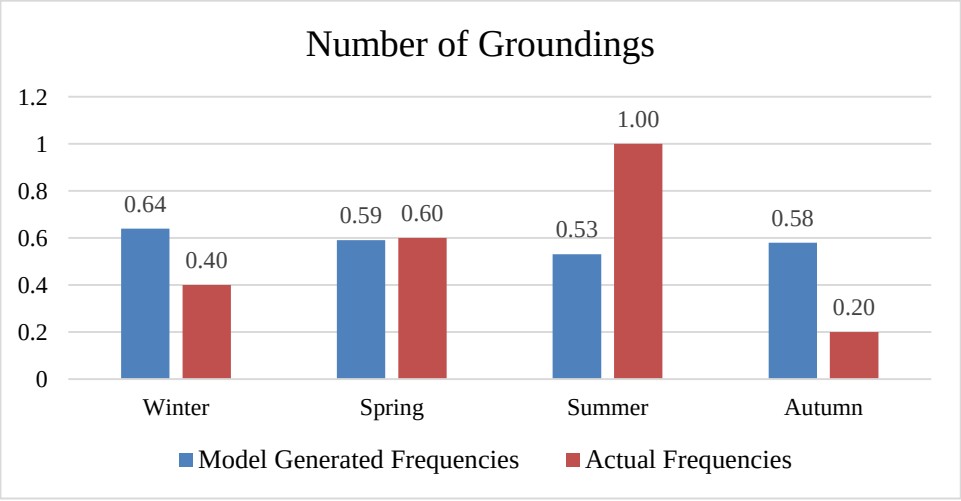

Figure 5.5. Groundings at each season in the average transit traffic density scenario.

Figure 5.6 displays the effect of day light on the estimated and actual number of groundings in the average transit traffic period. In the observed data, most groundings occur at night, while least groundings occur in the afternoon hours. Accordingly, the model predicts highest grounding frequency for nighttime and the lowest frequency for the afternoon hours. Therefore, the model is successful in mimicking the day light effect on number of groundings.

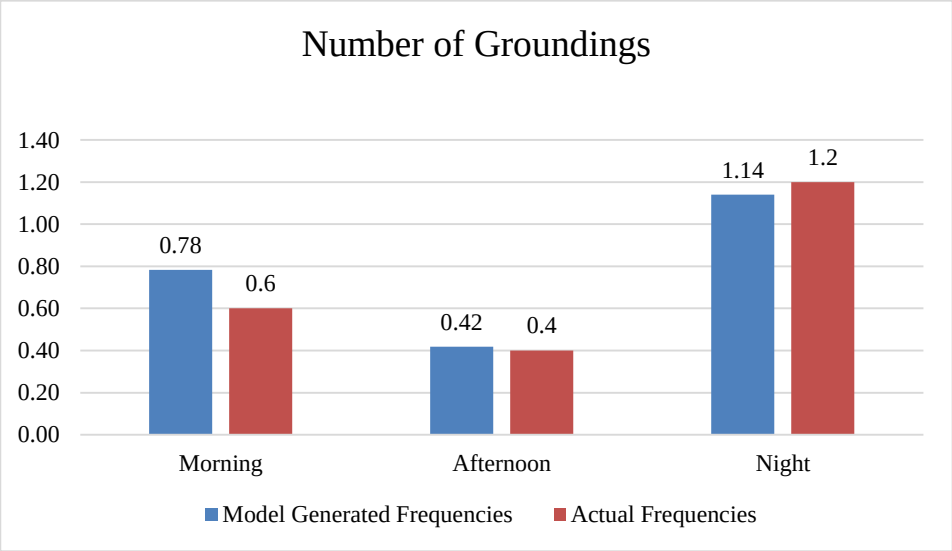

Figure 5.6. Groundings at different times of day in the average transit traffic density scenario.

5.2.2. Groundings Comparisons Based on the Higher Transit Traffic Scenario

In order to analyze the effect of higher traffic density on the number of groundings, the estimated number of groundings under higher traffic density case (based on the 2008 data) are compared with the actual number of groundings in "the higher transit traffic density" period. As displayed in Table 5.12, in this scenario 2.607 groundings occur in a year on the average.

Table 5.12. Groundings in the higher transit traffic scenario.

Number of Groundings in the Heavy Transit Traffic	
average	2.61
standard deviation	0.01
PI left	2.58
PI_right	2.64

The estimated number of groundings in the higher transit traffic scenario are compared with the actual number of groundings in the higher transit traffic period as displayed in Table 5.13. The results are in line with the expectation that higher density of transit traffic increases the number of groundings. Moreover, the model results are close to the actual results (the model underestimates the annual grounding by 7% and underestimates the number of groundings per 100,000 vessels by 6%).

Table 5.13. Comparison of number of groundings in the higher transit traffic scenario.

Groundings	Number of Groundings	Number of Years Observed	Total Vessel Entrances	Groundings/year	Groundings/100,000 vessels
Actual Number of Groundings	14	5	275240	2.8	5.09
Grounding Resulting from the Model	2.61	1	54747	2.61	4.77

The low number of actual groundings in the higher transit traffic scenario does not really permit for a reliable sectoral analysis. Nevertheless, Table 5.14 displays the relative frequency of groundings at each sector, as estimated by the model and the actual case (for 5 years). According to the model results, groundings more frequently occur in sector 5. In the actual case, groundings occur most frequently in sector 8. So, again, in the higher transit traffic scenario, the model does not correctly mimick the actual groundings in 13 sectors, primarily because of the very low level of actual cases per sector.

Table 5.14. Groundings at each sector in the higher transit traffic scenario.

Sector	Model Generated Frequencies	Actual Frequencies
S1	0.215	0.2
S2	0.224	0
S3	0.180	0.2
S4	0.217	0
S5	0.224	0
S6	0.218	0
S7	0.218	1
S8	0.208	1
S9	0.223	0
S10	0.210	0.2
S11	0.205	0
S12	0.223	0
S13	0.218	0.2

Figure 5.7 displays the effect of season on the estimated and actual number of groundings in the higher transit traffic density scenario. In the observed time period, groundings occur most often in summer, while the least number of groundings are in spring (no groundings were observed). In the mathematical model, grounding frequency is highest in winter and lowest in summer. Therefore, the model is not successful in mimicking the season effect on the number of groundings. Again, the models predictions regarding seasonal variations is not good in the higher transit traffic density scenario, primarily since the number of actual realization per season is low for a reliable comparison.

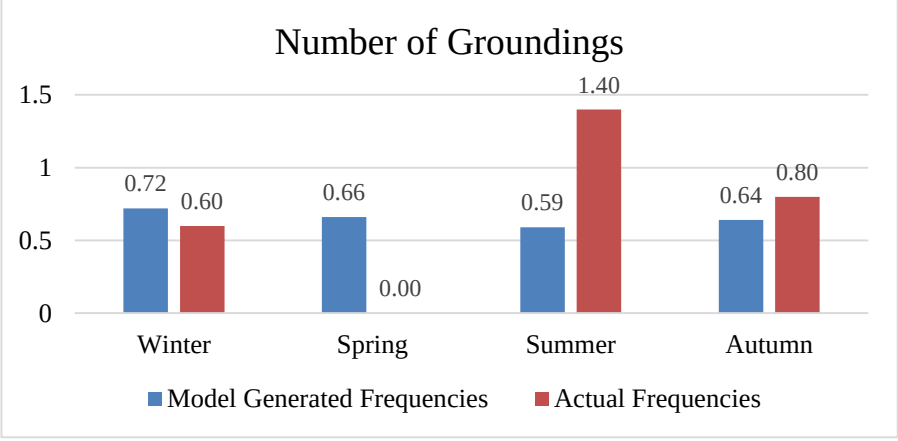

Figure 5.7. Groundings at each season in the higher transit traffic scenario.

Figure 5.8 displays the effect of day light on the estimated and actual number of groundings in the higher transit traffic period. In the observed data, most groundings occur at night, while least groundings occur in the afternoon hours. Accordingly, the model correctly predicts highest grounding frequency for nighttime and lowest frequency for the afternoon hours. Therefore, the model is successful in mimicking the day light effect on number of groundings.

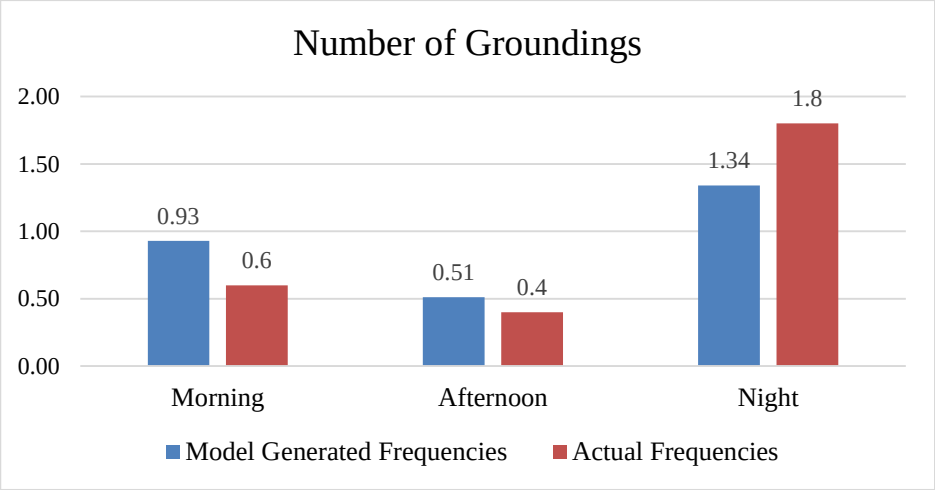

Figure 5.8. Groundings at different times of day in the higher transit traffic scenario.

5.2.3. Groundings Comparisons Based on the Lower Transit Traffic Scenario

In order to analyze the effect of lower transit traffic density on the number of groundings, the estimated number of groundings under lower transit traffic density case (based on the 2014 data) are compared with the actual number of groundings in "the lower transit traffic density" period. As displayed in Table 5.15, in this scenario 2.07 groundings occur in a year on the average.

Table 5.15. Groundings in the lower transit traffic scenario.

Number of Groundings at Low Transit Traffic	
average	2.07
standard deviation	0.01
PI_left	2.05
PI_right	2.09

The estimated number of groundings in the lower transit traffic scenario are compared with the actual number of groundings in the lower transit traffic period as displayed in Table 5.16. The results are in line with the expectation that lower density of transit traffic decreases the number of groundings. However, the model results are not close to the actual results.

Table 5.16. Comparison of number of groundings in the lower transit traffic scenario.

Groundings	Number of Groundings	Number of Years Observed	Total Vessel Entrances	Groundings/year	Groundings/100,000 vessels
Actual Number of Groundings	9	6	267734	1.5	3.36
Grounding Resulting from the Model	2.07	1	46215	2.07	4.48

The low number of actual groundings in the lower transit traffic scenario do not really permit for a reliable sectoral analysis. Nevertheless, Table 5.17 displays the relative frequency of groundings at each sector, as estimated by the model and the actual case (for 6 years). According to the model results, groundings most frequently occur in sector 5. In the actual case, groundings most frequently occur in sector 8. So, again in the lower transit traffic scenario, the model does not correctly mimick the actual groundings in 13 sectors, primarily because of the very low level of actual cases per sector.

Table 5.17. Groundings at each sector in the lower transit traffic scenario.

Sector	Model	Actual
S1	0.1708	0
S2	0.1774	0
S3	0.1428	0
S4	0.1718	0
S5	0.1776	0.1667
S6	0.1733	0
S7	0.1733	0.3333
S8	0.1652	0.8333
S9	0.1770	0.1667
S10	0.1664	0
S11	0.1627	0
S12	0.1770	0
S13	0.1726	0

Figure 5.9 displays the effect of season on the estimated and actual number of groundings in the lower transit traffic density scenario. In the observed time period, groundings occur most often in autumn, while in other seasons groundings occur equally frequently. In the mathematical model, grounding frequency is higher in winter and lowest in summer. Therefore, the model is not successful in mimicking the season effect on the number of groundings. Again, the models predictions regarding seasonal variations is not good in the lower transit traffic density scenario, primarily since the number of actual realization per season is low for a reliable comparison.

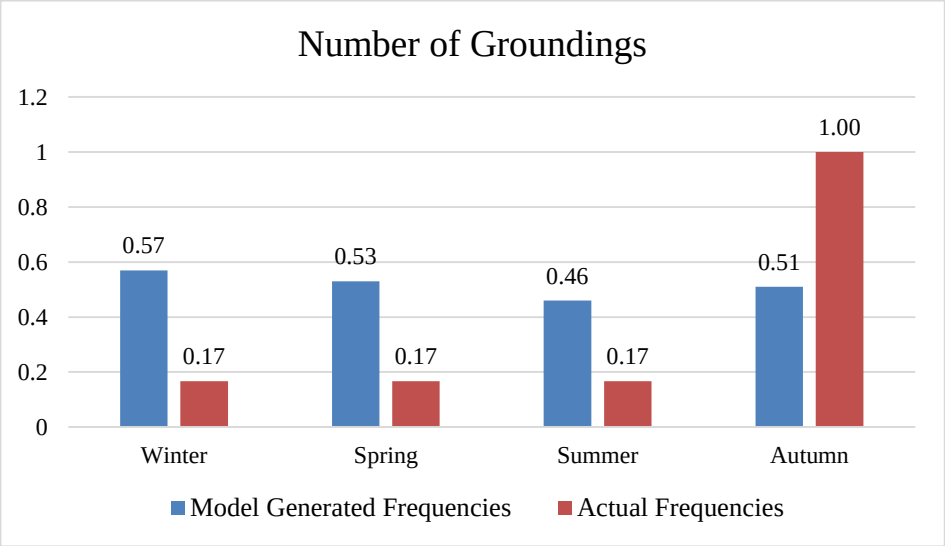

Figure 5.10. Groundings at each season in the lower transit traffic scenario.

Figure 5.11 displays the effect of day light on the estimated and actual number of groundings in the lower transit traffic period. In the observed data, all groundings occur at night. The model on the other hand predicts highest grounding frequency for nighttime, but also predicts a significant frequency of groundings for the afternoon hours. So, although the model is successful in mimicking the nighttime effect on the number of groundings, lack of groundings in other periods in the actual case prevent making a reliable comparison.

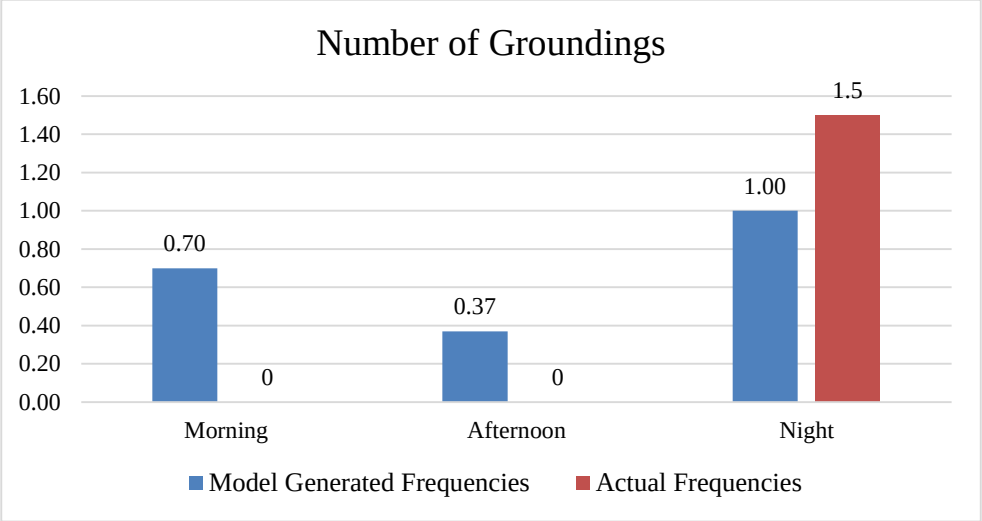

Figure 5.11. Groundings at different times of the day in the lower transit traffic scenario.

6. CONCLUSION

In this study, a quantitative risk analysis of maritime transit traffic in the Strait of Istanbul is performed. First, a simulation model is developed in order to mimic the actual transit traffic pattern in the Strait. The vessel activity data obtained from the VTS İstanbul, consisting of seven years (2008-2014) transit vessel traffic details provide a basis for the simulation model. Vessels are classified according to their cargo type, length and direction. Interarrival distribution of each vessel type is estimated based on the VTS data. Essentially, the VTS decides on the time and duration of daily traffic flow direction (north and south) time windows, type and entrance time of individual vessels according to judgements of VTS experts (in general complying with the R&R). In this study, instead of just relying on expert judgment, a scheduling algorithm is designed in order to decide the entrance time and vessel type by using both the R&R and past interentrance time statistics. Therefore, according to the simulation model, vessels approach to the Strait according to their class interarrival times and wait in queues until they are allowed to enter the Strait. Meanwhile, the scheduling algorithm decides the type and time of entering vessels. The model runs for both day and night time vessel traffic, during the seven years' period with 20 replications for each year. The performance measures of the simulation model are average interarrival times of each vessel class in northbound and southbound direction, average number of vessels entered the Strait and average interentrance times of each successive vessel pair in northbound and southbound direction.

In the simulation model, interarrival times of each vessel type in either direction are generated from specific interarrival time distribution of vessel classes estimated and fitted based on the actual interarrival times in the seven-year data. When the model generated interarrival times (based on each of the seven-year data) are compared with the real interarrival times of each vessel type, generated interarrival times for each vessel class in each direction are adequately representative of the real interarrival times of seven years.

The average number of vessels transited in northbound and southbound direction for seven years according to the scheduling algorithm are compared to the actual average number of vessels entered the Strait. The results are quite close to each other for all vessel classes.

In the simulation model, interentrance times of each vessel type in northbound and southbound directions are determined by random numbers (generated from the fitted distributions of actual interentrance times of each vessel type in northbound and southbound directions) and the R&R. Then, the model average interentrance times of each vessel type (determined by 20 simulation runs for each year from 2008 to 2014) are compared with the actual interentrance times of each vessel type (for each year from 2008 to 2014). The average interentrance times of successive northbound (southbound) class A vessel (determined by 20 simulation runs for each year from 2008 to 2014) are compared with the actual interentrance times of successive northbound (southbound) class A vessel (which is the most important vessel class in the daytime scheduling policy of the transit traffic in the Strait) and two results are found to be close to each other. Moreover, the average interentrance times (determined by 20 simulation runs for each year from 2008 to 2014) of successive northbound (southbound) class B, C, D, E and F vessels are compared with the real interentrance times and the result come close, as well.

Successive vessel entrance times of different vessel classes in each direction are also analyzed and the model results are compared with the actual interentrance pattern of corresponding transit vessel type pairs. In both traffic directions, most of the model generated successive interentrance times are close to the actual interentrance times. On the other hand, interentrance times of successive northbound and southbound class C and class F vessels, successive northbound and southbound class D and class F vessels and successive northbound and soutbound class E and class F vessels are considerably different from actual interentrance times of the corresponding vessel type pairs. The reason is that the developed scheduling algorithm applied to sequence the vessels in the Strait is based on the random numbers generated from interentrance time distributions of successive vessel types. In the indicated cases distributions to closely represent the actual interentrance times for the corresponding vessel pairs could not be determined, thus the results are different from each other.

In this study, the simulation model executes the scheduling algorithm to determine the sequence of transit vessels entering the Strait and the time of entrance during one-year period. In addition to that, probability of collisions in the Strait is estimated by multiplying the geometric collision probability with the collision causation probability and probability

of groundings in the Strait is estimated by multiplying the geometric grounding probability with the grounding causation probability. The geometric collision probabilities for each sector is obtained from [60]. The geometric collision probability is highest in sector 10 and lowest in sector 3. Moreover, [60] also shows that geometric collision probability is highest in winter and lowest in spring.

The geometric collision probability in the Strait is 0.027, which might be interpreted as, (disregarding other factors), two out of every 100 vessels colliding. This would lead to more than 1000 vessel collisions occurring in one year in the Strait, while the actual number of collisions is around 0.8 per year. Therefore, other factors, (such as the effect of the vessel captain's maneuver capability in case of being on a collision course) need be considered. These set of factors are taken into consideration by the collision causation probability, which is estimated through a Bayesian Network Analysis approach.

The first factor to analyze regarding collision is the direction of vessels. The results show that collision causation probability is higher for southbound vessels primarily since the prevailing southerly currents increase the likelihood of loss of control in that direction, which decrease the ability to maneuver.

Next, collision causation probabilities of Class A and B vessels turn out to be more favorable (lower) than other vessel classes primarily because,

(i) The safety culture of these classes are assumed to be perfect

(ii) Both class A and class B vessels are required to deploy pilot captains.

These two factors decrease the collision causation probability in either direction for class A and B vessels.

Another influential factor for the collision causation probability is the sectors. The results show that the collision causation probability is highest in sectors 1 and 13 in either direction, and lowest in sector 3 (which is the least dense sector) in either direction.

The season turns out to be an important external factor, for collision causation probabilities. The results show that the collision causation probability is highest in winter (due to adverse meteorological conditions) and lowest in summer.

Another important external factor is the time of day. The results show that in the mornings the collision causation probability is the highest (due to dense local traffic in the mornings) However, expected number of collisions is higher at nights since nighttime traffic lasts longer than morning traffic which leads more vessel transits.

Vessel traffic density in the Strait is another important external factor. The results show that under high intensity of local and transit vessel traffic, the collision causation probability is high and in low density of local and transit vessel traffic, the collision causation probability is low.

An important technical factor that affects the collision causation probability is machine failures. Potential machine failures noticeably increase the collision causation probability.

The effect of human factors such as fatigue and attention are also considered. As fatigue (working hours) increases, the collision causation probability increases and as attention span increases, detecting dangers and taking action gets easier, therefore, the causation collision probability decreases.

The geometric collision probability result for each vessel type entering the Strait at each sector is multiplied with the causation collision probability for each vessel type at each sector. Then, expected number of collisions for each vessel (which is the multiplication of each vessel's collision probability in each sector by one and then summed over all sectors) is summed up.to estimate the expected number of annual collisions. The total average number of collisions from simulation run results are then compared with the annual average of the realized number of collisions (obtained from [65]), on the overall. The average number of collisions from models runs (20 replications) is 0.82 collisions per year, whereas the realized number of collisions in the Strait is 0.79 collisions per year. The difference between these results can be attributed to various reasons. First, some of the actual collisions might be out of the boundaries of the sectors (determined by [60]) which are considered in this

study). Moreover, the Bayesian network designed for estimating the causation collision probability may not properly represent the impacts of some factors such as current and season due to lack of data.

Annual number of collisions in each season in the Strait is also observed. The model results for the number of collisions show that collisions occur more frequently in summer and winter whereas in autumn the frequency decreases. The actual results also displays a similar behaviour with the model results Next, annual number of collisions at different time time of day periods are also observed.The model results for the number of collisions show that number of collisions are highest at nights and lowest in the afternoons, whereas according to the actual results, number of collisions are highest at nights but lowest in the mornings. This difference between results can be attributed to low number of actual collisions.

Annual number of collisions for each traffic directions and vessel classes are also investigated in this study. According to the generated model results, number of collisions are higher in northbound vessels which is also the case for the actual number of collisions. Class D vessels in either direction are the vessels most frequently involved in collisions both in the model results and in the actual data. However, low number of observed collisions restrict a more detailed comparison.

In this study, geometric grounding probability is calculated using Equation 4.3. Then, a Bayesian Network is built and solved to estimate the grounding causation probability. The overall grounding probability is assumed to be the product of these two probabilities.

The first factor to analyze for estimating the grounding causation probability is the direction of vessels. The results show that the grounding causation probability is higher for southbound vessels, primarily since the prevailing southerly currents increase likelihood of the loss of control in that direction which decreases the ability to maneuver.

Grounding causation probabilities of Class A and B vessels turn out to be more favorable (lower) than other vessel classes primarily because,

(i) The safety culture of these classes are assumed to be perfect.
(ii) Both class A and class B vessels are required to deploypilot captains.

These two factors decrease the grounding causation probability in either direction for class A and B vessels.

Another important factor influencing the grounding causation probabilities is the sectors. The results show that the grounding causation probability is highest in sectors 4, 5 and 9 in northbound direction and in sectors 5 and 9 in southbound directions primarily due to higher number of transit vessels in these sectors).

The season is an important external factor influencing grounding causation probabilities. The results show that grounding causation probability is highest in winter (due to adverse meteorological conditions) and lowest in summer.

Another external factor is the availability of daylight. The results show that at nights the grounding causation probability is highest, whereas in the mornings the grounding causation probability is lowest.

Vessel traffic density in the Strait is another important external factor. The results show that under higher density of local and transit vessel traffic conditions, the grounding causation probability is higher and in lower density local and transit vessel traffic conditions, the grounding causation probability is lower.

Then expected number of groundings for each vessel (which is the multiplication of each vessel's grounding probability in each sector by one and then summed over all sectors) is summed up to estimate the expected number of annual groundings The total average number of groundings from simulation run results are then compared with the realized number of groundings (based on 16 years observed data). The average number of groundings from models runs (20 replications) is 2.342 groundings per year, whereas the actual annual average number of groundings in the Strait is 2.13. Annual number of groundings at each sector in the Strait is also observed. Accoridng to the model results, groundings occur more frequently in sector 5 and less frequently in sector 3.

Annual number of groundings at each sector is observed although the low number of actual groundings in the study period do not really permit for a reliable sectoral analysis in this study. According to the model, groundings occur most frequently in sector 5, however in actual case, groundings occur most frequently in sector 8. Annual number of groundings in each season is also observed. The model results regarding the number of groundings show that groundings occur most frequently in winter whereas in summer, the grounding frequency decreases. On the other hand, in the actual case, groundings occur most frequently in summer and grounding frequency decreases in spring. The model results regarding the daylight factor show that, in the Strait, number of groundings are highest at nighttime and lowest in the afternoons, this same trend is also observed in the actual data. Again, the number of observed groundings are low which restricts further and more reliable comparisons.

In order to better observe the effects of transit traffic density on the number of groundings, the overall period is divided into three (scenarios): average transit traffic scenario, higher transit traffic scenario and lower transit traffic scenario. First, the model results regarding the average transit traffic scenario and the actual case (which represents the average transit traffic) are compared. The model results estimates the annual number of groundings as 2.34 in the average transit traffic scenario, while in the actual case the average annual number of groundings is 2.20. Some additional factors are also analyzed under average transit traffic density. According to the model results, the grounding frequency is highest in sector 5 while in the actual case, groundings occur more frequently in sector 8 (in the average transit traffic density period). According to the model results, groundings occur more frequently in winter, while in actual case, groundings more frequently occur in summer (in the average transit traffic density period). According to both model results and the actual case, the groundings occur more frequently in the mornings and at nights (in the average transit traffic density period). Nevertheless, the actual number of groundings in the average transit traffic density period limits a reliable comparison.

Then, the model results regarding the higher transit traffic scenario and the actual case (which represents the higher transit traffic) are compared. The model results estimates the annual number of groundings as 2.61 in the higher transit traffic scenario, while in the actual case(in the higher transit traffic) the average annual number of groundings is 2.80. Moreover,

the actual case results show that as the transit traffic increases, the average annual number of groundings increases from 2.2 to 2.8. Some additional factors are also analyzed under higher transit traffic density. According to the model results, the grounding frequency is highest in sector 5 while in the actual case, groundings occur more frequently in sector 8 (in the higher transit traffic density period). According to the model results, groundings occur more frequently in winter while in actual case, groundings occur more frequently in summer (in the higher transit traffic density period). According to both model results and the actual case, the groundings occur more frequently in the mornings and at nights (in the higher transit traffic density period). Nevertheless, the actual number of groundings in the higher transit traffic density period restricts a reliable comparison.

Then, the model results regarding the lower transit traffic scenario and the actual case (which represents the lower transit traffic) are compared. The model results estimates the annual number of groundings as 2.07 in the lower transit traffic scenario, while in the actual case(in the lower transit traffic) the average annual number of groundings is 1.5. Moreover, the actual case results show that as the transit traffic decreases, the average annual number of groundings decreases from 2.2 to 1.5. Some additional factors are also analyzed under lower transit traffic density. According to the model results, the grounding frequency is highest in sector 5 while in the actual case, groundings occur more frequently in sector 8 (in the lower transit traffic density period). According to the model results, groundings occur more frequently in winter while in actual case, groundings occur more frequently in autumn (in the lower transit traffic density period). According to both model results and the actual case, the groundings occur more frequently in the mornings and at nights (in the lower transit traffic density period). Nevertheless, the actual number of groundings in the lower transit traffic density period do not allow a reliable comparison.

7. FURTHER STUDIES

This study forms a basis for the risk analysis of transit vessels navigating in the Strait regarding the probability of vessel collisions and groundings while systematizing the transit vessel traffic using a scheduling algorithm. There are still some improvable subjects for the further studies.

Although the scheduling algorithm provides quite a representative flow regarding the number of transit vessels entering the Strait and their interentrance time behavior, there are still some significant differences in interentrance times of some vessel pairs (especially for class F vessels) compared to the realized interentrance times. The scheduling algorithm may be revised to decrease those variations by adding some calibration factors.

While estimating geometric grounding probabilities, shoals in the Strait are not considered. Integrating these Strait characteristics to the model could improve the model's performance and results.

In the Bayesian network designed to quantify the maneuvering capability of the captains, the conditional probabilities of "the Current" node, is set to be 1 given various states of "the Wind" and "the Slice" nodes, due to lack of statistical and/or expert data. The conditional probabilities of the states of this node may be refined by doing extra studies. Vessel accidents is mainly controlled by the complex current climate within the Strait. This is only solved by integrating hydrodynamic current solver into this risk analysis.

Conditional probabilities of some nodes such as the transit traffic density and ship types in lane are found based on 2014 statistics. Those probabilities may be refined regarding long term frequencies.

Some arcs in Bayesian networks for both collision and grounding are not fully utilized again due to past data insufficiency. Once enough statistics are compiled, the Bayesian networks may be redesigned. Moreover, expert opinion extraction process may be expanded under more systematic conditions.

This study may be extended to the Çanakkale Strait whenever available data used in the model is obtained. Last but not the least, consequence analysis may be conducted so that a full risk analysis for the transit vessels entering the Turkish Straits is accomplished.

REFERENCES

1. GFP, *Maritime Transport and Port Operations*, https://gfptt.org/node/67, accessed at July 2017.

2. WRECK, *Greatest Maritime Disasters*, https://www.wrecksite.eu/, accessed at July 2017.

3. ITOPH, Sea Empress, Wales, UK, http://www.itopf.com/in-action/case-studies/case-study/sea-empress-milford-haven-wales-uk-1996/, accessed at July 2017.

4. Ince, A. and E. Topuz, "Modelling and Simulation for Safe and Efficient Navigation in Narrow Waterways", *Journal of Navigation*, Vol. 57 No. 1, pp. 53-71, 1996.

5. Gemi Trafik, Deniz Seyir Haritaları (Nautical Charts, http://www.gemitrafik.com/charts.htm, accessed at October 2016.

6. Ece, J., *Istanbul Bogazı Deniz Kazaları Analizi*, DEKAŞ Kültür Yayınları. 2007.

7. Viran, A., *Doing Risk Map of the Dense Traffic Region of Istanbul Strait (South Region) Based on Automatic Identification System (in Turkish)*, M. S. Thesis, Istanbul Technical University, 2014.

8. Deniz Haber Ajansı, *Boğazlardan Geçen Gemi Sayısı Azaldı, http://www.denizhaber.com.tr/bogazlardan-gecen-gemi-sayisi-azaldi-haber-60404.htm*, accessed at July 2017.

9. *Türk Boğazları Deniz Trafik Düzeni Tüzüğü, 1998, Regulation No: 98/11860*, Appeared on Turkish Official Gazette Date: 6 November 1998, No: 23515 mük., 1998.

10. Kornhauser, A.L. and W.A. Clark, “Quantitative Forecast of Vessel Casualties Resulting from Additional Oil Tanker Traffic Through the Bosphorus", Report, Associates, *Princeton,* New Jersey, 1995.

11. Bosphorus Strait News, *Causalties in the Strait, http://www.bosphorusstrait.com/the-bosporus-strait/incidents/,* accessed at July 2017.

12. Petersen, E.R. and A.J. Taylor, “An optimal scheduling system for the Welland Canal”, *Transportation science*, Vol. 22, No. 3, pp. 173-185, 1998.

13. Golkar, J., A. Shekhar and S. Buddhavarapu, “Panama Canal simulation model”, *Proceedings of 1998 Winter Simulation Conference*, IEEE Computer Society Press Los Alamitos, CA, USA, pp. 1229-1238, 1998.

14. Or, I. and I. Kahraman, “A simulation study of the accident risk in the Istanbul Channel”, *International Journal of Emergency Management*, Vol. 1, No. 2, pp. 110-124, 2002.

15. Franzese, L. A. G., L. O. Abdenur, R. C. Botter, D. Starks and A. R. Cano, “Simulating the Panama Canal: present and future”, *Proceedings of 2004 Winter Simulation Conference*, pp. 1835-1838, 2004.

16. Ulusçu, Ö. S., B. Özbaş, T. Altiok, I. Or and T. Yılmaz, “Transit Vessel Scheduling in the Strait of Istanbul”, *Journal of Navigation*, Vol. 62, No. 1, pp. 59-77. 2009a.

17. Almaz, A. Ö., *Investigation of Transit Maritime Traffic in the Strait of Istanbul through Simulation Modeling and Scenario Analysis,* M.S. Thesis, Bogazici University, 2006.

18. Cortès P., J. Munuzuri, J. Nicolas Ibanez and J. Gudix, “Simulation of Freight Traffic in the Seville Inland Port”, *Simulation Modelling and Practice and Theory*, Vol.15, No. 3, pp 256-271, 2007.

19. Özlem, Ş., *Simulation of the Vessel Traffic in the Strait of Istanbul*, M. S. Thesis, Bogazici University, 2011.

20. Candanoglu O, *Scheduling Transit Vessels in the Istanbul Strait*, M. S. Thesis, Bogazici University, 2013.

21. Amrozowicz, M., A. Brown and M. Golay, "A Probabilistic Analysis of Tanker Groundings", *Proceedings of the 1997 7th International Offshore and Polar Engineering Conference*, Honolulu, HI, pp. 313-320, 1997.

22. Amrozowicz, M. D., *The Quantitative Risk of Oil Tanker Groundings*, M.S. Thesis, Massachusetts Institute of Technology, 1996.

23. Merrick, J. R. W., J. R. van Dorp, J. P. Blackford, G. L. Shaw, J. Harrald and T. A. Mazzuchi, "A traffic density analysis of proposed ferry service expansion in San Francisco Bay using a maritime simulation model", *Reliability Engineering and System Safety*, Vol. 81, No. 2, pp. 119-132, 2003.

24. Merrick, J. R. W., J. R. van Dorp, T. Mazzuchi, J. R. Harrald, J. E. Spahn and M. Grabowski, "The Prince William Sound Risk Assessment", *Interfaces*, Vol. 32, No. 6, pp. 25-40, 2002.

25. Sotiralis P., N.P. Ventikos, R. Hamann, P. Golyshev and A.P. Teixeira, "Incorporation of human factors into ship collision risk models focusing on human centred design aspects", *Reliability Engineering & System Safety*, Vol. 156, pp. 210-227, 2016.

26. Itoh, K., T. Yamaguchi, J.P. Hansen, and F.R. Nielsen, "Risk analysis of ship navigation by use of cognitive simulation", *Cognitive Technology Work*, Vol.3, pp. 4-21, 2001.

27. Chauvin, C., Lardjane, S., Morel, G., Clostermann, J.P. and B. Langard, "Human and organizational factors in maritime accidents: analysis of collisions at sea using the HFACS", Accid. Anal. Prev., Vol.59, pp.26-37, 2013.

28. Ulusçu, Ö.S., B. Özbaş, B., T. Altıok, T. and İ. Or, "Risk analysis of the vessel traffic in the Strait of Istanbul", *Risk Analysis,* Vol. *29,* No. 10, pp.1454-1472, 2009.

29. Otay, N. E. and S. Özkan, "Stochastic prediction of maritime accidents in the Strait of Istanbul", *Proceedings of the 3rd International Conference on Oil Spills in the Mediterranean and Black Sea Regions,* Istanbul, Turkey, pp. 55–64, 2003.

30. Otay, E., and B. Tan. "Stochastic Modelling of Tanker Traffic Through Narrow Waterways.", *Proc. 1st International Conference on Oil Spills in the Mediterranean and Black Sea Regions,* Istanbul, Turkey, pp.85-96, 1998.

31. Tan, B., and E.N. Otay, "Modeling and Analysis of Vessel Casualties Resulting from Tanker Traffic Through Narrow Waterways", *Naval Research Logistics,* Vol. 46, No. 8, pp. 871-892, 1999.

32. Merrick, J. R. W., J. R. van Dorp, J. Harrald, T. Mazzuchi, J. E. Spahn and M. Grabowski, "A systems approach to managing oil transportation risk in Prince William Sound", *Systems Engineering*, Vol. 3, No. 3, pp. 128-142, 2000.

33. Harrald, J. R., T. A. Mazzuchi, J. Spahn, R. Van Dorp, J. Merrick, S. Shrestha and M. Grabowski, "Using system simulation to model the impact of human error in a maritime system", *Safety Science*, Vol. 30, No. 1-2, pp. 235-247, 1998.

34. Wheeler, T. A., Gawande, K. and S. Bespalko, "Development of Risk-Based Ranking Measures of Effectiveness for the United States Coast Guard's Vessel Inspection Program", *Risk Analysis*, Vol 17, pp. 333-340, 1997.

35. Merrick, J. R. W. and R. van Dorp, "Speaking the Truth in Maritime Risk Assessment", *Risk Analysis,* Vol. 26, No. 1, pp. 223-237, 2006.

36. Li. K. X., J. Yin, H.S. Bang, Z. Yang and J. Wang, “Bayesian network with quantitative input for maritime risk analysis”, *Transportmetrica A: Transport Science,* Vol. 10, No. 2, pp. 89-118, 2014.

37. Goerlandt, F. and J. Montewka, “A probabilistic model for accidental cargo oil outflow from product tankers in a ship–ship collision”, *Marine pollution bulletin*, Vol.79, No. 1-2, pp.130-144, 2014.

38. Goerlandt, F. and J. Montewka, “Maritime transportation risk analysis: review and analysis in light of some foundational issues”. *Reliability Engineering & System Safety*, Vol. 138, pp. 115-134, 2015.

39. Trucco, P., Cagno, E., Ruggeri, F. and O. Grande, “A Bayesian Belief Network modelling of organisational factors in risk analysis: A case study in maritime transportation”, *Reliability Engineering & System Safety*, Vol. 93, No. 6, pp. 845-856, 2008.

40. Akyuz, E. and M. Celik, “Utilisation of cognitive map in modelling human error in marine accident analysis and prevention”, *Safety science,* Vol.70, pp.19-28, 2014.

41. Eliopoulou, E. and A. Papanikolaou, “Casualty analysis of large tankers. *Journal of Marine Science and Technology”,* Vol.12, No.4, pp.240-250, 2007.

42. Sahin, B. and S. Kum, “Risk assessment of arctic navigation by using improved fuzzy-AHP approach”, *International Journal of Maritime Engineering,* Vol.157, No.4, p.241, 2015.

43. Montewka, J., Ehlers, S., Goerlandt, F., Hinz, T., Tabri, K. and P. Kujala, “A framework for risk assessment for maritime transportation systems-A case study for open sea collisions involving RoPax vessels”, *Reliability Engineering & System Safety*, Vol.124, pp. 142-157, 2014.

44. Macduff, T., “The Probability of Vessel Collisions”, *Ocean Industry,* Vol. 9, No. 9, 1974.

45. Fujii, Y., R. Oshima, H. Yamanouchi, and N. Mizuki, “Some factors affecting the frequency of accidents in marine traffic: I-the diameter of evasion for crossing encounters, II-the probability of stranding, III-the effect of darkness of the probability of collision and stranding”, *The Journal of Navigation*, Vol. *27,* No.2, pp.239-247, 1974.

46. Kite-Powell, H. L., N. M. Patrikalakis, D. Jin, S. L. Abrams, J. Jebsen, V. Papakonstantinou and S. C. Lin, *Formulation of a model for ship transit risk: Final project report, MIT Sea Grant College Program Report,* No. 96-19, Massachusetts Institute of Technology, Cambridge, Massachusetts, 1998.

47. Fowler, T.G. and E. Sørg˚ard, “Modeling Ship Transportation Risk”, *Risk Analysis*, Vol. 20, No. 2, pp. 225-244, 2000.

48. Kristiansen S., *Maritime Transportation: Safety Management and Risk Analysis,* New York: Butterworth-Heinemann**,** 2005.

49. Pedersen, P.T., “Collision and Grounding Mechanics”, *Proceedings of Wilderness Emergency Medical Technician,* Vol. 95, No. 1995, pp. 125-157, 1995.

50. Soares, C. Guedes, and A. P. Teixeira. “Risk assessment in maritime transportation”, *Reliability Engineering & System Safety,* Vol. 74, No. 3, pp. 299-309, 2001.

51. Otto, S., P. T. Pedersen, M. Samuelides and P. C. Sames, “Elements of risk analysis for collision and grounding of a RoRo passenger ferry”, *Marine Struct,* Vol. 15, No. 4-5, pp. 461–474, 2002.

52. Gucma, L. and E. Goryczko, “The Implementation of Oil Spill Costs Model in the Southern Baltic Sea Area to Assess the Possible Losses Due to Ships Collisions”,

TransNav: International Journal on Marine Navigation and Safety of Sea Transportation, Vol. 2, No. 4, 2008.

53. Hänninen, M., "Bayesian networks for maritime traffic accident prevention: benefits and challenges", *Accident Analysis & Prevention,* Vol. 73, pp. 305-312 73, 2014.

54. Aven, T., *Quantitative risk assessment - The Scientific Platform*, Cambridge University Press, 2011.

55. Knight, F. H. *Risk, uncertainty and Profit*, Sentry Press, New York, 1964.

56. Renn, O., *Concept of Risk: A Classification,* Krimsky, S: Social Theories of Risk, Westport, CT: Praeger, pp. 53–79, 1992.

57. Bernstein, P.L. and P.L. Bernstein, *Against the gods: The remarkable story of risk*, New York: Wiley, pp. 1269-1275, 1996.

58. Holton, Glyn A., "Defining Risk", *Financial Analysts Journal*, Vol. 60, No. 6, pp. 19–25, 2004.

59. SRA, *Society for Risk Analysis Glossary*, http://www.sra.org/sites/default /files/pdf/SRA-glossary-approved22june2015-x.pdf, accessed at October 2015.

60. Altan Y.C., *Analysis and Modeling of Maritime Traffic and Ship Collision in the Strait of Istanbul Based on Automatic Vessel Tracking System*, Bogazici University, 2017.

61. Fujii, Y. and R. Shiobara, "The Analysis of Traffic Accidents", Journal of Navigation, Vol. 24, No. 04, pp. 534-543, 1971.

62. Wiegerinck, W., W. Burgers. and B. Kappen, Bayesian Networks, Introduction and Practical Applications, *Handbook on Neural Information Processing* Vol. 49, pp. 401-431, 2017.

63. Devlet Meteoroloji İşleri, "İstanbul Kumköy İstasyonu Verileri", *Devlet Meteoroloji İşleri Bölge Müdürlüğü,* 2017.

64. The Navigator, *Bridge Resource Management: Working as a Cohesive Team*, The Nautical Institute, 2014.

65. Mazaheri, A., *Probabilistic modeling of ship grounding*, Helsinki University of Technology, pp. 48-56, 2009.

66. T.C. Ulaştırma, Denizcilik ve Haberleşme Bakanlığı Ana Arama Kurtarma Koordinasyon Merkezi, *Bölgeler İtibariyle Yıllara Göre Kaza/Olay İstatistikleri*, 2018.

APPENDIX A: INTERARRIVAL AND INTERENTRANCE DISTRIBUTIONS

Table A.1. Interarrival time distributions of vessel classes based on the actual transit traffic data of 2008.

Vessel type	Interarrival distribution	Parameters	Kolmogorov-Smirnov p-value
NB_A	Fatique Life (3P)	α=1.8677 β=189.11 γ=–5.8075	<0.05
SB_A	Gen. Pareto	k=-0.02393 s=276.85 m=-1.8065	0.97618
NB_B	Log-Pearson 3	a=13.69 b=-0.42633 g=10.897	<0.05
SB_B	Wakeby	a=64.252 b=2.5744 g=383.41 d=-0.02687 x=-5.231	0.99173
NB_C	Exponential	λ=0.0827	0.51589
SB_C	Weibull	a1=1.0109 a2=9.9819E+7 b=4.1976E+10	0.71386
NB_D	Phased Bi-Exponential	λ_1=0.03417 γ_1=0 λ_2=0.02269 γ_2=118.05	<0.05
SB_D	Pareto 2	α=11.949 β=321.39	<0.05
NB_E	Wakeby	k=284.69 a=1.064 b=3.2199E+5	0.99735
SB_E	Phased Bi-Exponential	λ_1=6.3336E-4 γ_1=1 λ_2=1.4242E-4 γ_2=3350.0	0.91659
NB_F	Phased Bi-Weibull	α_1=1.024 β_1=209.57 γ_1=0 α_2=0.84525 β_2=324.0 γ_2=26.7	0.1052
SB_F	Wakeby	α=292.75 β=0.01534 γ=22.107 δ=0.86884 ξ=2.6554	0.81536
NB_P	Gamma	α=0.66613 β=1070.3	0.95787
SB_P	Dagum	k=0.1964 α=3.1364 β=1457.6	0.47967

Table A.2. Interarrival time distributions of vessel classes based on the actual transit traffic data of 2009.

Vessel type	**Interarrival distribution**	**Parameters**
NB_A	Phased Bi-Weibull	α_1=0.95015 β_1=166.79 γ_1=0 α_2=0.45257 β_2=268.96 γ_2=108
SB_A	Wakeby	α=569.77 β=0.12633 γ=0 δ=0 ξ=-9.5459
NB_B	Lognormal	σ=1.4648 μ=5.1189
SB_B	Wakeby	α=417.46 β=0.0768 γ=0 δ=0 ξ=-2.7064
NB_C	Wakeby	α=102.37 β=-0.06154 γ=1.8357 δ=0.89303 ξ=-0.09886
SB_C	Wakeby	α=-19.453 β=8.5063 γ=119.33 δ=-0.02914 ξ=0
NB_D	Pareto 2	α=5.9014 β=165.99
SB_D	Phased Bi-Weibull	α_1=0.98961 β_1=30.505 γ_1=0 α_2=0.92038 β_2=28.992 γ_2=60
NB_E	Dagum	k=0.187 α=4.4473 β=4550.4
SB_E	Wakeby	α=-197.68 β=6.0781 γ=2894.9 δ=-0.22926 ξ=0
NB_F	Wakeby	α=-164.5 β=2.4367 γ=313.48 δ=0.04237 ξ=-1.6831
SB_F	Wakeby	α=–197.68 β=6.0781 γ=2894.9 δ=–0.22926 ξ=0
NB_P	Wakeby	α=-1070.4 β=2.58 γ=1104.0 δ=-0.0231 ξ=0
SB_P	Wakeby	α=-192.43 β=9.3925 γ=259.89 δ=0.12798 ξ=0

Table A.3. Interarrival time distributions of vessel classes based on the actual transit traffic data of 2010.

Vessel	**Interarrival distribution**	**Parameters**
NB_A	Frechet	α=0,61095 β=75,013
SB_A	Phased Bi-Weibul	α_1=0,97766 β_1=201,09 γ_1=0 α_2=0,59213 β_2=265,81 γ_2=131
NB_B	Gamma	α=0,95944 β=132,19
SB_B	Weibull	α=0,91328 β=32,997
NB_C	Wakeby	α=-689,27 β=2,2472 γ=2630,9 δ=-0,32371 ξ=57,96
SB_C	Weibull	α=0,81672 β=229,23
NB_D	Wakeby	α=-745,11 β=8,4144 γ=903,38 δ=0,09484 ξ=0
SB_D	Wakeby	α=137,21 β=1,464 γ=466,64 δ=0,00307 ξ=-3,8868
NB_E	Pearson 6	α_1=1,0416 α_2=6,3664E+7 β=2,3355E+10
SB_E	Gen. Gamma	k=1,0047 α=0,93883 β=133,51
NB_F	Weibull	α=0,95962 β=31,767
SB_F	Wakeby	α=-1080,3 β=2,525 γ=2506,9 δ=-0,19509 ξ=0
NB_P	Wakeby	α=-178,49 β=8,7564 γ=219,88 δ=0,1949 ξ=0
SB_P	Gen. Gamma	k=1,2633 α=0,54937 β=1707,7

Table A.4. Interarrival time distributions of vessel classes based on the actual transit traffic data of 2012.

Vessel type	**Interarrival**	**Parameters**
NB_A	Fatigue Life	α=2.4393 β=178.88
SB_A	Gen. Pareto	k=-0.17032 σ=690.04 μ=-2.9964
NB_B	Weibull	α=0.78982 β=373.93
SB_B	Gen. Pareto	k=-0.01539 σ=430.48 μ=-2.7983
NB_C	Wakeby	α=85.795 β=0.1119 γ=14.205
		δ=0.40201 ξ=-0.67931
SB_C	Gen. Gamma	k=1.015 α=0.93774 β=106.66
NB_D	Gamma	α=0.9023 β=43.962
SB_D	Weibull	α=0.94701 β=36.388
NB_E	Wakeby	α=-520.16 β=2.9142 γ=2037.3
		δ=-0.23654 ξ=14.868
SB_E	Gen. Gamma (4P)	k=1.3102 α=0.69267
		β=2251.2 γ=1.0
NB_F	Gen. Gamma	k=0.8429 α=0.93718 β=276.09
SB_F	Wakeby	α=-209.0 β=24.067 γ=212.63 δ=0.25308 ξ=0
NB_P	Dagum	k=0.20913 α=2.9548 β=1996.9
SB_P	Wakeby	α=-622.27 β=7.6014 γ=1086.2
		δ=-0.00579 ξ=-14.858

Table A.5. Interarrival time distributions of vessel classes based on the actual transit traffic data of 2013.

Vessel type	**Interarrival**	**Parameters**
NB_A	Fatigue Life (3P)	α=1.8209 β=217.77 γ=-6.8566
SB_A	Wakeby	α=601.93 β=0.04533 γ=0 δ=0 ξ=-3.4948
NB_B	Log-Logistic	α=1.1431 β=185.12
SB_B	Gen. Pareto	k=-0.01367 σ=405.67 μ=-1.5055
NB_C	Weibull	α=0.93241 β=40.834
SB_C	Weibull	α=0.96014 β=97.825
NB_D	Weibull	α=0.93241 β=40.834
SB_D	Weibull	α=0.93369 β=39.223
NB_E	Dagum	k=0.16538 α=4.6647 β=3120.0
SB_E	Gamma	α=1.3363 β=1133.5
NB_F	Pearson 6	α_1=0.59182 α_2=8.7598 β=3604.3
SB_F	Wakeby	α=-263.13 β=2.7121 γ=284.94 δ=0.17153 ξ=-0.74713
NB_P	Gen. Gamma	k=1.8437 α=0.36431 β=2352.4
SB_P	Gamma	α=0.76804 β=1302.4

Table A.6. Interarrival time distributions of vessel classes based on the actual transit traffic data of 2014.

Vessel type	**Interarrival distribution**	**Parameters**
NB_A	Fatigue Life	α=2.6291 β=166.45
SB_A	Wakeby	α=418.36 β=0.60214 γ=234.43 δ=0.28235 ξ=-4.8577
NB_B	Lognormal	σ=1.432 μ=4.9032
SB_B	Wakeby	α=103.82 β=0.33924 γ=187.19 δ=0.11857 ξ=-0.2363
NB_C	Gamma	α=0.90451 β=102.36
SB_C	Gen. Gamma	k=1.014 α=0.90233 β=104.29
NB_D	Weibull	α=0.85514 β=43.465
SB_D	Weibull	α=0.90965 β=43.823
NB_E	Wakeby	α=-1077.9 β=23.257 γ=1777.5 δ=-0.21974 ξ=0
SB_E	Wakeby	α=1022.9 β=1.0509 γ=863.61 δ=0.07923 ξ=-0.98351
NB_F	Kumaraswamy	α_1=0.60002 α_2=6.4991 a=3.7628E-15 b=6285.3
SB_F	Gamma	α=0.52437 β=549.95
NB_P	Gen. Pareto	k=0.00708 σ=829.1 μ=-14.553
SB_P	Gen. Pareto	k=-0.0069 σ=875.97 μ=-34.342

Table A.7. Successive northbound vessel entrance distributions based on the actual transit traffic data of 2008.

Direction	Vessel pairs	Interarrival distribution	Parameters
NB	**AA**	Cauchy	σ=11,052 μ=84,734
NB	**AC**	Gen. Extreme Value	k=0,1819 σ=15,426 μ=24,068
NB	**AD**	Burr (4P)	k=1,0798 α=2,488 β=9,509 γ=-0,48022
NB	**AE**	Gen. Extreme Value	k=0,33795 σ=18,669 μ=34,203
NB	**AF**	Dagum	k=0,38536 α=2,9873 β=65,344
NB	**CA**	Burr	k=1,8663 α=2,0093 β=50,179
NB	**CC**	Lognormal (3P)	σ=0,84687 μ=3,5716 γ=-2,0092
NB	**CD**	Log-Logistic (3P)	α=2,7713 β=8,501 γ=-1,0047
NB	**CE**	Lognormal	σ=0,85714 μ=3,7604
NB	**CF**	Log-Pearson 3	α=24,454 β=-0,22668 γ=8,5331
NB	**DA**	Log-Logistic (3P)	α=2,6236 β=9,2386 γ=-0,66895
NB	**DC**	Frechet (3P)	α=5,5424 β=28,387 γ=-20,639
NB	**DD**	Lognormal (3P)	σ=0,70847 μ=2,3687 γ=-1,4084
NB	**DE**	Log-Logistic (3P)	α=2,6106 β=12,824 γ=-0,41354
NB	**DF**	Pearson 6 (4P)	α_1=1,4448 α_2=11,049
NB	**EA**	Dagum	k=0,5279 α=4,4671 β=56,423
NB	**EC**	Gen. Pareto	k=-0,05714 σ=37,616 μ=5,1779
NB	**ED**	Pearson 5	α=1,2905 β=6,8082
NB	**EE**	Log-Logistic (3P)	α=1,9914 β=63,994 γ=0,69956
NB	**EF**	Kumaraswamy	α_1=0,70929 α_2=2,0265 a=1,1167 b=365,16
NB	**FA**	Dagum	k=0,81367 α=1,9346 β=57,659
NB	**FC**	Log-Pearson 3	α=26,4 β=-0,19718 γ=8,3928
NB	**FD**	Lognormal (3P)	σ=0,74487 μ=2,2354 γ=-1,436
NB	**FE**	Gen. Pareto	k=-0,07738 σ=90,298 μ=3,3782
NB	**FF**	Gen. Gamma	k=0,99028 α=0,93945 β=98,393

Table A.8. Successive southbound vessel entrance distributions based on the actual transit traffic data of 2008.

Direction	Vessel pairs	Interentrance distribution	Parameters	Parameters
SB	**AA**	Cauchy	σ=4,5911 μ=74,764	
SB	**AC**	Burr (4P)	k=0,2911 α=24,702	β=83,807 γ=-67,551
SB	**AD**	Burr (4P)	k=0,65923 α=4,5854	β=9,882 γ=-2,7223
SB	**AE**	Lognormal (3P)	σ=0,57145 μ=3,5458 γ=3,4711	
SB	**AF**	Dagum	k=0,37687 α=3,095 β=71,11	
SB	**CA**	Burr	k=1,5401 α=3,0026 β=33,669	
SB	**CC**	Lognormal (3P)	σ=0,81889 μ=3,4712 γ=-1,09	
SB	**CD**	Burr (4P)	k=0,72494 α=4,1354	β=8,7791 γ=-2,1532
SB	**CE**	Burr	k=0,5887 a=3,256 b=25,545	
SB	**CF**	Gen. Gamma (4P)	k=0,38234 α=5,8879	β=0,2483 γ=-0,02242
SB	**DA**	Dagum (4P)	k=0,96086 α=3,8598	β=15,827 γ=-1,7184
SB	**DC**	Dagum (4P)	k=1,0389 α=3,6327	β=11,708 γ=-1,8879
SB	**DD**	Lognormal (3P)	σ=0,68379 μ=2,4007 γ=-	
SB	**DE**	Dagum	k=0,63673 α=3,9129 β=16,169	
SB	**DF**	Pearson (5)	k=3,3721 α=29,001 β=-2,9054	
SB	**EA**	Dagum	k=0,99703 α=4,1351 β=39,676	
SB	**EC**	Burr	k=1,9586 α=1,994 β=59,27	
SB	**ED**	Burr (4P)	k=0,3632 α=8,7985	β=12,388 γ=-7,0558
SB	**EE**	Burr	k=0,66232 α=2,8864 β=54,096	
SB	**EF**	Gen. Gamma	k=1,074 α=0,70428 β=198,88	
SB	**FA**	Dagum	k=0,69502 α=2,4409 β=46,96	
SB	**FC**	Log-Pearson 3	α=18,502 β=-0,21766 γ=7,257	
SB	**FD**	Gen. Gamma (4P)	k=0,75532 α=2,6158	β=3,0931 γ=5,2904E-
SB	**FE**	Gamma (3P)	α=0,82285 β=81,512 γ=4,3	
SB	**FF**	Gen. Pareto	k=-0,00111 σ=104,77 μ=-	

Table A.9. Successive northbound vessel entrance distributions based on the actual transit traffic data of 2009.

Direction	Vessel pairs	Interentrance	Parameters
NB	AA	Dagum (4P)	k=0.69029 α=6.4535 β=46.729 γ=43.384
NB	AC	Gen. Extreme Value	k=0.12413 σ=14.525 μ=23.135
NB	AD	Gen. Gamma	k=0.41642 α=10.334 β=0.03563
NB	AE	Gen. Extreme Value	k=0.33157 σ=20.076 μ=38.864
NB	AF	Wakeby	α=43.155 β=1.4512 γ=17.821 δ=0.36212 ξ=0.62986
NB	BB	Wakeby	α=3627.2 β=74.069 γ=14.89 δ=0.44722 ξ=0
NB	BC	Wakeby	α=78.689 β=5.5887 γ=10.19 δ=0.38396 ξ=2.726
NB	BD	Wakeby	α=20.044 β=7.6443 γ=7.1335 δ=0.14863 ξ=1.0145
NB	BE	Wakeby	α=187.91 β=0.59322 γ=0 δ=0 ξ=22.634
NB	BF	Burr	k=2.2545 α=1.3095 β=76.236
NB	CA	Dagum	k=0.87499 α=2.6532 β=35.216
NB	CB	Wakeby	α=75.11 β=5.3912 γ=10.203 δ=0.37939 ξ=2.8426
NB	CC	Pearson 6	α_1=2.4047 α_2=3.717 β=52.497
NB	CD	Log-Logistic	α=2.4568 β=7.6541
NB	CE	Log-Logistic	α=1.9457 β=41.703
NB	CF	Wakeby	α=17.709 β=0.22965 γ=8.9099 δ=0.23813 ξ=0.59295
NB	DA	Dagum	k=0.61263 α=3.0838 β=19.517
NB	DB	Burr	k=1.5821 α=2.0567 β=15.684
NB	DC	Gen. Extreme Value	k=0.1972 σ=5.2738 μ=7.9269
NB	DD	Gen. Gamma	k=0.37434 α=10.47 β=0.02146
NB	DE	Wakeby	α=30.785 β=3.4238 γ=4.7632 δ=0.50429 ξ=1.6502
NB	DF	Wakeby	α=9.7854 β=6.8836 γ=8.1556 δ=-0.02079 ξ=0.26931
NB	EA	Dagum	k=0.48456 α=5.5261 β=62.649
NB	EB	Wakeby	α=151.37 β=0.80283 γ=0 δ=0 ξ=2.1711
NB	EC	Log-Gamma	α=16.569 β=0.1986
NB	ED	Pearson 6	α_1=2.5739 α_2=5.0417 β=18.026
NB	EE	Johnson SB	γ=0.56409 δ=0.53605 λ=294.27 ξ=10.406
NB	EF	Wakeby	α=34.151 β=8.1778 γ=79.471 δ=-0.1218 ξ=0
NB	FA	Wakeby	α=69.902 β=3.5419 γ=35.947 δ=0.13208 ξ=3.0869
NB	FB	Gen. Extreme Value	k=0.3136 σ=21.731 μ=24.069
NB	FC	Johnson SB	γ=1.8623 δ=0.84691 λ=235.99 ξ=0.44051
NB	FD	Wakeby	α=28.656 β=17.719 γ=10.372 δ=-0.041 ξ=0.06741
NB	FE	Weibull (3P)	α=1.2859 β=102.38 γ=1.1443
NB	FF	Gen. Pareto	k=-0.09317 σ=71.097 μ=0.70804

Table A.10. Successive southbound vessel entrance distributions based on the actual transit traffic data of 2009.

Direction	Vessel pairs	Interentrance distribution	Parameters
SB	**AA**	Wakeby	a=216.68 b=10.644 g=4.9118 d=0.44527 x=49.939
SB	**AC**	Burr (4P)	k=0.36449 a=7.0984 b=27.775 g=-10.329
SB	**AD**	Wakeby	a=32.378 b=8.4062 g=4.94 d=0.28868 x=1.3961
SB	**AE**	Wakeby	a=32.378 b=8.4062 g=4.94 d=0.28868 x=1.3961
SB	**AF**	Phased Bi-Weibull	a_1=0.98999 b_1=59.937 g_1=0 a_2=1.1461 b_2=52.288 g_2=22
SB	**BB**	Wakeby	a=30080.0 b=634.02 g=23.159 d=0.30415 x=0
SB	**BC**	Burr (4P)	k=0.69737 a=5.0327 b=28.437 g=-7.5545
SB	**BD**	Burr	k=0.82408 a=2.9921 b=7.4196
SB	**BE**	Log-Gamma	a=37.275 b=0.11359
SB	**BF**	Wakeby	a=22.021 b=1.5487 g=29.669 d=0.18301 x=0.36804
SB	**CA**	Burr	k=1.5493 a=2.9984 b=33.857
SB	**CB**	Burr (4P)	k=0.69737 a=5.0327 b=28.437 g=-7.5545
SB	**CC**	Wakeby	a=31.238 b=6.9419 g=30.546 d=0.12467 x=4.3236
SB	**CD**	Log-Logistic	a=2.9751 b=7.5479
SB	**CE**	Log-Logistic (3P)	a=2.9398 b=27.808 g=2.1731
SB	**CF**	Wakeby	a=21.31 b=15.086 g=24.174 d=0.13024 x=0
SB	**DA**	Dagum	k=0.67175 a=3.9095 b=16.751
SB	**DB**	Log-Logistic	a=3.062 b=12.711
SB	**DC**	Dagum	k=0.66908 a=3.6778 b=12.31
SB	**DD**	Lognormal	s=0.7669 m=2.3746
SB	**DE**	Inv. Gaussian	l=51.709 m=15.595
SB	**DF**	Lognormal	s=0.88392 m=1.9439
SB	**EA**	Wakeby	a=62.119 b=2.846 g=15.308 d=-0.05316 x=12.842
SB	**EB**	Wakeby	a=2170.6 b=103.39 g=234.21 d=-0.8198 x=0
SB	**EC**	Johnson SB	g=2.1041 d=0.89052 l=262.37 x=3.3592
SB	**ED**	Wakeby	a=58.952 b=16.177 g=5.1282 d=0.17064 x=0.53008
SB	**EE**	Wakeby	a=100.07 b=0.44498 g=0 d=0 x=8.4314
SB	**EF**	Wakeby	a=38.237 b=4.46 g=90.024 d=-0.15969 x=-3.5265
SB	**FA**	Pearson 6	a_1=1.9793 a_2=1.2249E+5 b=2.5347E+6
SB	**FB**	Burr	k=1.6945 a=1.5467 b=61.622
SB	**FC**	Wakeby	a=292.63 b=44.94 g=29.937 d=-0.00107 x=-2.9125
SB	**FD**	Gen. Gamma	k=0.51345 a=5.5004 b=0.37164
SB	**FE**	Johnson SB	g=1.1756 d=0.71168 l=208.87 x=4.5387
SB	**FF**	Wakeby	a=48.144 b=0.19642 g=24.217 d=0.10674 x=0

Table A.11. Successive northbound vessel entrance distributions based on the actual transit traffic data of 2010.

Direction	Vessel pairs	Interentrance distribution	Parameters
NB	**AA**	Log-Logistic (3P)	α=8,9921 β=63,353 γ=22,698
			σ=11,052 μ=84,734
NB	**AC**	Gen. Extreme Value	k=0,27407 σ=14,144 μ=23,238
NB	**AD**	Wakeby	α=14,225 β=2,8217 γ=5,1104
			δ=0,2964 ξ=1,1134
NB	**AE**	Burr	k=0,33704 α=4,6513 β=26,213
NB	**AF**	Wakeby	α=45,341 β=0,49309 γ=6,0789
			δ=0,49316 ξ=0,31057
NB	**CA**	Burr	k=1,8663 α=2,0093 β=50,179
NB	**CC**	Lognormal (3P)	σ=0,84687 μ=3,5716 γ=-2,0092
NB	**CD**	Log-Logistic (3P)	α=2,7713 β=8,501 γ=-1,0047
NB	**CE**	Lognormal	σ=0,85714 μ=3,7604
NB	**CF**	Log-Pearson 3	α=24,454 β=-0,22668 γ=8,5331
NB	**DA**	Log-Logistic (3P)	α=2,6236 β=9,2386 γ=-0,66895
NB	**DC**	Frechet (3P)	α=5,5424 β=28,387 γ=-20,639
NB	**DD**	Lognormal (3P)	σ=0,70847 μ=2,3687 γ=-1,4084
NB	**DE**	Log-Logistic (3P)	α=2,6106 β=12,824 γ=-0,41354
NB	**DF**	Pearson 6 (4P)	α_1=1,4448 α_2=11,049
NB	**EA**	Dagum	k=0,5279 α=4,4671 β=56,423
NB	**EC**	Gen. Pareto	k=-0,05714 σ=37,616 μ=5,1779
NB	**ED**	Pearson 5	α=1,2905 β=6,8082
NB	**EE**	Log-Logistic (3P)	α=1,9914 β=63,994 γ=0,69956
NB	**EF**	Kumaraswamy	α_1=0,70929 α_2=2,0265
NB	**FA**	Dagum	k=0,81367 α=1,9346 β=57,659
NB	**FC**	Log-Pearson 3	α=26,4 β=-0,19718 γ=8,3928
NB	**FD**	Lognormal (3P)	σ=0,74487 μ=2,2354 γ=-1,436
NB	**FE**	Gen. Pareto	k=-0,07738 σ=90,298 μ=3,3782
NB	**FF**	Gen. Gamma	k=0,99028 α=0,93945 β=98,393

Table A.12. Successive southbound vessel entrance distributions based on the actual transit traffic data of 2010.

Direction	Vessel pairs	Interentrance distribution	Parameters
SB	**AA**	Log-Logistic (3P)	α=9,2967 β=49,18 γ=26,185
SB	**AC**	Wakeby	α=103,19 β=9,3592 γ=11,97 δ=0,33643 ξ=4,9038
SB	**AD**	Dagum	k=1,3398 α=2,4376 β=7,4477
SB	**AE**	Wakeby	α=118,1 β=8,7845 γ=11,028 δ=0,32793 ξ=10,401
SB	**AF**	Dagum	k=0,61739 α=1,8551 β=46,692
SB	**CA**	Burr	k=1,5401 α=3,0026 β=33,669
SB	**CC**	Lognormal (3P)	σ=0,81889 μ=3,4712 γ=-1,09
SB	**CD**	Burr (4P)	k=0,72494 α=4,1354
SB	**CE**	Burr	k=0,5887 a=3,256 b=25,545
SB	**CF**	Gen. Gamma (4P)	k=0,38234 α=5,8879
SB	**DA**	Dagum (4P)	k=0,96086 α=3,8598
SB	**DC**	Dagum (4P)	k=1,0389 α=3,6327
SB	**DD**	Lognormal (3P)	σ=0,68379 μ=2,4007 γ=-1,2963
SB	**DE**	Dagum	k=0,63673 α=3,9129 β=16,169
SB	**DF**	Pearson (5)	k=3,3721 α=29,001 β=-2,9054
SB	**EA**	Dagum	k=0,99703 α=4,1351 β=39,676
SB	**EC**	Burr	k=1,9586 α=1,994 β=59,27
SB	**ED**	Burr (4P)	k=0,3632 α=8,7985
SB	**EE**	Burr	k=0,66232 α=2,8864 β=54,096
SB	**EF**	Gen. Gamma	k=1,074 α=0,70428 β=198,88
SB	**FA**	Dagum	k=0,69502 α=2,4409 β=46,96
SB	**FC**	Log-Pearson 3	α=18,502 β=-0,21766 γ=7,257
SB	**FD**	Gen. Gamma (4P)	k=0,75532 α=2,6158
SB	**FE**	Gamma (3P)	α=0,82285 β=81,512 γ=4,3
SB	**FF**	Gen. Pareto	k=-0,00111 σ=104,77 μ=-0,256

Table A.13. Successive northbound vessel entrance distributions based on the actual transit traffic data of 2012.

Direction	Vessel pairs	Interentrance	Parameters
NB	**AA**	Log-Logistic (3P)	α=7.6093 β=53.728 γ=33.419
NB	**AC**	Gen. Extreme Value	k=0.18862 σ=12.555 μ=20.012
NB	**AD**	Gen. Extreme Value	k=0.24884 σ=5.0126 μ=7.4216
NB	**AE**	Burr	k=0.45712 α=3.7644 β=28.52
NB	**AF**	Wakeby	α=0 β=0 γ=49.082 δ=0.03509 ξ=1.377
NB	**BB**	Burr	k=0.31461 α=8.7911 β=59.492
NB	**BC**	Wakeby	α=65.981 β=5.5359 γ=10.107 δ=0.30896 ξ=2.5418
NB	**BD**	Burr	k=1.2043 α=2.2849 β=10.063
NB	**BE**	Wakeby	α=-213.59 β=4.2484 γ=249.62 δ=-0.69989 ξ=14.6
NB	**BF**	Wakeby	α=25.628 β=3.2112 γ=31.105 δ=0.14823 ξ=0.67168
NB	**CA**	Wakeby	α=111.59 β=6.8683 γ=19.427 δ=0.04812 ξ=3.7583
NB	**CB**	Pearson 6 (4P)	α_1=6.3343 α_2=6.403 β=30.3 γ=-2.1941
NB	**CC**	Log-Logistic	α=2.0334 β=27.47
NB	**CD**	Log-Logistic	α=2.5706 β=7.7879
NB	**CE**	Wakeby	α=37.986 β=4.5193 γ=30.831 δ=0.06192 ξ=6.0019
NB	**CF**	Wakeby	α=99.241 β=105.2 γ=23.4 δ=0.02201 ξ=0
NB	**DA**	Wakeby	α=36.571 β=4.4657 γ=7.4828 δ=0.25428 ξ=1.4638
NB	**DB**	Gen. Gamma	k=0.48672 α=8.4303 β=0.17428
NB	**DC**	Gen. Extreme Value	k=0.18342 σ=5.1324 μ=7.6978
NB	**DD**	Gen. Gamma	k=0.55861 α=5.2128 β=0.68531
NB	**DE**	Dagum	k=0.74153 α=2.706 β=14.364
NB	**DF**	Wakeby	α=8.6111 β=2.049 γ=6.6951 δ=0.21115 ξ=0.56225
NB	**EA**	Burr	k=0.52877 α=3.5257 β=35.224
NB	**EB**	Johnson SB	γ=0.43679 δ=0.71388 λ=322.07 ξ=-0.83666
NB	**EC**	Frechet (3P)	α=2.2792 β=34.527 γ=-13.25
NB	**ED**	Burr (4P)	k=0.38606 α=4.0191 β=6.9798 γ=-1.3389
NB	**EE**	Burr (4P)	k=28.859 α=1.2055 β=1792.1 γ=3.8564
NB	**EF**	Phased Bi-Exponential	l1=0.01227 g1=0 l2=0.04367 g2=230
NB	**FA**	Wakeby	α=56.143 β=2.0151 γ=22.855 δ=0.26646 ξ=1.6582
NB	**FB**	Dagum	k=0.46372 α=2.5904 β=65.395
NB	**FC**	Gen. Pareto	k=0.0506 σ=25.309 μ=1.9642
NB	**FD**	Wakeby	α=10.403 β=5.0916 γ=9.6862 δ=0.0362 ξ=0.74506
NB	**FE**	Johnson SB	γ=1.2267 δ=0.62883 λ=300.57 ξ=2.0785
NB	**FF**	Dagum	k=0.34893 α=2.9285 β=103.21

Table A.14. Successive southbound vessel entrance distributions based on the actual transit traffic data of 2012.

Direction	Vessel pairs	Interentrance	Parameters
SB	**AA**	Cauchy	σ=5.0527 μ=76.545
SB	**AC**	Gen. Extreme Value	k=0.1952 σ=11.114 μ=20.039
SB	**AD**	Burr	k=0.62874 α=3.5049 β=7.2643
SB	**AE**	Burr	k=0.23841 α=6.7379 β=19.942
SB	**AF**	Wakeby	α=39.833 β=0.64371 γ=12.136 δ=0.41581 ξ=-0.27503
SB	**BB**	Wakeby	α=0 β=0 γ=27.791 δ=0.30035 ξ=49.575
SB	**BC**	Wakeby	α=78.593 β=6.8107 γ=8.205 δ=0.32887 ξ=3.9325
SB	**BD**	Burr	k=0.70643 α=3.1125 β=7.3524
SB	**BE**	Burr	k=1220.1 α=1.6235 β=11454.0
SB	**BF**	Gen. Extreme Value	k=0.34935 σ=22.824 μ=22.935
SB	**CA**	Gen. Logistic	k=0.3001 σ=9.7434 μ=30.886
SB	**CB**	Burr (4P)	k=0.77 α=3.3587 β=24.08 γ=-1.2425
SB	**CC**	Burr	k=0.36613 α=2.7146 β=15.453
SB	**CD**	Log-Logistic	α=2.9633 β=7.9127
SB	**CE**	Fatigue Life (3P)	α=0.70097 β=39.236 γ=-3.4848
SB	**CF**	Fatigue Life	α=1.1441 β=13.92
SB	**DA**	Wakeby	α=36.173 β=4.6175 γ=4.8782 δ=0.35323 ξ=3.0826
SB	**DB**	Log-Logistic	α=2.9427 β=12.131
SB	**DC**	Burr	k=1.3047 α=2.934 β=11.46
SB	**DD**	Gen. Pareto	k=-0.06462 σ=12.89 μ=2.9425
SB	**DE**	Dagum	k=0.8818 α=3.4263 β=12.992
SB	**DF**	Lognormal	s=0.84145 m=2.0814
SB	**EA**	Wakeby	α=78.311 β=3.8034 γ=11.892 δ=0.4746 ξ=12.213
SB	**EB**	Wakeby	α=-173.98 β=9.9795 γ=184.44 δ=-0.63146 ξ=14.592
SB	**EC**	Burr (4P)	k=0.1131 α=518.95 β=1266.7 γ=-1256.0
SB	**ED**	Burr (4P)	k=0.52996 α=4.9962 β=9.3432 γ=-2.978
SB	**EE**	Log-Logistic	α=2.0734 β=58.167
SB	**EF**	Wakeby	α=-15.317 β=0.79302 γ=60.192 δ=0.005 ξ=0.31271
SB	**FA**	Burr	k=1.2712 α=1.8849 β=46.95
SB	**FB**	Burr	k=2.2357 α=1.4851 β=73.812
SB	**FC**	Wakeby	α=57.399 β=15.385 γ=21.077 δ=0.081 ξ=0.32339
SB	**FD**	Gen. Gamma	k=0.39876 α=10.093 β=0.03158
SB	**FE**	Log-Logistic (3P)	α=1.7082 β=42.277 γ=-0.1814
SB	**FF**	Dagum	k=0.33959 α=3.1502 β=100.75

Table A.15. Successive northbound vessel entrance distributions based on the actual transit traffic data of 2013.

Direction	Vessel pairs	Interentrance distribution	Parameters
NB	**AA**	Log-Logistic (3P)	α=7.6093 β=53.728 γ=33.419
NB	**AC**	Gen. Extreme Value	k=0.18862 σ=12.555 μ=20.012
NB	**AD**	Gen. Extreme Value	k=0.24884 σ=5.0126 μ=7.4216
NB	**AE**	Burr	k=0.45712 α=3.7644 β=28.52
NB	**AF**	Gen. Pareto	k=0.03509 σ=49.082 μ=1.377
NB	**BB**	Burr	k=0.31461 α=8.7911 β=59.492
NB	**BC**	Wakeby	α=65.981 β=5.5359 γ=10.107 δ=0.30896 ξ=2.5418
NB	**BD**	Burr	k=1.2043 α=2.2849 β=10.063
NB	**BE**	Wakeby	α=-213.59 β=4.2484 γ=249.62 δ=-0.69989 ξ=14.6
NB	**BF**	Wakeby	α=25.628 β=3.2112 γ=31.105 δ=0.14823 ξ=0.67168
NB	**CA**	Wakeby	α=111.59 β=6.8683 γ=19.427 δ=0.04812 ξ=3.7583
NB	**CB**	Pearson 6 (4P)	α_1=6.3343 α_2=6.403 β=30.3 γ=-2.1941
NB	**CC**	Log-Logistic	α=2.0334 β=27.47
NB	**CD**	Log-Logistic	α=2.5706 β=7.7879
NB	**CE**	Wakeby	α=37.986 β=4.5193 γ=30.831 δ=0.06192 ξ=6.0019
NB	**CF**	Wakeby	α=99.241 β=105.2 γ=23.4 δ=0.02201 ξ=0
NB	**DA**	Wakeby	α=36.571 β=4.4657 γ=7.4828 δ=0.25428 ξ=1.4638
NB	**DB**	Gen. Gamma	k=0.48672 α=8.4303 β=0.17428
NB	**DC**	Gen. Extreme Value	k=0.18342 σ=5.1324 μ=7.6978
NB	**DD**	Gen. Gamma	k=0.55861 α=5.2128 β=0.68531
NB	**DE**	Dagum	k=0.74153 α=2.706 β=14.364
NB	**DF**	Wakeby	α=8.6111 β=2.049 γ=6.6951 δ=0.21115 ξ=0.56225
NB	**EA**	Wakeby	α=135.06 β=3.1285 γ=5.1409 δ=0.40976 ξ=8.4067
NB	**EB**	Johnson SB	γ=0.42539 δ=0.54147 λ=287.03 ξ=11.845
NB	**EC**	Log-Logistic (3P)	α=2.2443 β=23.436 γ=-0.78711
NB	**ED**	Burr	k=0.80861 α=2.5026 β=8.8402
NB	**EE**	Gen. Pareto	k=-0.07456 σ=73.826 μ=7.6556
NB	**EF**	Wakeby	α=-136.49 β=1.1664 γ=174.18 δ=-0.34659 ξ=2.0564
NB	**FA**	Gen. Logistic	k=0.33391 σ=20.717 μ=44.537
NB	**FB**	Pearson 6	α_1=1.6599 α_2=4.9166 β=120.94
NB	**FC**	Wakeby	α=19.275 β=9.1204 γ=22.708 δ=0.09472 ξ=1.1233
NB	**FD**	Lognormal	σ=0.86788 μ=2.226
NB	**FE**	Lognormal	σ=1.1955 μ=3.6348
NB	**FF**	Wakeby	α=61.724 β=3.2166 γ=42.504 δ=0.07634 ξ=-1.0617

Table A.16. Successive southbound vessel entrance distributions based on the actual transit traffic data of 2013.

Direction	Vessel pairs	Interentrance distribution	Parameters
SB	**AA**	Cauchy	σ=5.0527 μ=76.545
SB	**AC**	Gen. Extreme Value	k=0.1952 σ=11.114 μ=20.039
SB	**AD**	Burr	k=0.62874 α=3.5049 β=7.2643
SB	**AE**	Burr	k=0.23841 α=6.7379 β=19.942
SB	**AF**	Wakeby	α=39.833 β=0.64371 γ=12.136 δ=0.41581 ξ=-0.27503
SB	**BB**	Gen. Pareto	k=0.30035 σ=27.791 μ=49.575
SB	**BC**	Wakeby	α=78.593 β=6.8107 γ=8.205 δ=0.32887 ξ=3.9325
SB	**BD**	Burr	k=0.70643 α=3.1125 β=7.3524
SB	**BE**	Burr	k=1220.1 α=1.6235 β=11454.0
SB	**BF**	Gen. Extreme Value	k=0.34935 σ=22.824 μ=22.935
SB	**CA**	Gen. Logistic	k=0.3001 σ=9.7434 μ=30.886
SB	**CB**	Burr (4P)	k=0.77 α=3.3587 β=24.08 γ=-1.2425
SB	**CC**	Burr	k=0.36613 α=2.7146 β=15.453
SB	**CD**	Log-Logistic	α=2.9633 β=7.9127
SB	**CE**	Fatigue Life	α=0.81028 β=34.076
SB	**CF**	Log-Logistic	α=2.9633 β=7.9127
SB	**DA**	Burr (4P)	k=0.66647 α=4.4629 β=15.118 γ=-2.4944
SB	**DB**	Log-Logistic	α=2.9296 β=12.688
SB	**DC**	Log-Logistic	α=3.2318 β=10.46
SB	**DD**	Gen. Pareto	k=-0.12336 σ=14.368 μ=3.0982
SB	**DE**	Burr	k=0.8768 α=3.3425 β=11.69
SB	**DF**	Fatigue Life	α=0.91981 β=8.2575
SB	**EA**	Wakeby	α=83.542 β=3.5666 γ=9.8563 δ=0.45549 ξ=14.176
SB	**EB**	Gen. Gamma (4P)	k=4.3959 α=0.18329 β=235.65 γ=12.0
SB	**EC**	Dagum	k=1.3038 α=2.3983 β=19.563
SB	**ED**	Wakeby	α=38.894 β=8.7138 γ=4.4897 δ=0.33127 ξ=0.83094
SB	**EE**	Weibull (3P)	α=0.98777 β=69.171 γ=11.0
SB	**EF**	Weibull (3P)	α=0.87489 β=57.12 γ=1.0
SB	**FA**	Wakeby	α=49.497 β=2.094 γ=23.292 δ=0.26346 ξ=4.0
SB	**FB**	Burr (4P)	k=2.138 α=1.4801 β=70.333 γ=0.85299
SB	**FC**	Wakeby	α=23.511 β=6.9564 γ=19.919 δ=0.11192 ξ=1.25
SB	**FD**	Lognormal	σ=0.82427 μ=2.2248
SB	**FE**	Johnson SB	γ=1.3363 δ=0.70123 λ=315.62 ξ=2.4579
SB	**FF**	Wakeby	α=117.69 β=5.0325 γ=41.872 δ=0.10645 ξ=-3.0742

Table A.17. Successive northbound vessel entrance distributions based on the actual transit traffic data of 2014.

Direction	Vessel pairs	Interentrance distribution	Parameters
NB	**AA**	Wakeby	α=120.95 β=5.8314 γ=5.2222 δ=0.46364 ξ=62.476
NB	**AC**	Wakeby	α=98.591 β=11.191 γ=19.091
NB	**AD**	Johnson SB	δ=0.01238 ξ=2.0805 γ=6.0344 λ=1997.9 ξ=1.5729 δ=1.103
NB	**AE**	Burr	k=0.35395 α=4.6455 β=23.537
NB	**AF**	Wakeby	α=39.085 β=1.673 γ=27.691 δ=0.24075 ξ=-0.90868
NB	**BB**	Wakeby	α=562.69 β=9.4318 γ=29.053 δ=0.24146 ξ=-12.347
NB	**BC**	Wakeby	α=54.386 β=5.5666 γ=11.201 δ=0.18849 ξ=2.2459
NB	**BD**	Wakeby	α=27.264 β=9.9857 γ=8.2848 δ=0.13112 ξ=1.3072
NB	**BE**	Fatigue Life (3P)	α=0.6776 β=85.579 γ=-16.606
NB	**BF**	Wakeby	α=20.644 β=1.4141 γ=24.01 δ=0.22022 ξ=1.1537
NB	**CA**	Burr	k=1.5422 α=2.5798 β=38.836
NB	**CB**	Burr	k=2.1123 α=1.9416 β=38.514
NB	**CC**	Burr	k=0.44824 α=2.3229 β=15.76
NB	**CD**	Burr	k=1.297 α=2.3595 β=9.7205
NB	**CE**	Log-Pearson 3	α=23.386 β=-0.16102 γ=7.1948
NB	**CF**	Wakeby	α=4.5639 β=1.1575 γ=15.468 δ=0.1676 ξ=0.98453
NB	**DA**	Pearson 5 (3P)	α=4.2098 β=82.379 γ=-5.7337
NB	**DB**	Gen. Gamma	k=0.45416 α=8.9082 β=0.11812
NB	**DC**	Wakeby	α=26.929 β=6.4258 γ=6.9611 δ=0.1008 ξ=1.0745
NB	**DD**	Gen. Gamma	k=0.59265 α=4.6802 β=1.1459
NB	**DE**	Log-Logistic (3P)	α=2.518 β=14.414 γ=-0.8476
NB	**DF**	Wakeby	α=8.7737 β=3.2605 γ=8.8684 δ=0.12849 ξ=0.50302
NB	**EA**	Wakeby	α=105.8 β=2.4255 γ=4.7145 δ=0.5367 ξ=8.9585
NB	**EB**	Wakeby	α=125.52 β=0.34925 γ=0 δ=0 ξ=2.5617
NB	**EC**	Log-Logistic (3P)	α=2.3733 β=21.799 γ=0.07168
NB	**ED**	Gen. Logistic	k=0.47481 σ=4.7879 μ=10.816
NB	**EE**	Wakeby	α=80.885 β=0.08647 γ=0 δ=0 ξ=9.5525
NB	**EF**	Weibull (3P)	α=0.79986 β=64.412 γ=1.0
NB	**FA**	Dagum	k=0.60995 α=2.3717 β=61.469
NB	**FB**	Wakeby	α=27.773 β=3.0069 γ=29.89 δ=0.15686 ξ=1.6622
NB	**FC**	Wakeby	α=20.771 β=7.6831 γ=20.403 δ=0.09914 ξ=1.3123
NB	**FD**	Wakeby	α=11.498 β=1.7111 γ=7.32 δ=0.17393 ξ=1.0802
NB	**FE**	Wakeby	α=67.833 β=0.02519 γ=0 δ=0 ξ=3.4809
NB	**FF**	Wakeby	α=75.656 β=4.0023 γ=45.85 δ=0.05416 ξ=-2.2468

Table A.18. Successive southbound vessel entrance distributions based on 2014.

Direction	Vessel pairs	Interentrance	Parameters
SB	**AA**	Cauchy	σ=5.2219 μ=75.257
SB	**AC**	Wakeby	α=133.23 β=13.791 γ=13.327 δ=0.19754 ξ=3.7354
SB	**AD**	Burr	k=0.61456 α=2.9179 β=7.4984
SB	**AE**	Burr	k=0.43829 α=4.5153 β=24.49
SB	**AF**	Wakeby	α=43.124 β=0.44766 γ=5.9884 δ=0.52574 ξ=0.31692
SB	**BB**	Wakeby	α=811.05 β=13.55 γ=35.609 δ=0.16814 ξ=-18.851
SB	**BC**	Wakeby	α=56.136 β=4.9905 γ=8.4181 δ=0.35259 ξ=3.0122
SB	**BD**	Burr	k=0.67516 α=2.8516 β=8.067
SB	**BE**	Wakeby	α=99.088 β=0.24929 γ=0 δ=0 ξ=2.8979
SB	**BF**	Wakeby	α=30.391 β=0.786 γ=13.041 δ=0.37735 ξ=0.13617
SB	**CA**	Dagum	k=1.3705 α=2.965 β=25.597
SB	**CB**	Wakeby	α=49.311 β=4.0668 γ=11.147 δ=0.28301 ξ=3.2793
SB	**CC**	Lognormal	σ=0.79161 μ=3.2214
SB	**CD**	Burr	k=0.92737 α=2.9707 β=7.8601
SB	**CE**	Wakeby	α=46.616 β=0.4016 γ=0.02476 δ=0.98703 ξ=6.5685
SB	**CF**	Burr	k=0.67525 α=2.6314 β=7.1959
SB	**DA**	Wakeby	α=46.802 β=6.3739 γ=6.9903 δ=0.35777 ξ=2.7904
SB	**DB**	Gen. Extreme Value	k=0.29792 σ=5.7871 μ=10.219
SB	**DC**	Log-Logistic	α=3.2397 β=10.885
SB	**DD**	Wakeby	α=18.654 β=0.95806 γ=3.0961 δ=0.45715 ξ=2.3191
SB	**DE**	Burr (4P)	k=0.65123 α=3.3209 β=11.187 γ=-0.49591
SB	**DF**	Wakeby	α=15.276 β=0.49469 γ=0.68463 δ=0.70645 ξ=0.68801
SB	**EA**	Wakeby	α=135.8 β=5.8453 γ=12.369 δ=0.4334 ξ=7.9807
SB	**EB**	Weibull	α=1.2929 β=95.484
SB	**EC**	Dagum	k=1.1018 α=2.3803 β=23.402
SB	**ED**	Burr	k=0.74057 α=2.6606 β=7.9606
SB	**EE**	Johnson SB	γ=1.0574 δ=0.64679 λ=313.17 ξ=7.4185
SB	**EF**	Weibull (3P)	α=0.79045 β=41.844 γ=1.0
SB	**FA**	Dagum	k=0.67131 α=2.5511 β=46.76
SB	**FB**	Dagum	k=0.54095 α=2.5252 β=52.129
SB	**FC**	Gen. Gamma	k=0.47185 α=5.697 β=0.49661
SB	**FD**	Lognormal	σ=0.85956 μ=2.2299
SB	**FE**	Pearson 6	α_1=1.4906 α_2=5.1147 β=160.05
SB	**FF**	Wakeby	α=118.19 β=3.6478 γ=33.085 δ=0.18229 ξ=-3.4457

APPENDIX B: COMPARISON OF MODEL GENERATED AND ACTUAL INTERARRIVAL TIMES

Table B.1. Comparison of interarrival times for 2008.

Vessel Type	Model Average	Actual case	PI left	PI right	Fall in range
NB AA	562.3	502	458.85	665.75	TRUE
NB BB	379.5	414	332.3	426.7	TRUE
NB CC	121.061	120.51	120.26	121.87	TRUE
NB DD	30.427	30	29.611	31.243	TRUE
NB EE	1493.4	1550	1105.2	1881.6	TRUE
NB FF	232.1	350	208.13	256.07	FALSE
NB PP	615.4	713	468.82	761.98	TRUE
SB AA	595.8	501	496.16	695.44	TRUE
SB BB	406.4	408	368.81	443.99	TRUE
SB CC	121.8	121	115.47	128.13	TRUE
SB DD	31.096	29	30.335	31.857	FALSE
SB EE	1457.3	1510	1349.7	1564.9	TRUE
SB FF	173.55	350	137.6	209.5	FALSE
SB PP	597.5	694	481.25	713.75	TRUE

Table B.2. Comparison of interarrival times for 2009.

Vessel Type	Model Average	Actual case	PI left	PI right	Fall in range
NB AA	502.35	490	458.3441	546.3559	TRUE
NB BB	480.8268	382	327.8704	633.7831	TRUE
NB CC	116	113	107.5507	124.4493	TRUE
NB DD	34	31	32.69624	35.30376	FALSE
NB EE	2391.45	2372	1754.577	3028.323	TRUE
NB FF	279.25	278	255.7146	302.7854	TRUE
NB PP	766.65	778	621.1642	912.1358	TRUE
SB AA	497.8	497	444.3524	551.2476	TRUE
SB BB	383.2	387	354.2637	412.1363	TRUE
SB CC	114.65	114	109.2312	120.0688	TRUE
SB DD	31.1	34	29.86315	32.33685	FALSE
SB EE	2366.95	2327	2057.321	2676.579	TRUE
SB FF	277.8	280	247.4866	308.1134	TRUE
SB PP	773.6	785	617.8222	929.3778	TRUE

Table B.3. Comparison of interarrival times for 2010.

Vessel	Average	Actual Case	PI left	PI right	Fall in range
NB AA	419.338	519	349.1496	489.5264	FALSE
NB BB	423.705	385	339.5263	507.8837	TRUE
NB CC	127.3	127	118.9417	135.6583	TRUE
NB DD	34.2	34	32.55087	35.84913	TRUE
NB EE	1827.85	1833	1592.518	2063.182	TRUE
NB FF	254.6	256	226.8083	282.3917	TRUE
NB PP	910.45	1919	730.9031	1089.997	FALSE
SB AA	516.4	520	464.8827	567.9173	TRUE
SB BB	385.45	383	343.0333	427.8667	TRUE
SB CC	125.6	125	117.8429	133.3571	TRUE
SB DD	32.15	33	30.67785	33.62215	TRUE
SB EE	1802.6	1791	1345.613	2259.587	TRUE
SB FF	251.05	255	223.7808	278.3192	TRUE
SB PP	952.4	937	757.2352	1147.565	TRUE

Table B.4. Comparison of interarrival times for 2012.

Vessel	Average	Actual Case	PI left	PI right	Fall in range
NB AA	585.4	583	501.1548	669.6452	TRUE
NB BB	427.95	420	361.1464	494.7536	TRUE
NB CC	101.15	100	95.27948	107.0205	TRUE
NB DD	39.7	38	37.81068	41.58932	TRUE
NB EE	1524.45	1530	1223.338	1825.562	TRUE
NB FF	284.3	279	237.4718	331.1282	TRUE
NB PP	1014.8	979	740.8326	1288.767	TRUE
SB AA	587.95	587	536.3326	639.5674	TRUE
SB BB	417.45	421	367.5062	467.3938	TRUE
SB CC	99.4	99	93.65755	105.1424	TRUE
SB DD	36.9	38	35.66315	38.13685	TRUE
SB EE	1528.2	1531	1302.241	1754.159	TRUE
SB FF	275.1	276	249.2245	300.9755	TRUE
SB PP	1013.15	993	875.5851	1150.715	TRUE

Table B.5. Comparison of interarrival times for 2013.

Vessel	Average	Actual Case	PI left	PI right	Fall in range
NB AA	568.55	564	477.0038	660.0962	TRUE
NB BB	411.25	401	352.5973	469.9027	TRUE
NB CC	96.95	99	92.34514	101.5549	TRUE
NB DD	42	42	42	42	TRUE
NB EE	1511.4	1519	1237.927	1784.873	TRUE
NB FF	274.5	273	246.5224	302.4776	TRUE
NB PP	1022.7	1010	859.9388	1185.461	TRUE
SB AA	576.75	572	511.4336	642.0664	TRUE
SB BB	396.5	399	354.9943	438.0057	TRUE
SB CC	100.25	99	96.83152	103.6685	TRUE
SB DD	40.00	40	40	40	TRUE
SB EE	1528.9	1515	1210.165	1847.635	TRUE
SB FF	267.5	272	229.1222	305.8778	TRUE
SB PP	1037.15	998	960.115	1114.185	TRUE

Table B.6. Comparison of interarrival times for 2014.

Vessel	Average	Actual Case	PI left	PI right	Fall in range
NB AA	568.1	567	479.66	656.44	TRUE
NB BB	375.5	284	307.84	443.16	FALSE
NB CC	92.8	93	88.76	96.84	TRUE
NB DD	41.92	46	41.152	42.696	FALSE
NB EE	1399	1413	1281.9	1516.1	TRUE
NB FF	293.2	287	253.02	333.38	TRUE
NB PP	830.6	820	727.24	933.86	TRUE
SB AA	569.7	583	501.13	638.17	TRUE
SB BB	288.9	290	265.37	312.33	TRUE
SB CC	94.04	93	90.954	97.119	TRUE
SB DD	46.24	46	45.351	47.119	TRUE
SB EE	1428	1436	1260	1596.8	TRUE
SB FF	277.3	284	223.78	330.82	TRUE
SB PP	758.4	836	753.81	762.99	FALSE

APPENDIX C: COMPARISON OF MODEL GENERATED AND ACTUAL NUMBER OF VESSEL TRANSITS

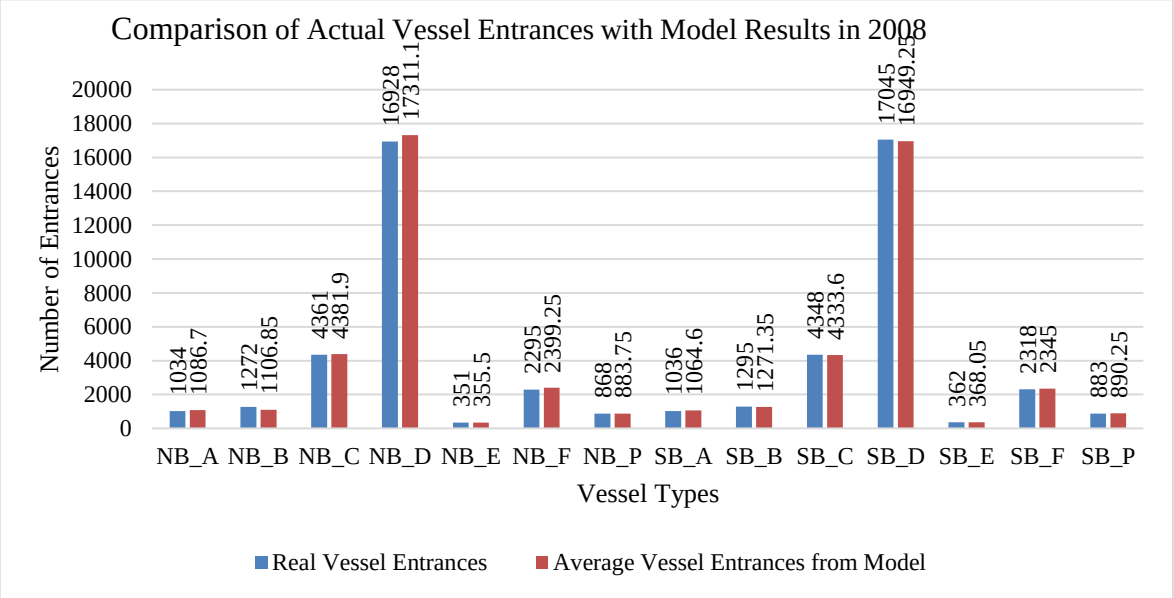

Figure C.1. Comparison of vessel transits in 2008.

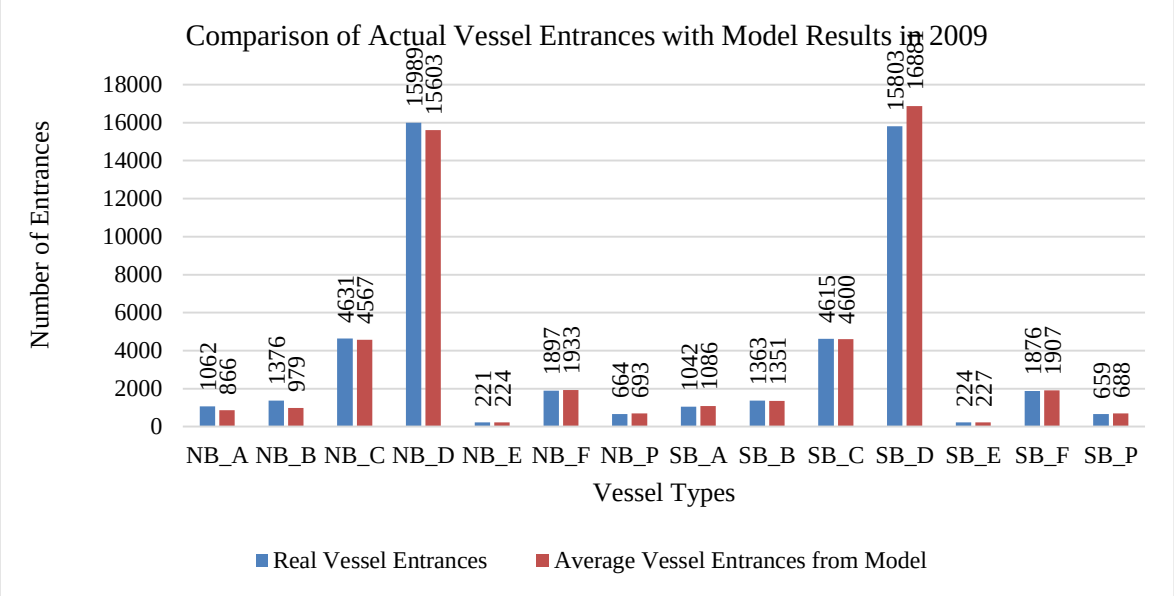

Figure C.2. Comparison of vessel transits in 2009.

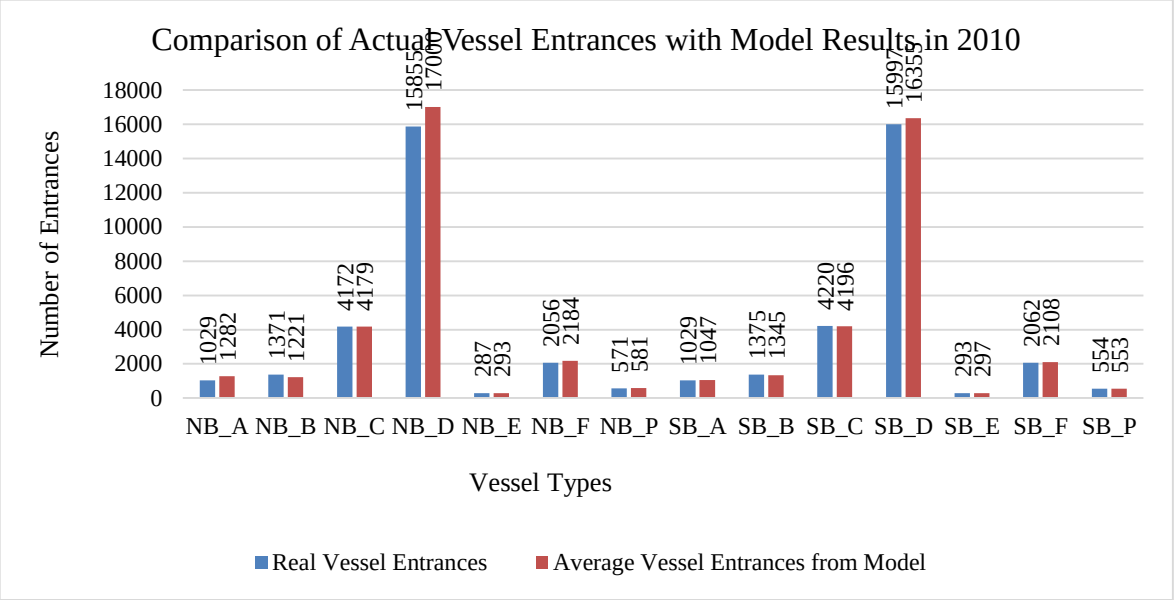

Figure C.3. Comparison of vessel transits in 2010.

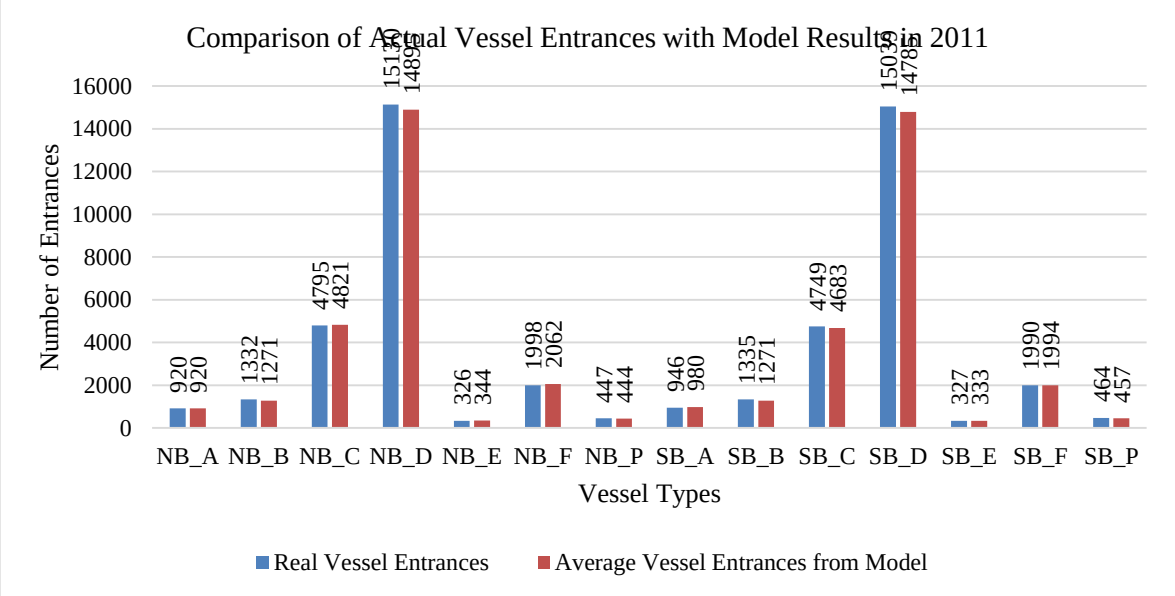

Figure C.4. Comparison of vessel transits in 2011.

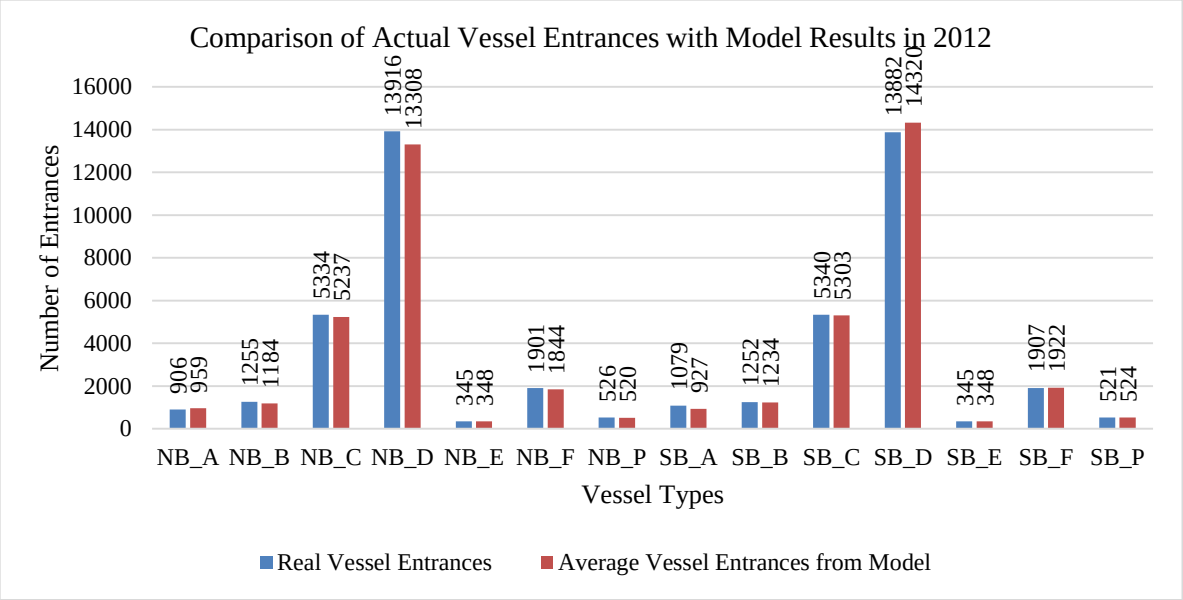

Figure C.5. Comparison of vessel transits in 2012.

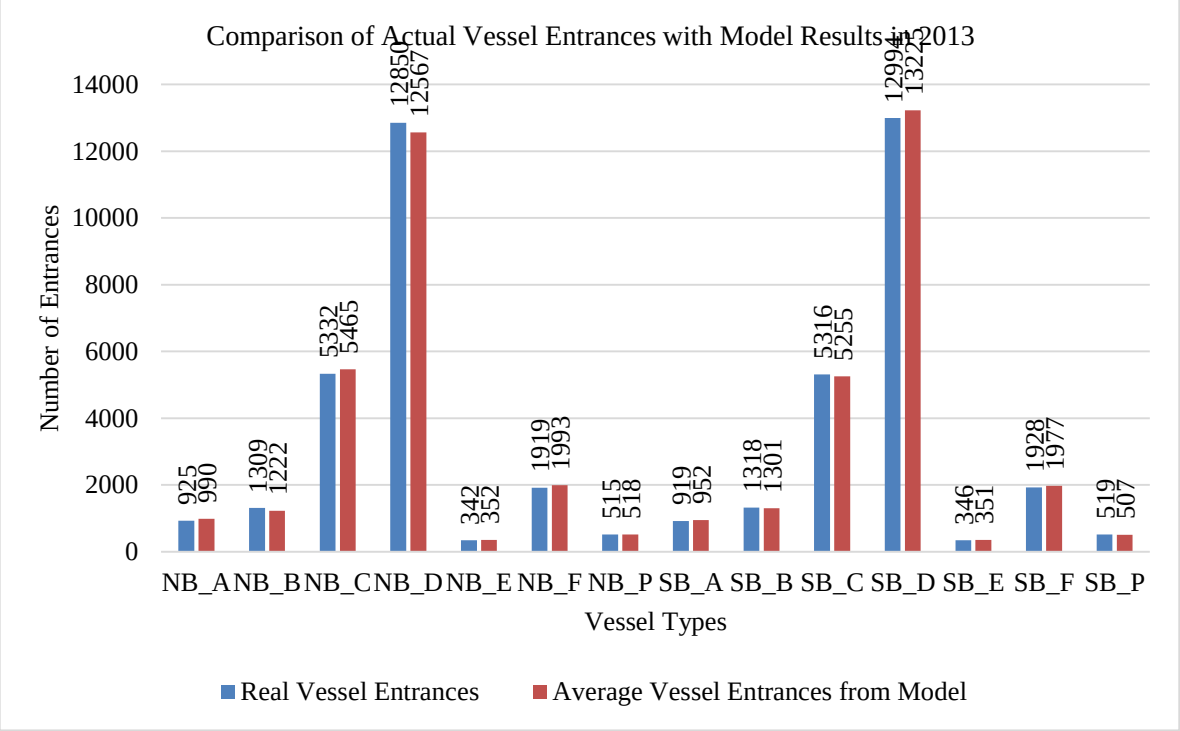

Figure C.6. Comparison of vessel transits in 2013.

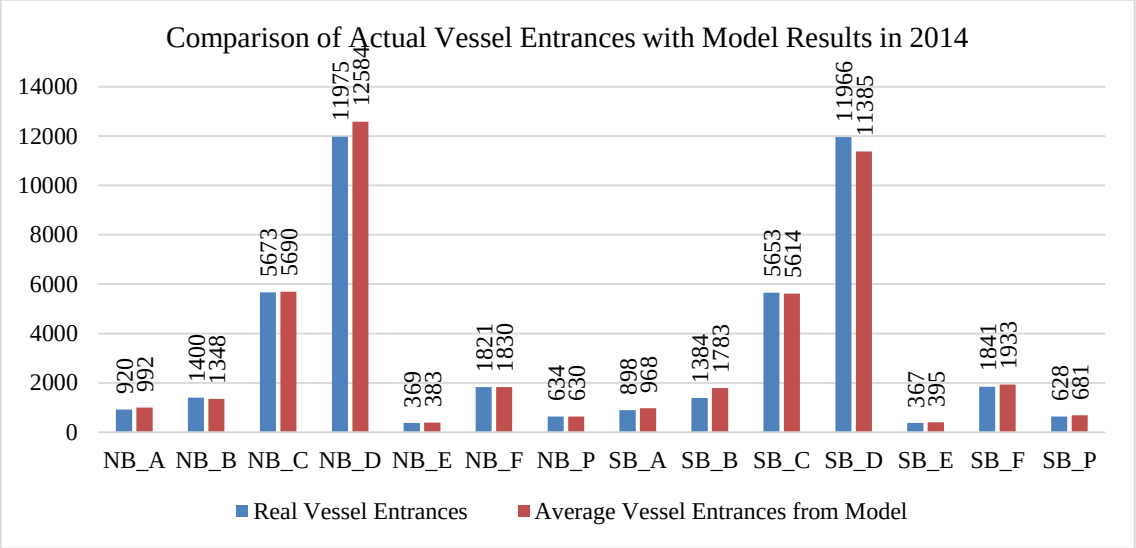

Figure C.7. Comparison of vessel transits in 2014.

APPENDIX D: COMPARISON OF MODEL GENERATED AND ACTUAL VESSEL INTERENTRANCE TIMES

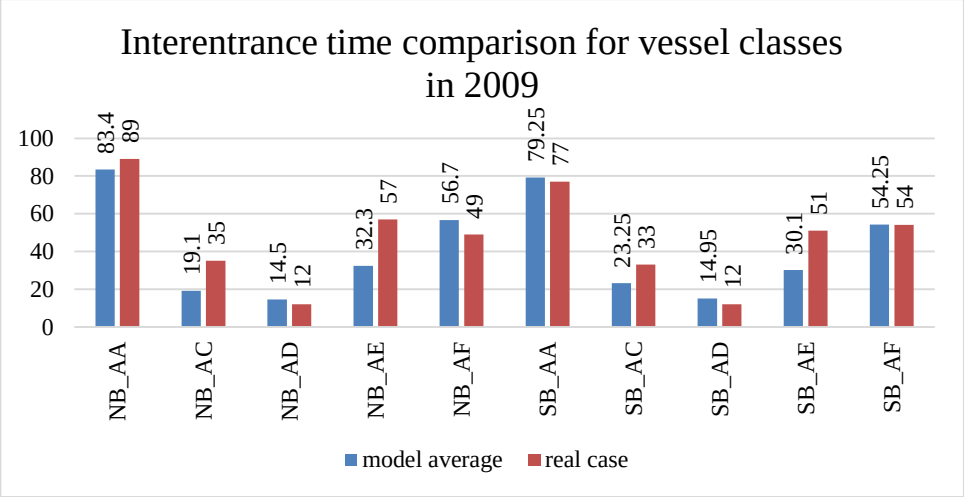

Figure D.1. Vessel interentrance time comparison for class A and successive classes in 2009.

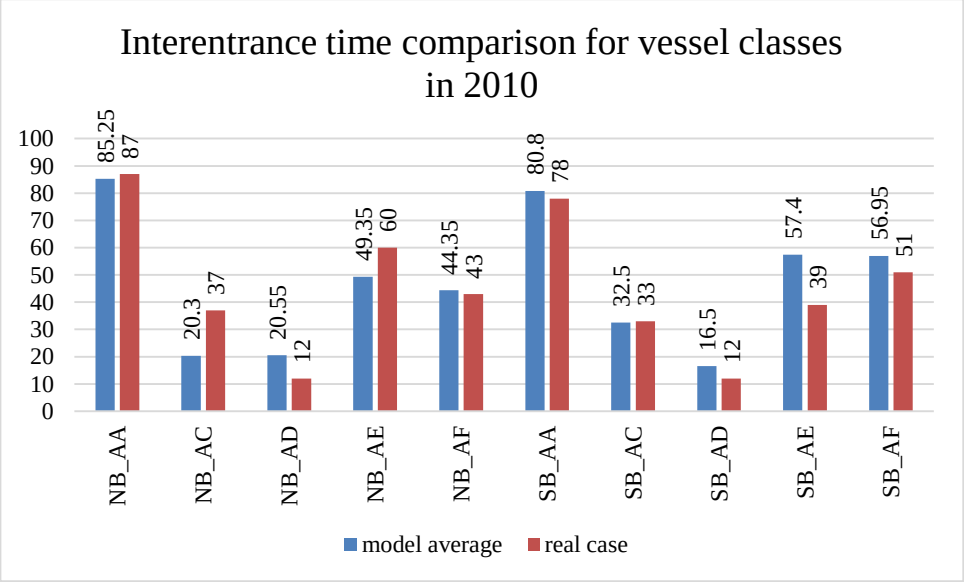

Figure D.2. Vessel interentrance time comparison for class A and successive classes in 2010.

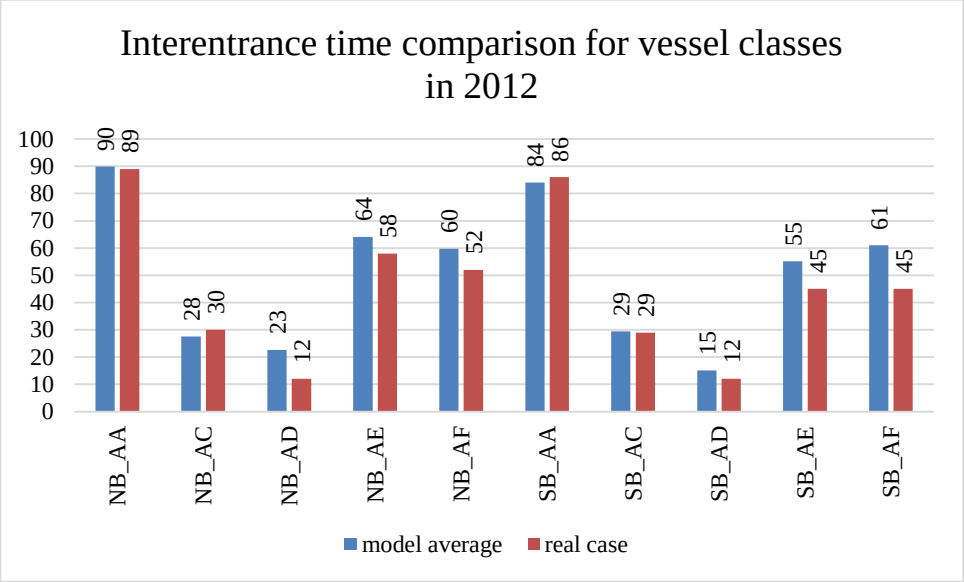

Figure D.3. Vessel interentrance time comparison for class A and successive classes in 2012.

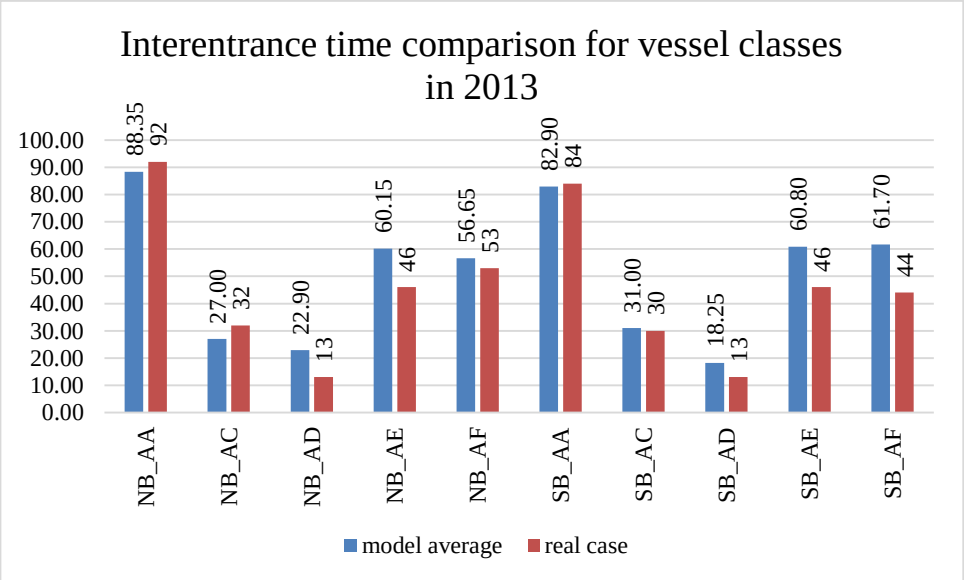

Figure D.4. Vessel interentrance time comparison for class A and successive classes in 2013.

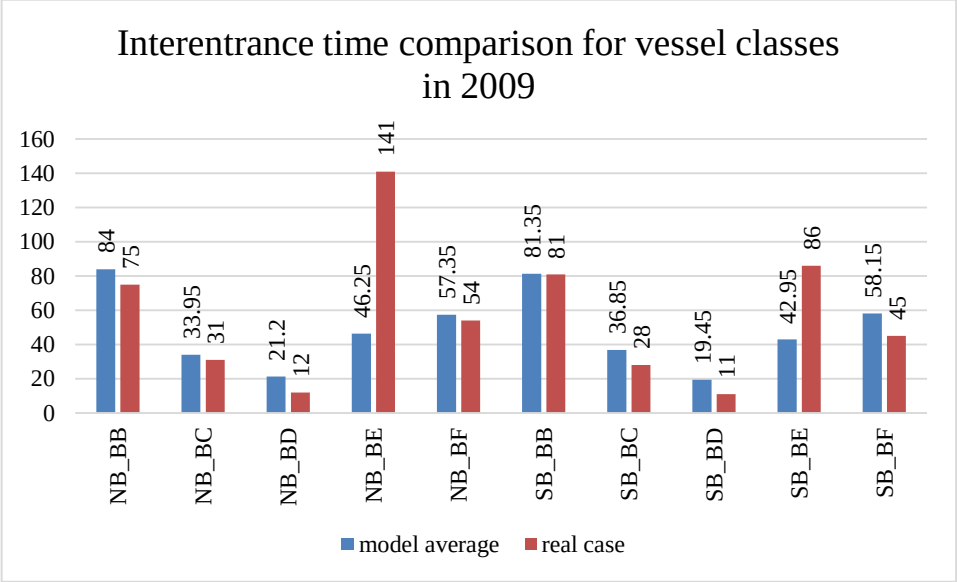

Figure D.5. Vessel interentrance time comparison for class B and successive classes in 2009.

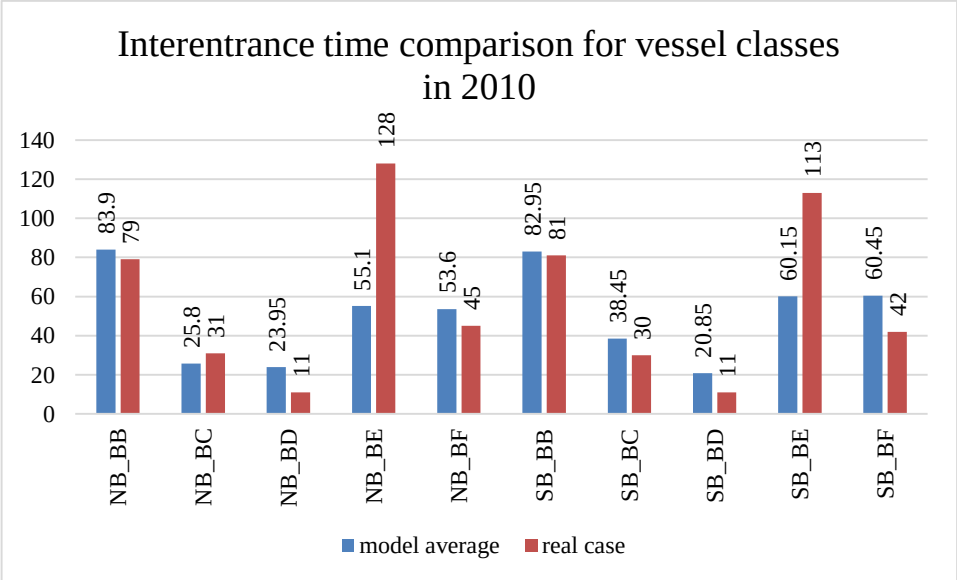

Figure D.6. Vessel interentrance time comparison for class B and successive classes in 2010.

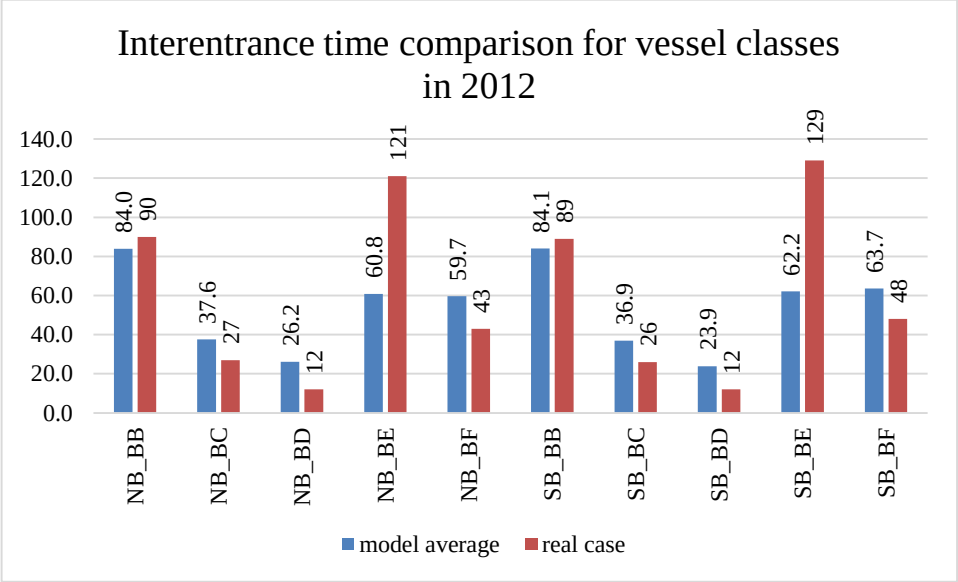

Figure D.7. Vessel interentrance time comparison for class B and successive classes in 2012.

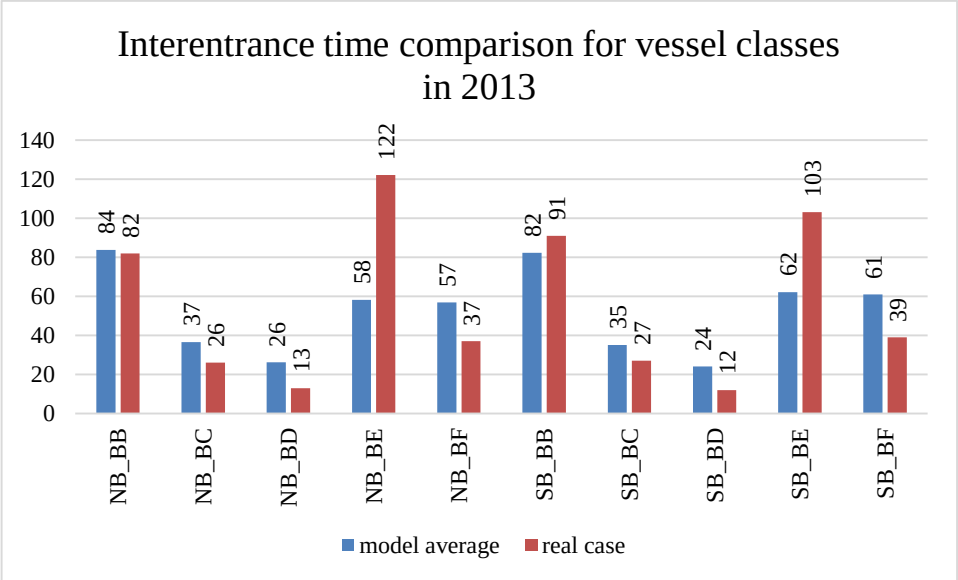

Figure D.8. Vessel interentrance time comparison for class B and successive classes in 2013.

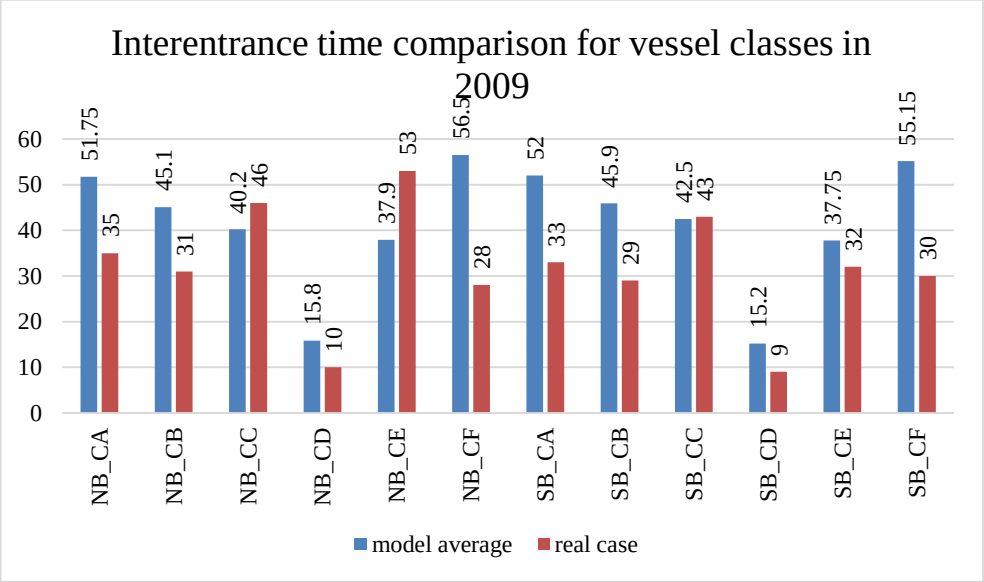

Figure D.9. Vessel interentrance time comparison for class C and successive classes in 2009.

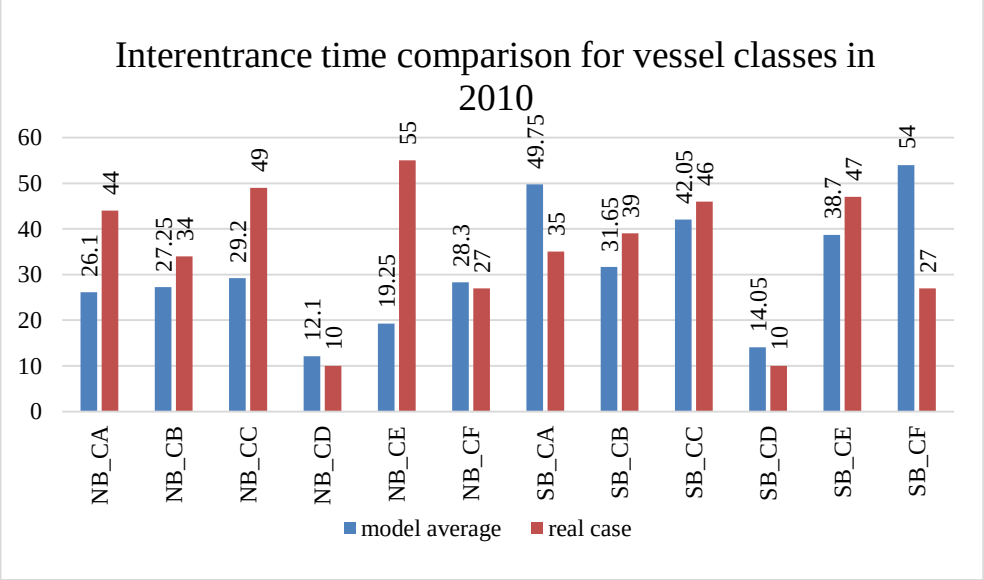

Figure D.10. Vessel interentrance time comparison for class C and successive classes in 2010.

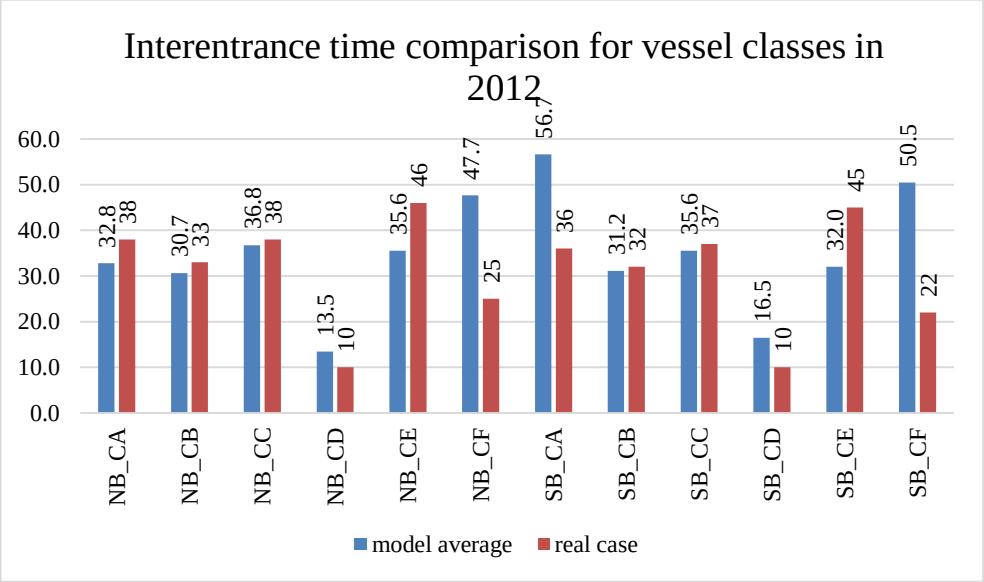

Figure D.11. Vessel interentrance time comparison for class C and successive classes in 2012.

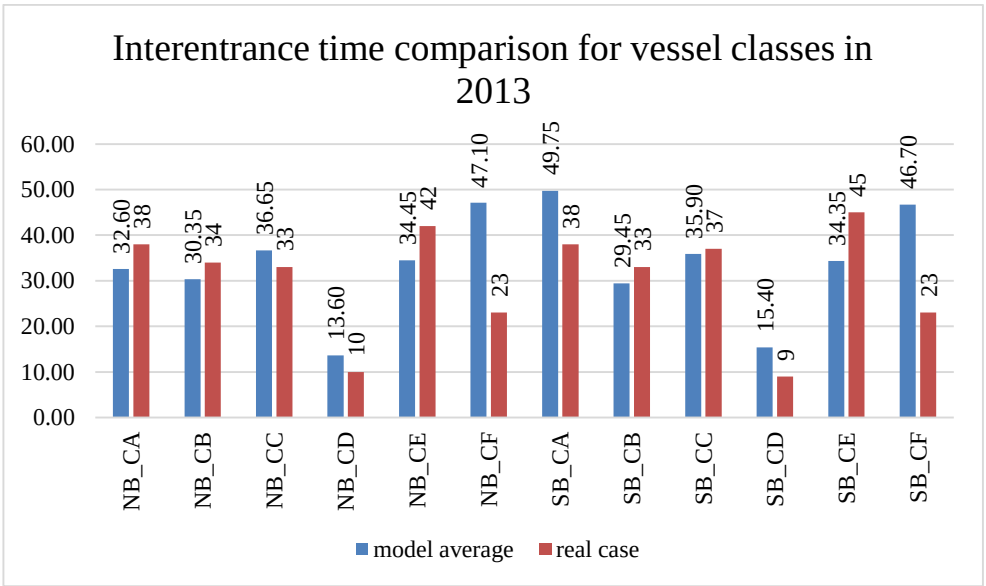

Figure D.12. Vessel interentrance time comparison for class C and successive classes in 2013.

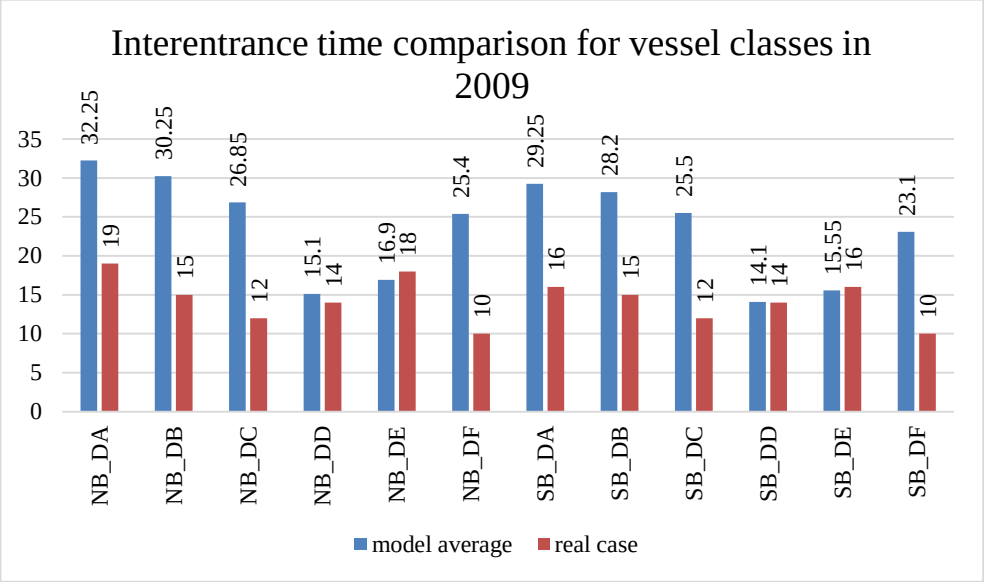

Figure D.13. Vessel interentrance time comparison for class D and successive classes in 2009.

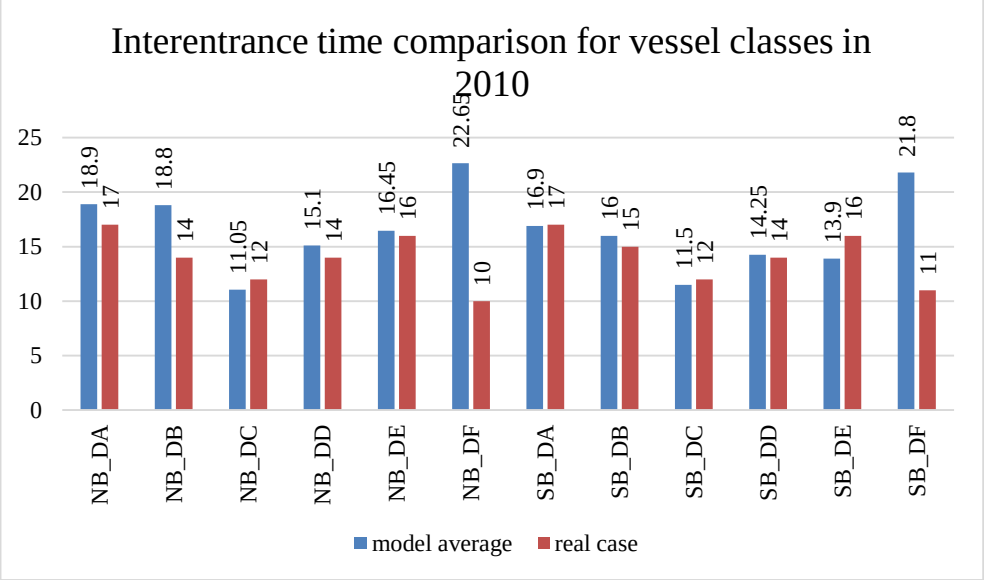

Figure D.14. Vessel interentrance time comparison for class D and successive classes in 2010.

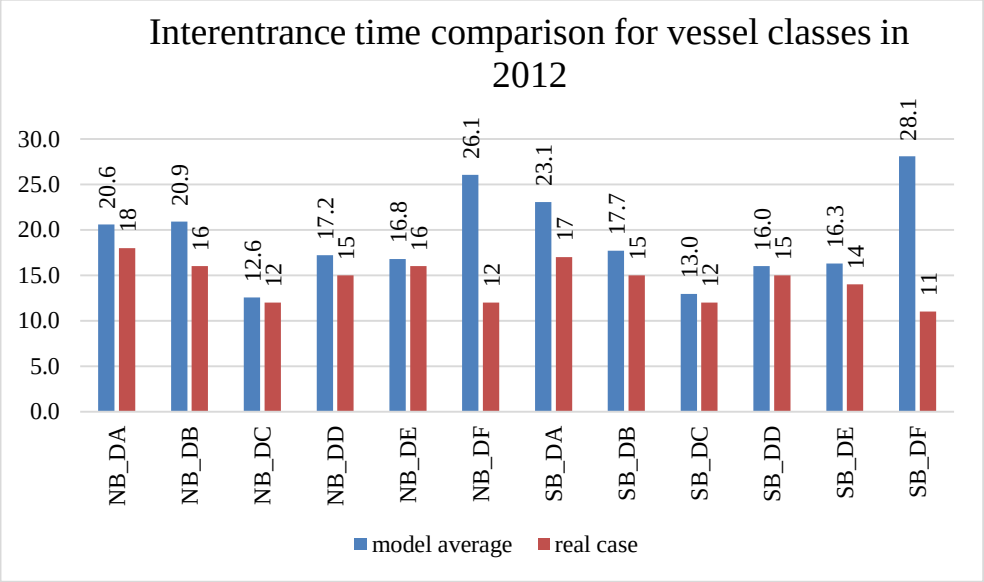

Figure D.15. Vessel interentrance time comparison for class D and successive classes in 2012.

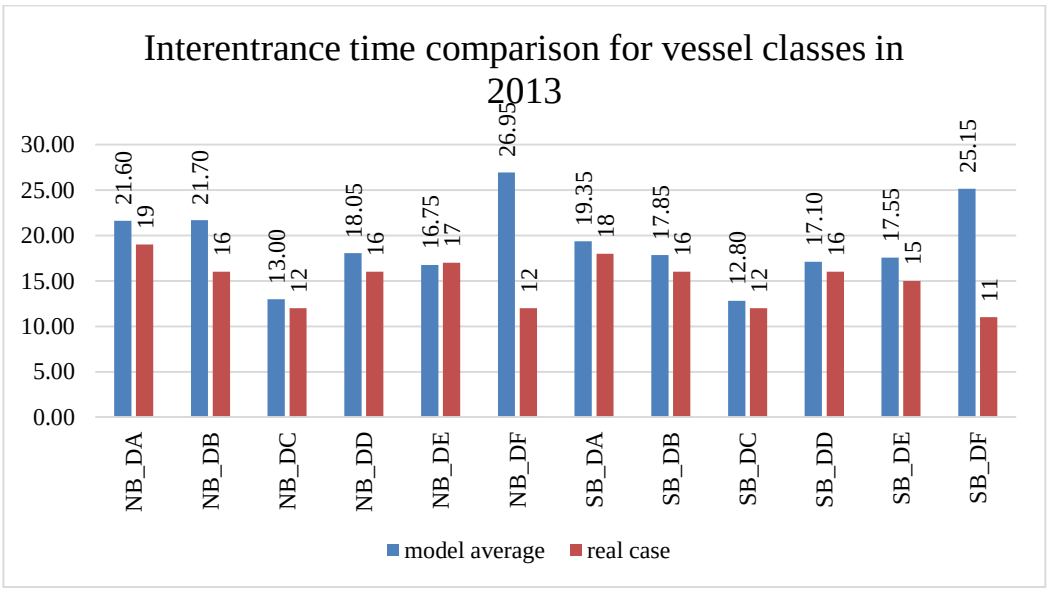

Figure D.16. Vessel interentrance time comparison for class D and successive classes in 2013.

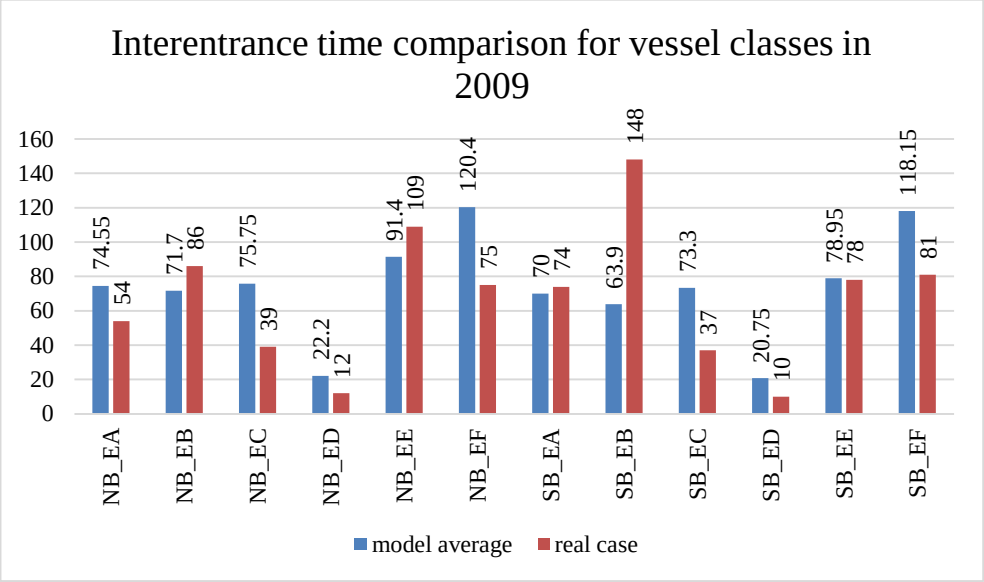

Figure D.17. Vessel interentrance time comparison for class E and successive classes in 2009.

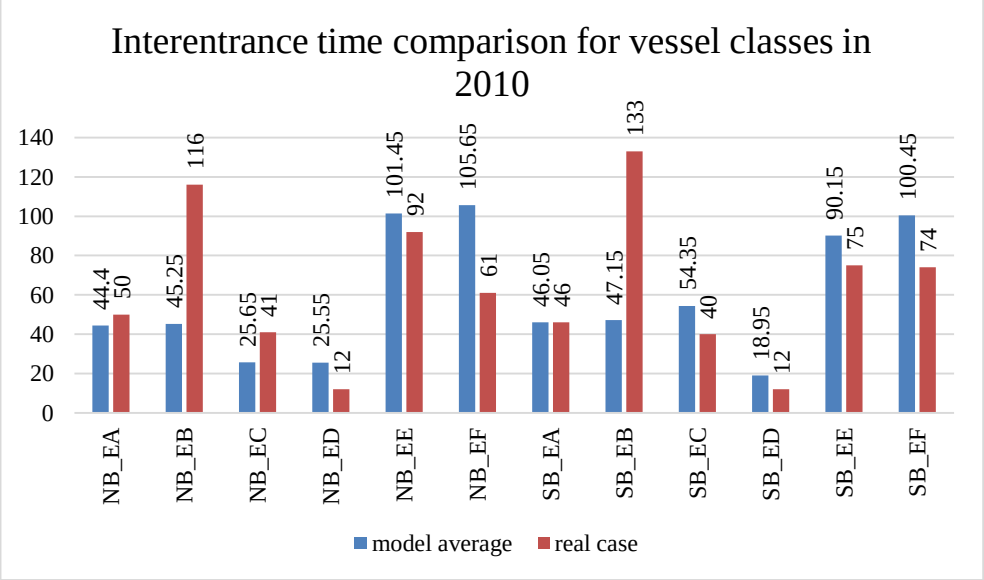

Figure D.18. Vessel interentrance time comparison for class E and successive classes in 2010.

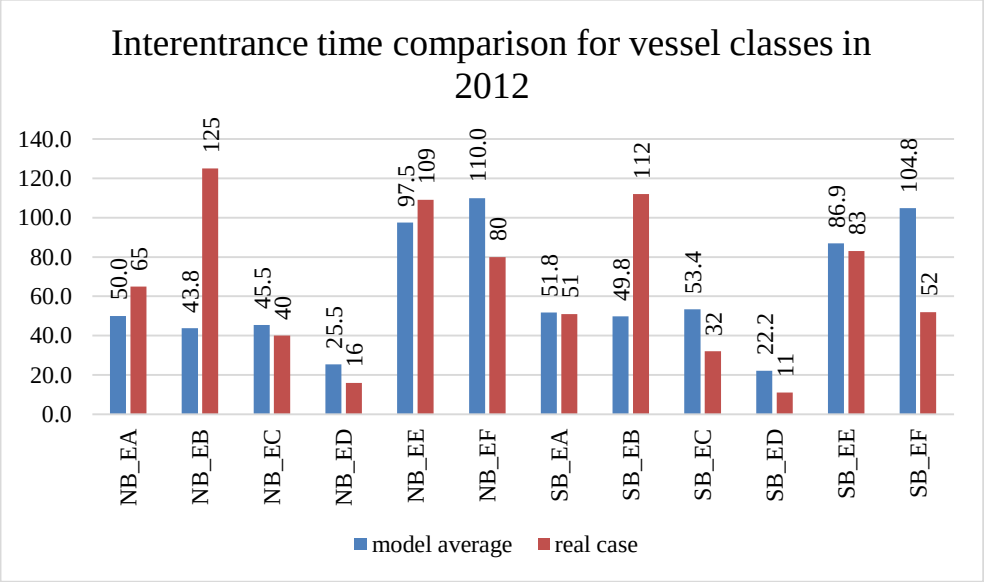

Figure D.19. Vessel interentrance time comparison for class E and successive classes in 2012.

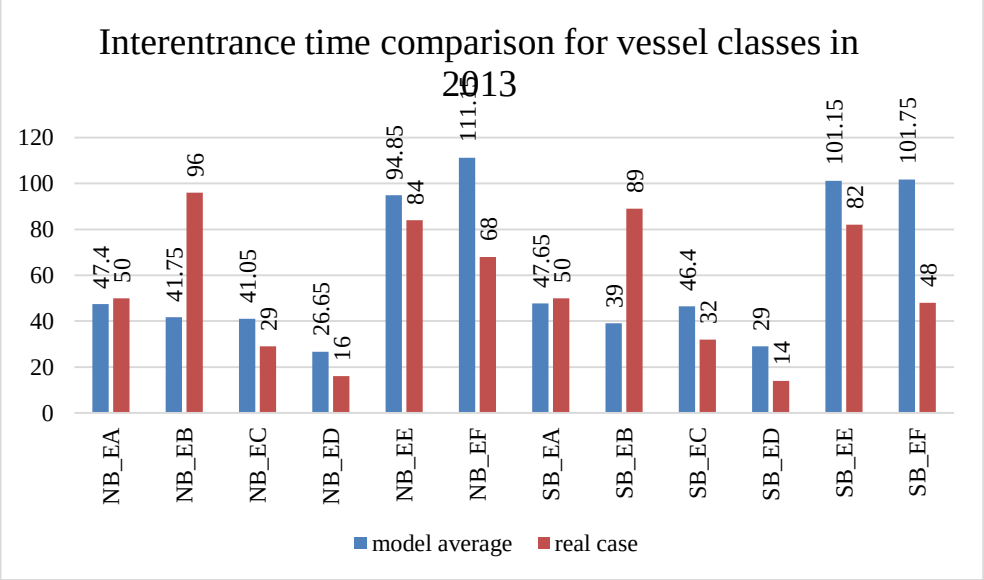

Figure D.20. Vessel interentrance time comparison for class E and successive classes in 2013.

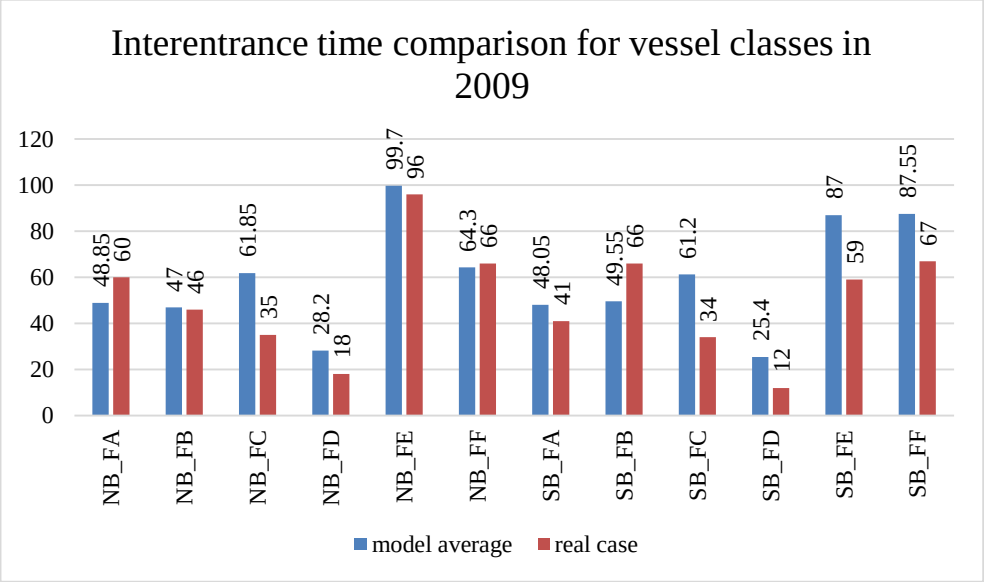

Figure D.21. Vessel interentrance time comparison for class F and successive classes in 2009.

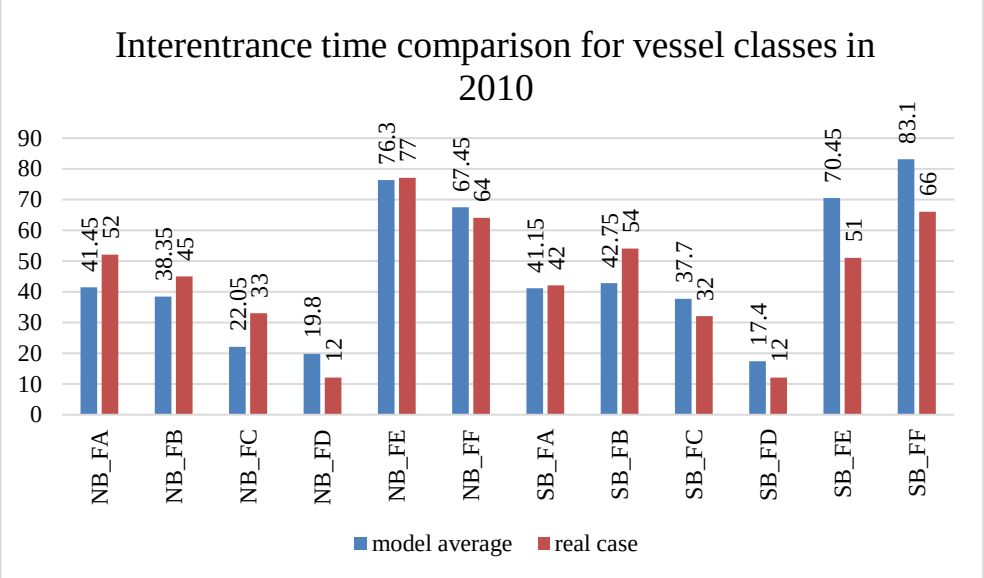

Figure D.22. Vessel interentrance time comparison for class F and successive classes in 2010.

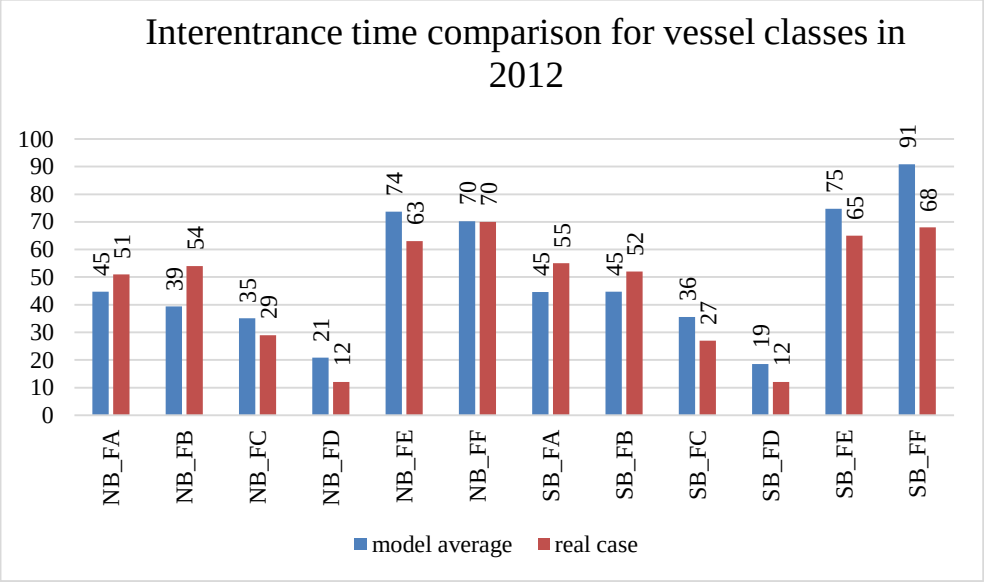

Figure D.23. Vessel interentrance time comparison for class F and successive classes in 2012.

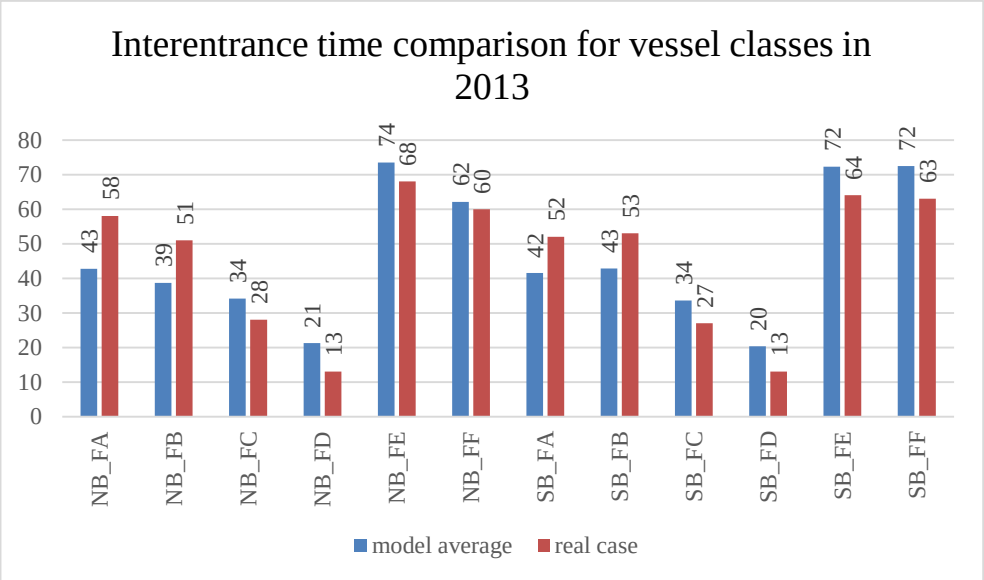

Figure D.24. Vessel interentrance time comparison for class F and successive classes in 2013.